

25. PELAGIC SEDIMENTS¹

G. ARRHENIUS

1. Concept of Pelagic Sedimentation

The term pelagic sediment is often rather loosely defined. It is generally applied to marine sediments in which the fraction derived from the continents indicates deposition from a dilute mineral suspension distributed throughout deep-ocean water. It appears logical to base a precise definition of pelagic sediments on some limiting property of this suspension, such as concentration or rate of removal. Further, the property chosen should, if possible, be reflected in the ensuing deposit, so that the criterion in question can be applied to ancient sediments.

Extensive measurements of the concentration of particulate matter in sea-water have been carried out by Jerlov (1953); however, these measurements reflect the sum of both the terrigenous mineral sol and particles of organic (biotic) origin. Aluminosilicates form a major part of the inorganic mineral suspension; aluminum is useful as an indicator of these, since this element forms 7 to 9% of the total inorganic component,² and can be quantitatively determined at concentration levels down to 3×10^{-10} (Sackett and Arrhenius, 1962). Measurements of the amount of particulate aluminum in North Pacific deep water indicate an average concentration of 23 $\mu\text{g/l}$. of mineral suspensoid, or 10 mg in a vertical sea-water column with a 1 cm^2 cross-section at oceanic depth. The mass of mineral particles larger than 0.5μ constitutes 60%, or less, of the total. From the concentration of the suspensoid and the rate of fallout of terrigenous minerals on the ocean floor, an average passage time (Barth, 1952) of less than 100 years is obtained for the fraction of particles larger than 0.5μ . For the finer particles the average passage time is longer, such as more than 200 (but considerably less than 600) years.

A mechanism which possibly contributes significantly to the removal of coarse suspensoid is aggregation in the gut of filter-feeding animals; this phenomenon has been observed by Rex and Goldberg (1958). Gravitative settling of single grains could account for the deposition of most particles larger than a few microns, but for smaller grains this mechanism is inadequate since the settling time required by Stokes' law³ is several orders of magnitude larger than the passage time actually observed ($< 10^2$ years).⁴

¹ Much of the information presented in this chapter is the result of research partly carried out under Contract No. AT (11-1)-34 with the U.S. Atomic Energy Commission, partly sponsored by the Petroleum Research Fund of the American Chemical Society (ACS PRF Unsolicited Award 875-C6). The generous support from these agencies is gratefully acknowledged.

² Data from the Pacific Ocean (Sackett and Arrhenius, 1962); determinations from the English Channel give similar values (Armstrong, 1958).

³ 7800 years for a 0.1μ spherical particle of density 2.6 through 2900 m of the oceanic-water column at 10°C .

⁴ The passage time is defined as the time at which the mass of particles originally present in the water column has been reduced to $1/e$ of the original value. This occurs when the

Coagulation of unprotected colloids at high electrolyte concentration has been demonstrated by von Smoluchovski (1917) to be a second-order reaction with a rate constant of the order 2×10^{-2} . If in the coarse ($> 0.5 \mu$) part of the oceanic mineral suspensoid the average particle diameter is taken to be 1μ , in agreement with the particle-size distribution found in the sediment,¹ the number of particles per ml is 7×10^3 . In 3×10^9 sec (100 years, which is the maximum passage time given above for this fraction), coagulation by such a reaction would reduce the original particle concentration by a factor of 4×10^{11} , i.e. all particles in 5×10^7 ml of sea-water, or a 100 cm^2 oceanic-water column, would be aggregated together.

If a similar reasoning is applied to the fine fraction of the suspensoid ($0.01-0.5 \mu$), in which an average particle diameter of 0.05μ is assumed, the initial particle content of 3×10^7 per ml should be reduced to 6×10^{-15} of the original value in 10^{10} sec (300 years) which, as indicated above, is a probable passage time for this fraction. This aggregation would comprise all particles in this size range contained in a 400-cm^2 water column.

It is obvious that the rate of coagulation by such a reaction is far more rapid than the rate of removal actually observed in the open ocean. Rates of the order required by von Smoluchovski's theory prevail, however, in concentrated suspensions such as in shallow seas and off river mouths (see e.g. Gripenberg, 1934). It is possible that one of the organic components of sea-water, present in concentrations several orders of magnitude higher than that of the mineral suspensoid, might decrease its rate of coagulation. Whether this is correct or not, the low concentration of the suspensoid in the open ocean, its abnormally low rate of coagulation, and, therefore, its long passage time, permitting wide areal distribution, are observed properties which contrast with the properties of the more concentrated, rapidly flocculating, and, therefore, locally varying hydrosol observed in some coastal areas. Pelagic sediments may consequently be defined on the basis of a maximum value for the rate of deposition of the terrigenous component. This value seems to fall in the range of millimeters per thousand years. Within the basins accumulating pelagic sediments, the terrigenous deposition rate appears to vary not much more than one order of magnitude (5×10^{-5} to 5×10^{-4} cm/year), whereas values much higher and varying by several orders of magnitude are characteristic of the sediments fringing the continents. An attempt to outline the area covered by pelagic sediments, as defined above, is made in Fig. 1.

The rapidly accumulating sediments on the continental slope are unstable, and when the structures fail, coherent masses of sediment slide or slump. When water infiltrates the sliding masses, the concentrated suspensions slide as

particles have settled $(1-1/e)$ of the height of the water column, or $(1-1/2.72) \times 4600 = 2900$ m on the average.

¹ The particle-size frequency distribution of the sediment is not identical with the corresponding distribution in the suspensoid for reasons discussed in Sackett and Arrhenius (1962), but this effect is too small to be considered in the order-of-magnitude computation above.

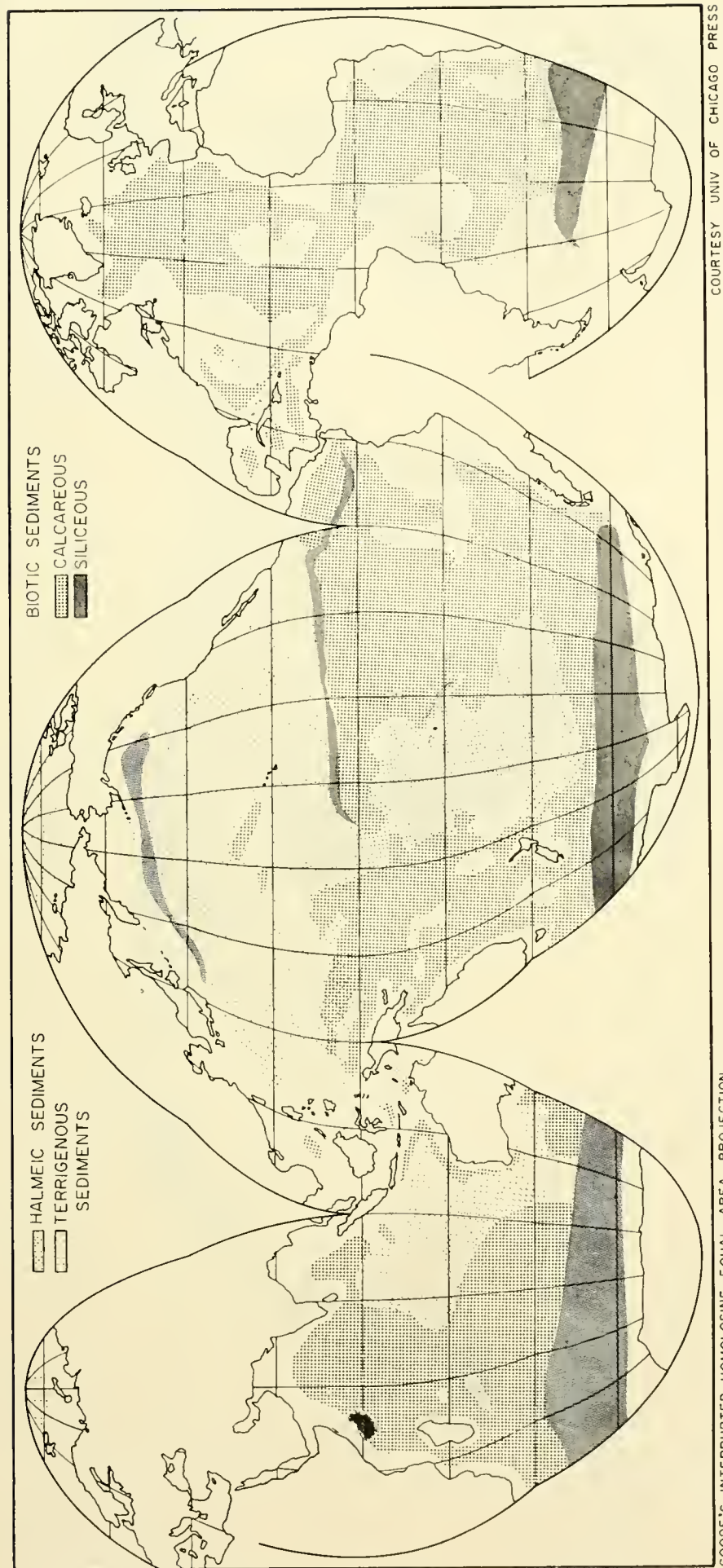


Fig. 1. Present areal distribution of pelagic sediments. The term halmeic has been used to indicate those sediments where the major component is formed from solution in sea-water. Sediments dominantly made up of minerals transported from the continents (regardless of origin of exchangeable cations) have been designated as terrigenous. The boundaries shown in the map are approximate in most areas owing to lack of precise information on the critical properties of the sediment. The generalization due to the small scale has necessitated the omission of features with small areal extension. Local occurrences of pyroclastic and halmeic deposits, the latter mostly phosphorite and manganese oxide rocks, and of biotic sediments such as coral reefs and pteropod ooze are consequently not shown. Features with intricate limits such as the fast accumulating sediments funneled into pelagic areas along submarine canyons, as in some parts of the Atlantic Ocean, are omitted for the same reason.

The map attempts to represent present conditions, characterized by relatively narrow zones of rapidly depositing sediments around the continents, compared to the conditions during Pleistocene epochs with a maximum rate of sediment transport.

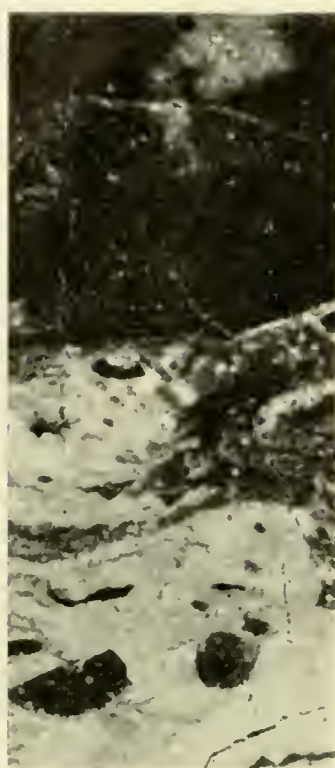


Fig. 2. Abyssal plains and feeding channels in the North Pacific. Depths in meters. Shaded areas indicate hilly topography. (Modified from Hurley, 1960.)

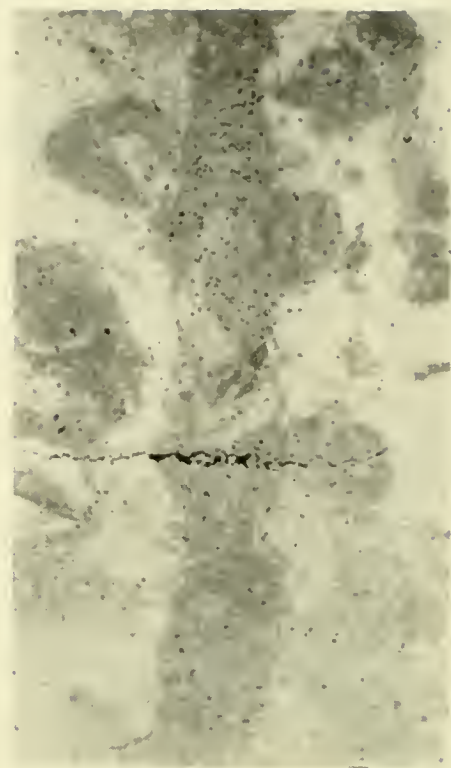
high-speed turbidity currents, invading the unprotected areas of the deep-ocean floor adjacent to the shelf slope, and smoothing the original topography to almost level abyssal plains (Kuenen, 1950; Heezen *et al.*, 1959; Menard, 1959; Hurley, 1960). Rises or trenches protect areas separated from the continental shelf from invasion by turbidity currents; in the absence of topographic barriers such as in the Gulf of Alaska and in large parts of the Atlantic Ocean, detrital sediments are, or were once, spread over extensive areas of the deep ocean by this mechanism (Fig. 2). On the other hand, some pelagic deposits accumulate close to the coast in areas where river discharge is low, where topographic protection is provided and where currents prevent fine-grained clastics from accumulating, such as on banks and rises, or where the clastic erosion products are efficiently funneled into deep catchment basins by submarine canyons (Shepard, 1948; Kuenen, 1950; Emery, 1960; Inman and Chamberlain, 1960). Iron and manganese oxide rocks, phosphorite and glauconite deposits, coral reefs, pteropod and foraminiferal oozes are thus frequently found in local areas close to the continents.

Although few measurements exist which permit quantitative estimates of the rate of deposition of the terrigenous component, i.e. the parameter suggested as a basis for division of marine sediments into pelagic and rapidly accumulating ones, the large differences in accumulation rate between these two sediment types often permit their recognition on the basis of a number of easily observed features. One of these is evidence of reworking of the sediment by organisms. Benthic animals appear to be distributed over all areas of the ocean floor where free oxygen is available, even at the greatest depths. Studies of the mixing of sediments across unconformities demonstrate that although single worm burrows might occasionally penetrate as deep as 20–30 cm, the mean mixing depth, above which 50% of the extraneous material is located, is of the order of 4–5 cm. In pelagic sediments the time required for burial of such a layer under another equally thick one varies between 10^3 and 10^5 years. The longer time is typical of areas with a low rate of deposition of organic remains, where a correspondingly low population-density of benthic animals is sustained. The total amount of reworking of a given stratum before ultimate burial might, therefore, not vary as much as the total rate of deposition within the area of pelagic sedimentation. When adjacent strata have different colors or shades, the mixing process causes a typical mottled appearance (Fig. 3). In pelagic sediments without a color stratification, the mud-eating animals leave less conspicuous traces, but their presence is indicated by fecal pellets, annelid jaws, and other fossil remains including chemical reduction structures. Non-pelagic deep-sea sediments, on the other hand, are deposited so rapidly that the sparse benthic population does not have enough time to disturb the strata as extensively as in pelagic deposits with similar population densities, and the original stratification is preserved, often in minute detail. Examples are the thin laminations often present in graded beds, deposited by turbidity currents, and laminae of volcanic ash.

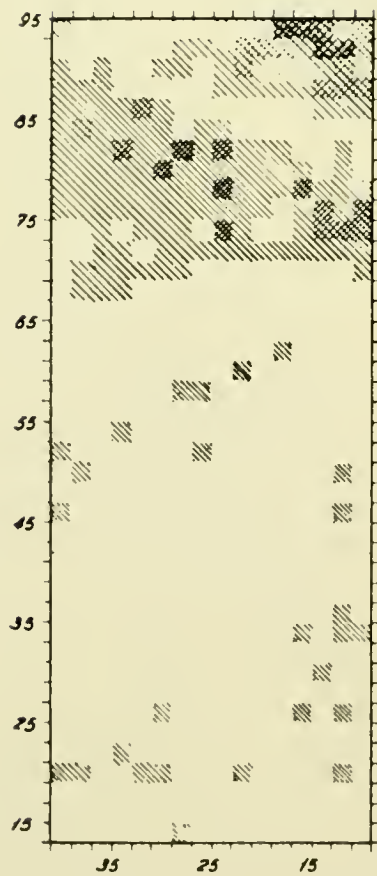
Another effect of the low rate of detrital deposition, characteristic of pelagic



CH 40
0-8 cm



CH 30
16-24 cm



CH 30
40-48 cm



Fig. 3. Mixing by animal burrowing in pelagic sediments. The photograph CH 30 (16–24 cm) contains an unusually long vertical worm burrow extending through the section (8 cm). CH 40 (0–8 cm) demonstrates by tone contrast the redistribution of sediment over the boundary between layers of clay and calcareous ooze.

The section CH 30 (40–48 cm) contains an unconformity between Middle Tertiary and Quaternary sediment. The evaluation of a radioautograph of this section (adjacent to the photograph) distinguishes between the highly alpha-active Quaternary sediment and the inactive Tertiary, and demonstrates the extent and distribution of mixing of material from the two strata.

The total number of alpha tracks generated in the surface of the section CH 30 (40–48 cm) during six weeks was counted, and the average activity in each 4 mm^2 surface unit is shown in the radioautograph evaluation in the following intensity shades, graded in units of 10^{-4} alpha particles per $\text{cm}^2 \text{ sec}$:

No surface tone	0–2.0
Line hatched	2.1–5.0
Cross hatched	5.1–9.3
Double cross hatched	9.4–16.6

The linear scale in millimeters (relative to an arbitrary origin) is indicated at the edge of the diagram. (From Picciotto and Arrhenius, unpublished.)

sediments, is the high percentage of authigenic minerals, extra-terrestrial material, and fossil remains of planktonic organisms. Further, with a similar rate of diagenesis in pelagic and neritic deposits, considerably more rapid increase in shear strength with depth in the sediment is found in the former than in the latter (Fig. 4). Bramlette (1961) has pointed out that the redox

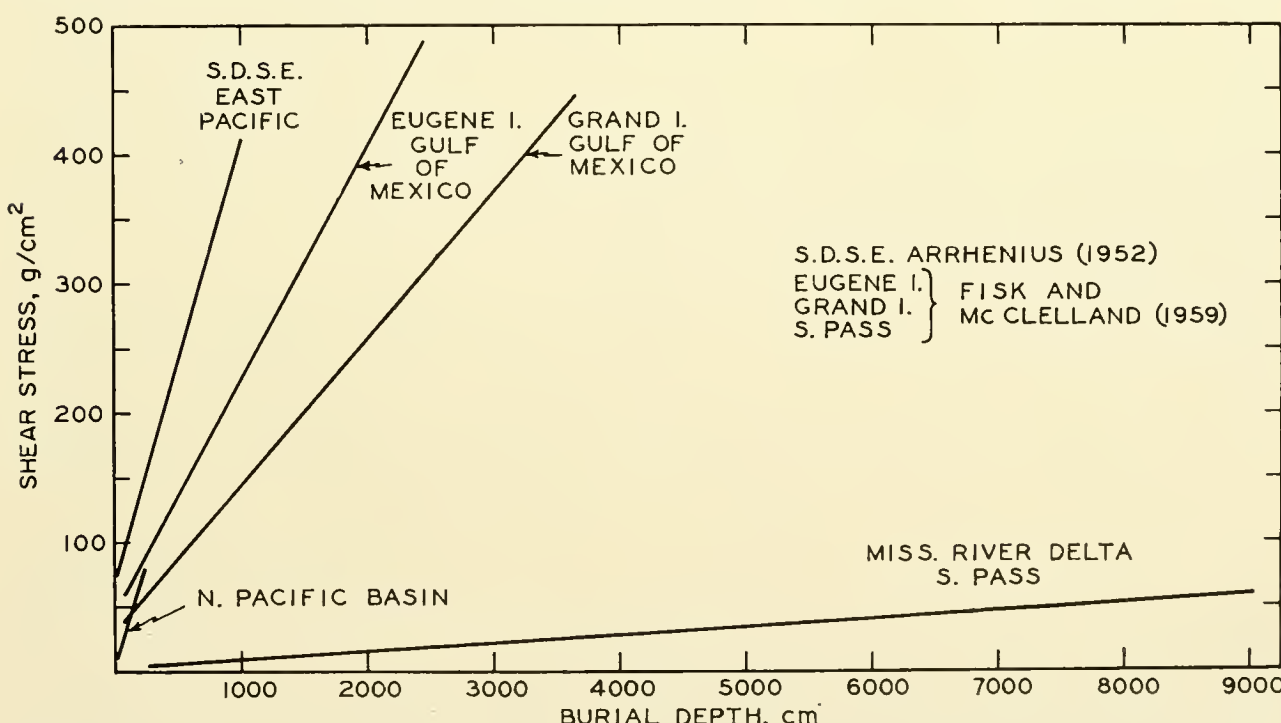


Fig. 4. Induration of sediment as a function of burial depth in pelagic sediments (Swedish Deep-Sea Expedition, East Pacific, N. Pacific basin) and in rapidly accumulating clay sediments (max. rate: Miss. delta). (From Moore, 1960.)

state of the sediment is mainly determined by the duration of contact with the oxidizing bottom water. This property consequently reflects the total rate of deposition, and Bramlette suggests a high degree of oxidation as one criterion for pelagic sediments.

Any single one of the criteria for pelagic versus high-rate sedimentation might be insufficient when applied alone. In cases where several indications occur jointly, conclusions regarding the order of magnitude of the sedimentation rate can apparently be safely drawn. The reliability of such conclusions is illustrated by the fact that estimates of the rate of deposition of different types of pelagic sediments, made before the advent of nuclear age-determination methods, have in general proved correct within surprisingly narrow limits. Even if the number of absolute age determinations will remain relatively limited, the suggested definition of pelagic sediments on the basis of a maximal value for the rate of deposition of the terrigenous component thus appears rational and practical.

2. Composition

Attempts to classify pelagic sediments have been based either on appearance and composition, or on the ultimate origin of the components. A rigorous application of the latter scheme has been attempted by Grabau (1904) and Schott (1935), and recently in a modified form by Goldberg (1954), further applied by Arrhenius (1959). However, at this time not enough is known of the ultimate origin and mode of accretion of some of the minerals making up the sediment (cf. Pettijohn, 1949, p. 184). To indicate the general distribution of different types of pelagic sediments it is consequently necessary to limit genetic classifications to major groups, except in the case of biotic sediments which can be identified morphologically. The origin of the major inorganic component in most areas has not been established with certainty; the term "red clay" has come into general use, although a red hue is seldom dominant and clay minerals sometimes are not the major mineral group.

Although introducing additional technical terminology is deprecable, the discussion of pelagic sediments on a genetic basis warrants some modification of existing terms. It appears feasible to distinguish minerals which crystallized in sea-water from those which formed in magmas, in hydrothermal solution, or by weathering under acidic conditions. This distinction is important, inasmuch as only the first group can be used to interpret the physicochemical state of the ocean in the past. These minerals are here described as *halmeic* (from $\alpha\lambda\mu\eta$; sea-water). Conversely, the properties of the third group of components frequently furnish information on the processes acting on the lithosphere and on the transport of this group of minerals into the pelagic environment. The minerals derived from the exposed surface of the lithosphere are here designated as *terrigenous*. Minerals and mineraloids deposited into the ocean by volcanic eruption are described as *pyroclastic*. Solids secreted by living organisms are referred to as *biotic*.

In the map showing the distribution of pelagic sediments (Fig. 1), this broad genetic classification is attempted, based in some instances on assumptions which, admittedly, are as yet unproven. However, the account given below of the composition of such sediments is based solely on the observed properties of the constituent minerals, whose possible sources of origin are discussed subsequently. In this way the basic observations have been separated from the interpretations.

A. Elements and Oxides

Iron and manganese oxide mineral aggregates constitute one of the major types of rock encountered on the ocean floor; according to Menard (unpublished) about 10% of the pelagic area of the Pacific is covered by such nodules. Measurements from the northeast Pacific by Skornyakova (1960) and Mero (1960a) give similar averages and indicate a considerable local variability in concentration (Fig. 5).

The nodules consist of intimately intergrown crystallites of different minerals; among those identified, besides detrital minerals and organic matter, are opal, goethite, rutile, anatase, barite, nontronite, and at least three manganese oxide minerals of major importance, described by Buser and Grütter (1956), Grütter and Buser (1957, 1959). One of these minerals, identical with a synthetic phase described in the chemical literature as $\delta\text{-MnO}_2$, forms aggregates of randomly oriented sheet units as small as 50–100 Å. The other two minerals possess a double layer structure similar to that of lithiophorite and to synthetic phases, in chemical nomenclature called manganites.¹ These consist of ordered sheets of MnO_2 , alternating with disordered layers of metal ions, co-ordinated with water, hydroxyl and probably also other anions. The most prevalent cations in the disordered layer are Mn^{2+} and Fe^{3+} . It is assumed that Na, Ca, Sr, Cu, Cd, Co, Ni, and Mo also substitute in this part of the structure. Two species of this general type have been observed, one with a basal spacing of 10 Å, the other with 7 Å. Buser has interpreted the 10 Å spacing as due to the existence of two discrete layers, OH and H_2O , whereas in the collapsed structure these groups are assumed to form a single layer, but owing to the disorder, the structure has not yet been precisely described. Synthesis experiments demonstrate that the three manganese oxide minerals represent increasing degrees of oxidation at formation in the order 10 Å “manganite,” 7 Å “manganite”, and $\delta\text{-MnO}_2$. Buser has pointed out the potential use of this information in interpreting the conditions of formation of pelagic sediments.

Recent determinations of the bulk composition of manganese nodules have been made by Goldberg (1954), by Riley and Sinhaseni (1958), and by Mero (1960, and unpublished), and specific elements have been reported on by a number of authors. Mero's data, compiled in Table I, demonstrate the wide

¹ Not identical with the mineral manganite, $\gamma\text{-MnOOH}$, which is monoclinic–pseudo-rhombic and isotypical with the diaspore group (Strunz, 1957).

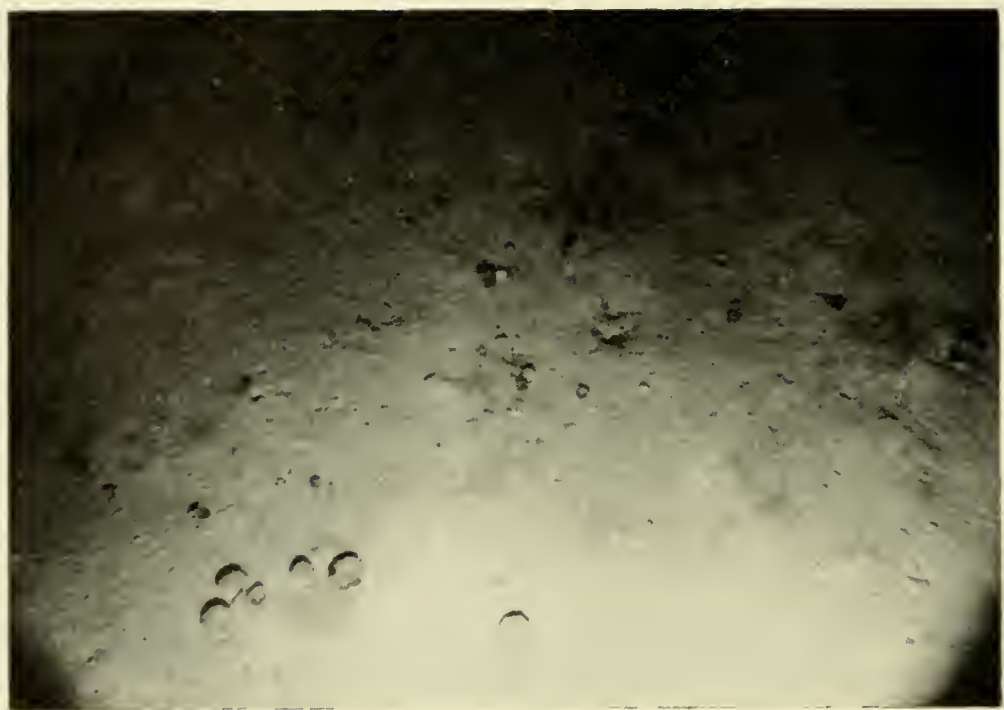


Fig. 5. Two photographs from the floor of the Atlantic Ocean, taken a few hundred feet apart, show the marked local variability in concentration of manganese nodules. (Photo: Bruce Heezen, Lamont Geological Observatory, Columbia University.) The locality is further discussed by Heezen *et al.* (1959), who include a third photograph from the same station (pl. 11, fig. 6).

TABLE I
Bulk Chemical Composition of Manganese Nodules from the Pacific and Atlantic Oceans as Determined by X-Ray Spectrography^a

Element	Pacific Ocean			Atlantic Ocean		
	Maximum	Minimum	Average	Maximum	Minimum	Average
B	0.06	0.007	0.029	0.05	0.009	0.03
Na	4.7	1.5	2.6	3.5	1.4	2.3
Mg	2.4	1.0	1.7	2.4	1.4	1.7
Al	6.9	0.8	2.9	5.8	1.4	3.1
Si	20.1	1.3	9.4	19.6	2.8	11.0
K	3.1	0.3	0.8	0.8	0.6	0.7
Ca	4.4	0.8	1.9	3.4	1.5	2.7
Sc	0.003	0.001	0.001	0.003	0.002	0.002
Ti	1.7	0.11	0.67	1.3	0.3	0.8
V	0.11	0.021	0.054	0.11	0.02	0.07
Cr	0.007	0.001	0.001	0.003	0.001	0.002
Mn	50.1	8.2	24.2	21.5	12.0	16.3
Fe	26.6	2.4	14.0	25.9	9.1	17.5
Co	2.3	0.014	0.35	0.68	0.06	0.31
Ni	2.0	0.16	0.99	0.54	0.31	0.42
Cu	1.6	0.028	0.53	0.41	0.05	0.20
Zn	0.08	0.04	0.047	—	—	—
Ga	0.003	0.0002	0.001	—	—	—
Sr	0.16	0.024	0.081	0.14	0.04	0.09
Y	0.045	0.033	0.016	0.024	0.008	0.018
Zr	0.12	0.009	0.063	0.064	0.044	0.054
Mo	0.15	0.01	0.052	0.056	0.013	0.035
Ag	0.0006	—	0.0003	—	—	—
Ba	0.64	0.08	0.18	0.36	0.10	0.17
La	0.024	0.009	0.016	—	—	—
Yb	0.0066	0.0013	0.0031	0.007	0.002	0.004
Pb	0.36	0.02	0.09	0.14	0.08	0.10
Ignition loss at 500°C	39.0	15.5	25.8	30.0	17.5	23.8

^a Concentrations are given in weight per cent. (Data from Mero, unpublished.)

variability in the concentrations of cobalt, nickel, copper, iron and molybdenum relative to manganese in the nodules. Arrhenius and Korkisch (1959) have pointed out that eddy diffusion is an insufficient transport mechanism for a number of the heavy metals found in manganese nodules, including the rare earth elements, thorium and uranium. They consequently assume that the vertical-transport mechanism described on page 677 below controls the transfer

of many of the heavy metals from sea-water to sediment. High concentrations of a specific element at the ocean floor would under these conditions be expected in areas with a high rate of biological extraction of this element in the surface layer. Mero (*op. cit.*) has established a regional regularity in the elemental composition of the nodules (Fig. 6), and assumes that the regional variations



Fig. 6. Regional variation in chemical composition of manganese nodules. Regions marked A are characterized by ratios Mn/Fe less than 1; B-areas conversely have exceptionally high ratios Mn/Fe (ranging from 12 to 50). In areas marked C the nickel and copper content of the nodules is unusually high. D denotes regions with large amounts of cobalt (0.7–2.1%) in the nodules. (Mero, unpublished, modified from Mero, 1960a.)

in copper and nickel content of the nodules are controlled by the process referred to above.

Arrhenius and Korkisch (1959) have attempted to separate from each other the different minerals constituting the nodules, in order to establish the details of their structure and the localization of the heavy metal ions. The results demonstrate (Table II) that copper and nickel are concentrated in the manganese oxide phases. Cobalt, part of the nickel and most of the chromium are distributed between these and the acid-soluble group of the non-manganese

minerals, dominated by goethite and disordered FeOOH. With increasing cobalt concentration in the rock, more of it substitutes in the manganese oxide minerals, which may achieve concentrations of well above 1% of cobalt, nickel, and copper. A variable fraction (mostly $\frac{1}{3}$ to $\frac{2}{3}$) of the soluble iron prevails in the form of goethite and in some instances as nontronite (the acid-soluble fraction of sample no. 2, Dwd HD 72, in Table II contains one-third nontronite). The remainder of the soluble iron is located in the manganese oxide minerals substituting for divalent manganese (Buser, *op. cit.*). Conversely, between a tenth and one per cent of manganese is always found in the separation group which contains the goethite, probably substituting as Mn³⁺ for Fe³⁺ in this

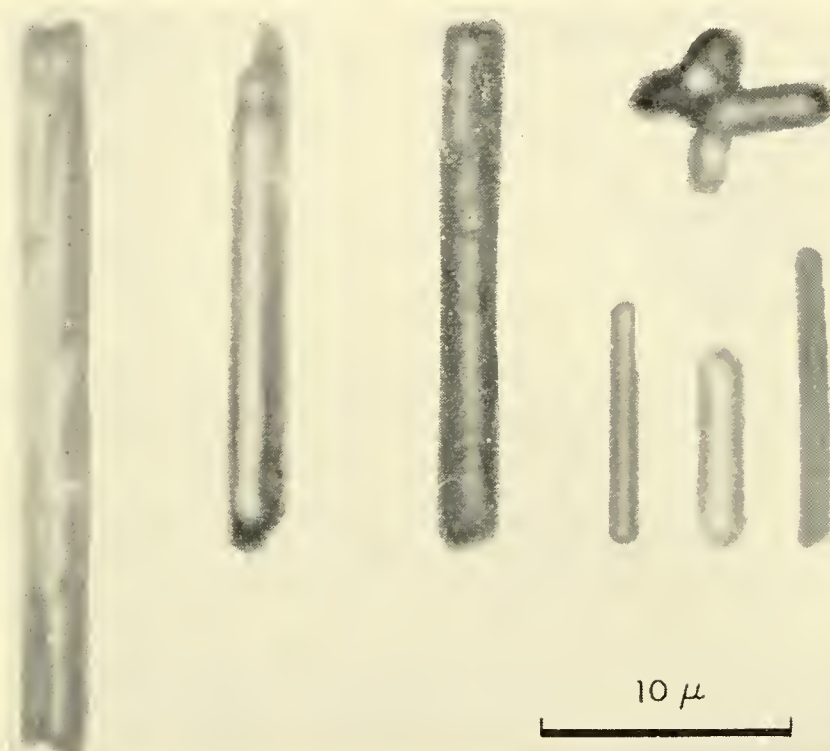


Fig. 7. Rutile needles and multiple twin, Cap. 49 BG, Quaternary, North Equatorial Pacific.

mineral. This group also tends to concentrate the major fractions of molybdenum, lead, titanium, scandium, the rare earth elements, and thorium. It is as yet uncertain which of the minerals constituting the group is responsible for the accumulation of the first four of these elements; it appears that thorium and the rare earth elements largely prevail as phosphates.

The elements barium and strontium in manganese nodules appear to be partitioned between the manganese oxide structures and the barite-celestite solid solutions (see also Section 2-B). These latter crystals account for the occasional high barium content of the acid-soluble and insoluble fractions in Table II. Titanium in the insoluble residue (Table II) is present as small euhedral crystals of rutile (Fig. 7) and anatase, the rutile frequently twinned on 011. The relatively high niobium content of the insoluble residue is probably

TABLE

Distribution of Elements between Minerals Soluble in 1M Hydroxylamine Residue of

Sample number, region and position	Fraction	Percent of total mass	Cu	Ni	Co ^a	Cr	Fe	Mn
AA2 high Mn $28^{\circ} 23'N, 126^{\circ} 57'W$	reducible acid sol. residue	43.6 47.6 8.8	2000 200 45	1100 300 30	33 80 0	7 20 60	4400 4400 15,000	major 8000 800
Dwd HD 72 high Mn $25^{\circ} 31'S, 85^{\circ} 14'W$	reducible acid sol. residue	70.0 13.8 16.0	800 210 20	2200 1100 7	3300 9900 35	7 28 0	30,000 240,000 100,000	major 8000 45
AA 4711 high Mn, Ni, Cu $07^{\circ} 48'S, 94^{\circ} 06'W$	reducible acid sol. residue	84.4 4.6 11.0	3000 500 90	>1000 >1000 40	250 700 0	4 50 17	10,000 90,000 17,000	major 4500 300
Alb 13 high Ni, Cu $09^{\circ} 57'N, 137^{\circ} 47'W$	reducible acid sol. residue	82.5 3.3 14.2	10,000 200 25	9900 200 25	1100 40 0	14 50 30	80,000 60,000 6000	major 2500 40
AA 4721 high Ni, Cu $08^{\circ} 08'S, 104^{\circ} 11'W$	reducible acid sol. residue	54.5 22.8 22.5	7000 450 90	7700 1400 20	440 660 0	3 70 12	130,000 120,000 18,000	major 2500 200
Dwd BD 4 high Co $13^{\circ} 20'S, 146^{\circ} 30'W$	reducible acid sol. residue	84.25 11.4 4.3	1000 250 20	3100 150 25	9300 180 0	6 60 5	30,000 140,000 3,000	major 3500 p. tr.
Nth Hol 10 low Mn $40^{\circ} 14'N, 15^{\circ} 52'W$	reducible acid sol. residue $\rho > 3.0$ residue $\rho < 3.0$		5900 1000 250 140	1000 1700 25 25	900 1000 8 9	83 81 62 58		major 8000 700 500

^a 0 = below sensitivity limit.

The reducible fraction contains the manganese oxide minerals. The acid-soluble fraction consists mainly of goethite and, if present, the cations from hydrous aluminosilicates (the high iron content in the acid-soluble fraction of Dwd HD72 is partly caused by a nontronite with $n\gamma = 1.598$; $\text{Fe}^{3+} = 15\%$). Further, such apatite crystals in which substitution with rare-earth ions is only partial are dissolved to a small extent in the weakly acid hydroxylamine hydrochloride and extensively in the hydrochloric acid, which accounts for the high concentration of rare earths, thorium, and possibly for the molybdenum and lead found in the acid-soluble fraction. When considerable barite is present, as in AA 4711, the corrosion of the crystallites yields appreciable amounts of barium, but the major fraction of the mineral is left in the residue.

II

Hydrochloride (Reducible); in 1M HCl (Acid-Soluble) and in the Insoluble Manganese Nodules

Mo	Pb ^b	Ti ^c	Sc	La	Y	Yb	Zr ^c	Th ^c	Ba,	Sr	Nb
220	p. tr.	242	0	220	17	2	70	0	3000	450	p. tr.
150	p. tr.	1400	8	150	55	6	114	8.5	3000	45	p. tr.
2	0	4000	15	2	15	1	390	37.5	1000	100	0
250	60	785	4	200	130	9	61.4	0	500	200	p. tr.
700	150	7600	0	300	250	20	36.3	58.4	1000	50	30
11	0	3330	0	0	0	0	343	0	140	3	40
250	p. tr.	2860	0	90	60	4	162	16.6	3000	300	p. tr.
1000	65	5800	60	350	450	45	112	0	2000	60	16
0	0	2500	18	0	10	1	1670	8.3	20,000	300	20
300	35	182	0	250	120	12	20	17	500	350	p. tr.
800	20	15,800	110	0	15	2	236	58.3	3000	200	40
4	0	4000	12	0	13	1	1430	57.1	5000	250	110
130	p. tr.	555	0	250	150	14	125	0	900	1000	p. tr.
400	60	6200	30	170	200	18	84.2	5.1	600	60	10
1	0	3570	0	0		1	1570	0	2000	50	10
300	40	562	5	280	130	13	120	57.1	3000	350	p. tr.
1000	300	15,600	16	450	400	20	363	27.2	500	65	50
15	0	122,900	20	0	0	0	4290	114.0	80	0	700
0	0	250	0	0	0	0	820	3.6	400	2600	0
26	300	3820	p. tr.	500	240	20	828	60.0	19,000	400	20
0	100	10,000	14	0	50	10	930	0.7	3200	300	20
0	110	1560	11	0	53	8	831	0.8	1000	330	21

^b p. tr. = possible traces.^c Colorimetric determination.

The residue also contains the terrigenous minerals, which are embedded in the nodules in varying amounts (mainly quartz, feldspar [of which the calcic plagioclase is partly dissolved by HCl], pyroxene, hornblende, mica residue and spinels), further authigenic opal, authigenic and terrigenous rutile and anatase (carrying the niobium), and finally the more complete authigenic pseudomorphs of rare-earth zirconium-thorium phosphates after apatite. The residue of Nth Hol 10 was separated in two density fractions by centrifugation in a Clerici solution with $\rho = 3.0$.

Concentrations are given in parts per million. (Spectrographic analyses by A. Chodos and E. Godijn, California Institute of Technology; colorimetric measurements of Zr, Ti, and Th by J. Korkisch, University of Vienna.)

due to substitution in rutile. The origin of the titanium oxide minerals is still uncertain; it appears probable that the rutile is terrigenous but the anatase might develop *in situ* (cf. Correns, 1937, 1954; Teodorovich, 1958).

The ferromanganese nodules range in size from a few microns, suspended in the sediment or coating other minerals, to intergrowths forming slabs several meters wide. The nodules have alternating growth zones of high and low

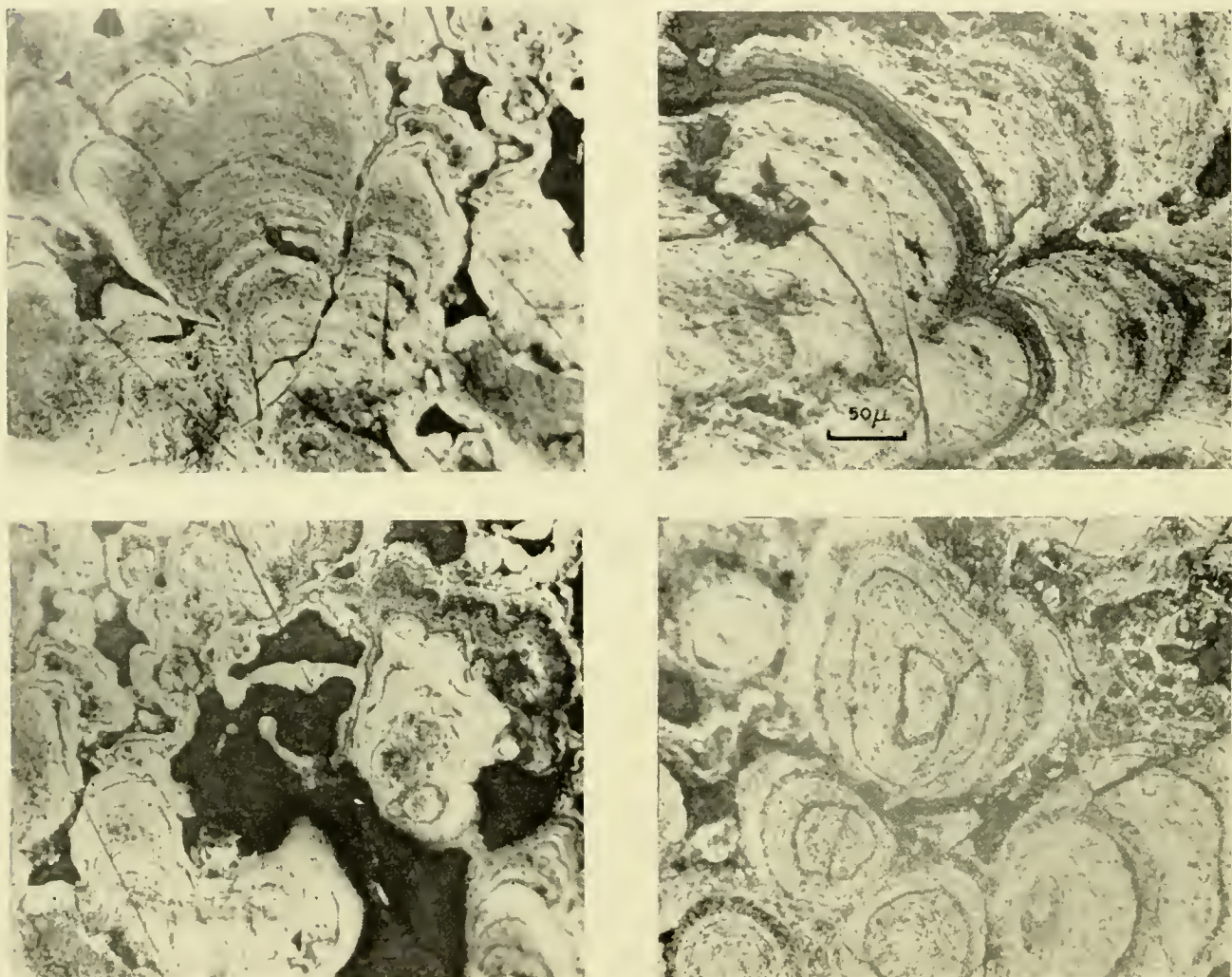


Fig. 8. Zonal growth in manganese nodule (16810, South Pacific). Reflected light. White = manganese oxide minerals; grey = goethite; black = mounting medium (polyvinyl resin) filling voids.

goethite content (Figs. 8 and 9). Detailed information on the distribution of macroscopic concretions over the present sediment surface has been obtained through deep-sea bottom photography (Fig. 5) such as by Owen, Shipek, Menard and Dietz in Dietz (1955), Menard and Shipek (1958), Heezen *et al.* (1959), Shipek (1960), and Zenkevitch (1959), and by sampling of the sediment surface (Skornyakova, *op. cit.*). Large nodules and crusts appear to accrete on topographic highs, or in other areas with a low total rate of deposition, where the growing nuclei are not buried by other sedimentary components. The rate of accretion was in the range of 10^{-5} to 10^{-6} cm year $^{-1}$ in a nodule investigated by von Buttlar and Houtermans (1950) applying the results of Goldberg and

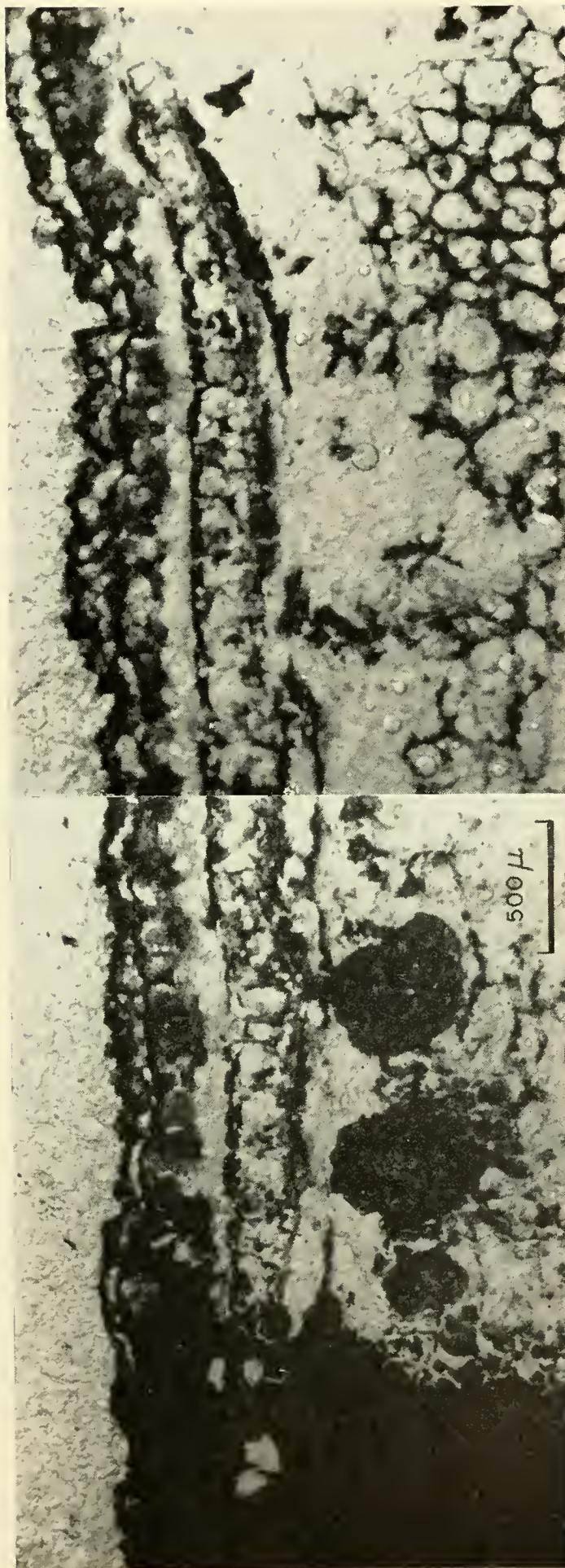


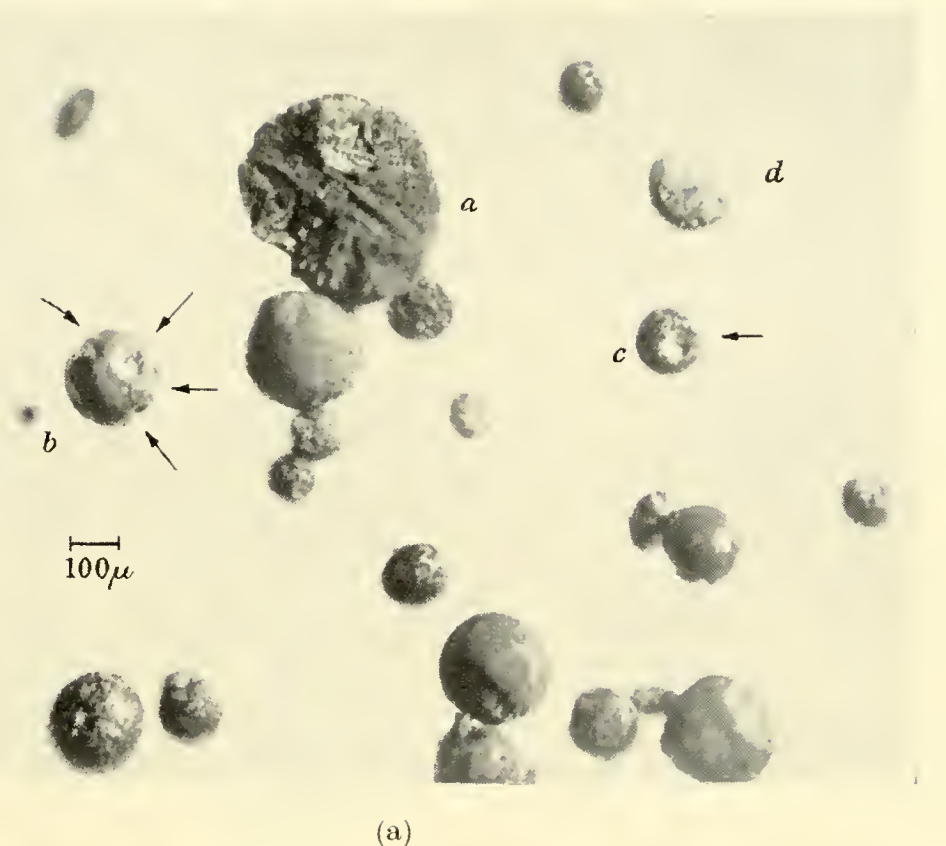
Fig. 9. Goethite network in manganese nodule from North Pacific (PAS 19121). Section cut normal to surface of nodule and manganese oxide minerals removed from right part of section by reduction with hydroxylamine, showing residual goethite texture. Untreated part of section, with remaining manganese oxide minerals, in opaque area to the left. Transmitted light.

Picciotto (1955) (Goldberg and Arrhenius, 1958, p. 198). Similar values are obtained for manganese micronodules in pelagic clays and zeolitites by integrating the manganese content in a column of known interval of time.

Several hypotheses have been advanced regarding the ultimate source of the manganese. Murray, in contrast to Renard (Murray and Renard, 1884) and lately Pettersson (1945, 1955, 1959), suggested that the manganese is derived from pyroclastics decomposing on the ocean floor; so far, no decomposition residue correspondingly deficient in manganese has been observed. Further, by order of magnitude, the manganese found on the ocean floor is accounted for by the amount of this element known to be continually lost from the continents (Kuenen, 1950, p. 390; Goldberg and Arrhenius, *op. cit.*; Wedepohl, 1960). Consequently many authors assume that the manganese on the ocean floor, other than the relatively small part which can be accounted for by decomposition *in situ* of basaltic pyroclastics, originates from dissolution of this element from continental rocks and from volcanic exhalates. Recent geochemical balance computations by Wedepohl (*op. cit.*) indicate that the volcanic exhalates are quantitatively important sources of manganese, iron, and other heavy metals with high halide vapor pressures. World-wide or large regional changes in the absolute rate of deposition of manganese in pelagic sediments could accordingly be due to variations in the rate of weathering on the continents, or in volcanic activity. Local or regional differences in the concentration of manganese in pelagic sediments, such as between the North and South Pacific at the present time or between Atlantic and Pacific sediments, can be accounted for by differences in dilution of the sediments with terrigenous material. Strata with a markedly increased manganese concentration, frequently found in pelagic sediments (see, for example, Arrhenius, 1952, pls. 2.51, 2.56; Revelle *et al.*, 1955, fig. 7; Pettersson, 1959), appear to correspond to periods of a lowered rate of total deposition, resulting in a decreased dilution of the halmeic oxide minerals with terrigenous silicates.

Whatever the ultimate source and mode of transportation of manganese and associated elements, several processes have been suggested to explain the mode of subsequent accretion of the manganese oxide minerals. One group involves various inorganic reactions (a review of these is given in Goldberg and Arrhenius, 1958); another group assumes organic (bacterial) mechanisms (Dieulafait, 1883; Butkevich, 1928; Dorff, 1935; Kalinenko, 1949; Ljunggren, 1953; Graham, 1959; Kriss, 1959). Goldberg and Arrhenius suggest specifically that manganese is removed from the bottom water by catalytic oxidation of manganese ion by colloidal ferric hydroxide at the sediment-water interface. In support of the biotic transfer Graham has demonstrated the presence of organic matter in the nodules. Although investigations in process (Galen Jones, unpublished) have demonstrated that the nodules contain bacteria capable of reducing manganese, it is difficult at the present time to evaluate the biotic hypothesis against an inorganic one.

Under the oxidizing conditions on the ocean floor, the only elemental mineral observed, besides carbon from burning forests and grasslands, is



(a)



(b)

Fig. 10. Cosmic spherules from deep-sea sediments: (a) silicate spherules; (b) magnetite-coated nickel-iron spherules. (From Hunter and Parkin, 1960.)

nickel iron in the form of droplets, formed by ablation of iron meteorites during their passage through the atmosphere (Fig. 10b). The total amount of such spherules has been estimated at a few thousand tons per year over the surface of the earth (Pettersson and Fredriksson, 1958), which is only a fraction of a per cent of the total accretion rate of cosmic matter estimated from satellite measurements of micrometeorite impacts (LaGow and Alexander, 1960). Associated with the partly oxidized metal spherules are chondrules (Fig. 10a) consisting of olivine and pyroxene,¹ which are crystalline and thus could hardly

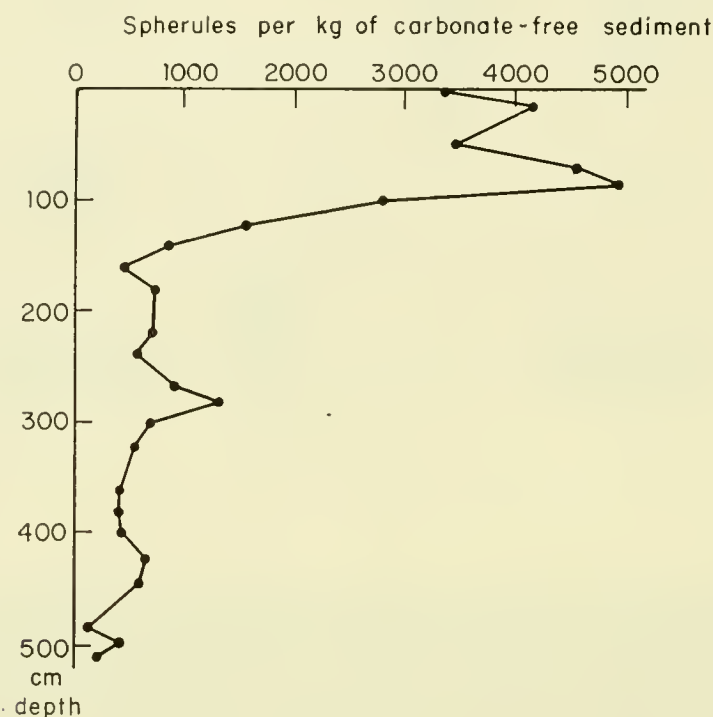


Fig. 11. Frequency of cosmic iron spherules as a function of depth in core 90, Swed. Deep-Sea Exped., from the West Pacific. (After Pettersson and Fredriksson, 1958.) Paleontological investigations by Bramlette and Riedel (quoted by Olausson, 1961) indicate an unconformity between Quaternary and Lower Miocene at about 56 cm depth.

have formed from molten drops in the atmosphere; these are probably original cosmic particles or fragments of chondritic meteorites breaking apart at entry into the atmosphere. Studies of the cosmic components of pelagic sediments were originally carried out by Murray and Renard (*op. cit.*). Recent extensive investigations by Hans Pettersson have focused on the variation in time of the accretion of cosmic material. The results of Pettersson and his co-workers (Pettersson and Fredriksson, 1958; Fredriksson, 1958; Castaing and Fredriksson, 1958; Laevastu and Mellis, 1955; Pettersson, 1959a; Fredriksson, 1959) indicate marked, world-wide changes in the rate of accretion of metallic spherules during Cenozoic times (Fig. 11). Hunter and Parkin (1960) have also

¹ The presence of this latter mineral is not evident from the work of Hunter and Parkin (1960) but has been established in similar chondrules by Murray and Renard (1891) and Bramlette (unpublished).

studied the metallic spherules and have investigated the nature of the silicate chondrules. The size distributions both of the nickel-iron spherules and of the olivine-pyroxene chondrules found on the deep ocean floor (Fig. 12) are in remarkable disagreement with the tentative size distribution of micrometeorites derived by impact counting from the satellites 1958 Alpha and 1959 Eta (LaGow and Alexander, *op. cit.*). An exponential increase in number of particles with decreasing size below 10–20 μ is indicated by the satellite observations, although cosmic particles from the ocean floor show a marked decrease in

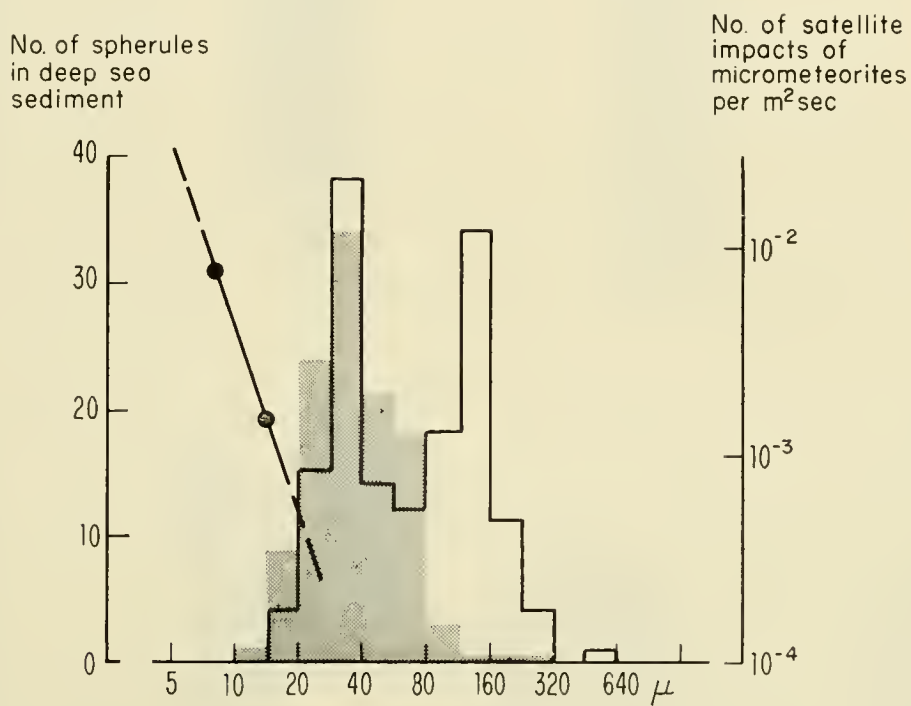


Fig. 12. Size distribution of cosmic spherules from pelagic sediments, and from micrometeorites in outer space. Shaded histogram = iron spherules; line-bounded histogram = silicate spherules from pelagic sediments (data from Hunter and Parkin, 1960); filled circles = impact observations from satellites 1958 Alpha and 1959 Eta (computed from data in LaGow and Alexander, 1960, assuming an average particle density of 3.0).

frequency below 25 μ and a comparatively large number of big (90 to 300 μ) silicate chondrules. This corroborates the idea that the cosmic material found on the ocean floor represents debris of meteorites, as suggested by Fredriksson (1959), rather than the original cosmic dust.

Large numbers of magnetic spherules of unknown origin and composition, ranging in size from less than a micron to several microns, are frequently observed in sediments (see, for example, Crozier, 1960). Analyses of such bodies indicate a heterogeneous origin. Many of the magnetic spherules previously assumed to have been derived from outer space have been shown by Fredriksson (1961) to consist of volcanic glass with inclusions of magnetite and metallic iron. Others, in size-range of 0.5–5 μ , appear to consist of goethite and might have been accreted by marine bacteria. It therefore appears necessary to define individual cosmic spherules not only on the basis of shape and magnetic properties but also on chemical composition. Considering the difficulties in

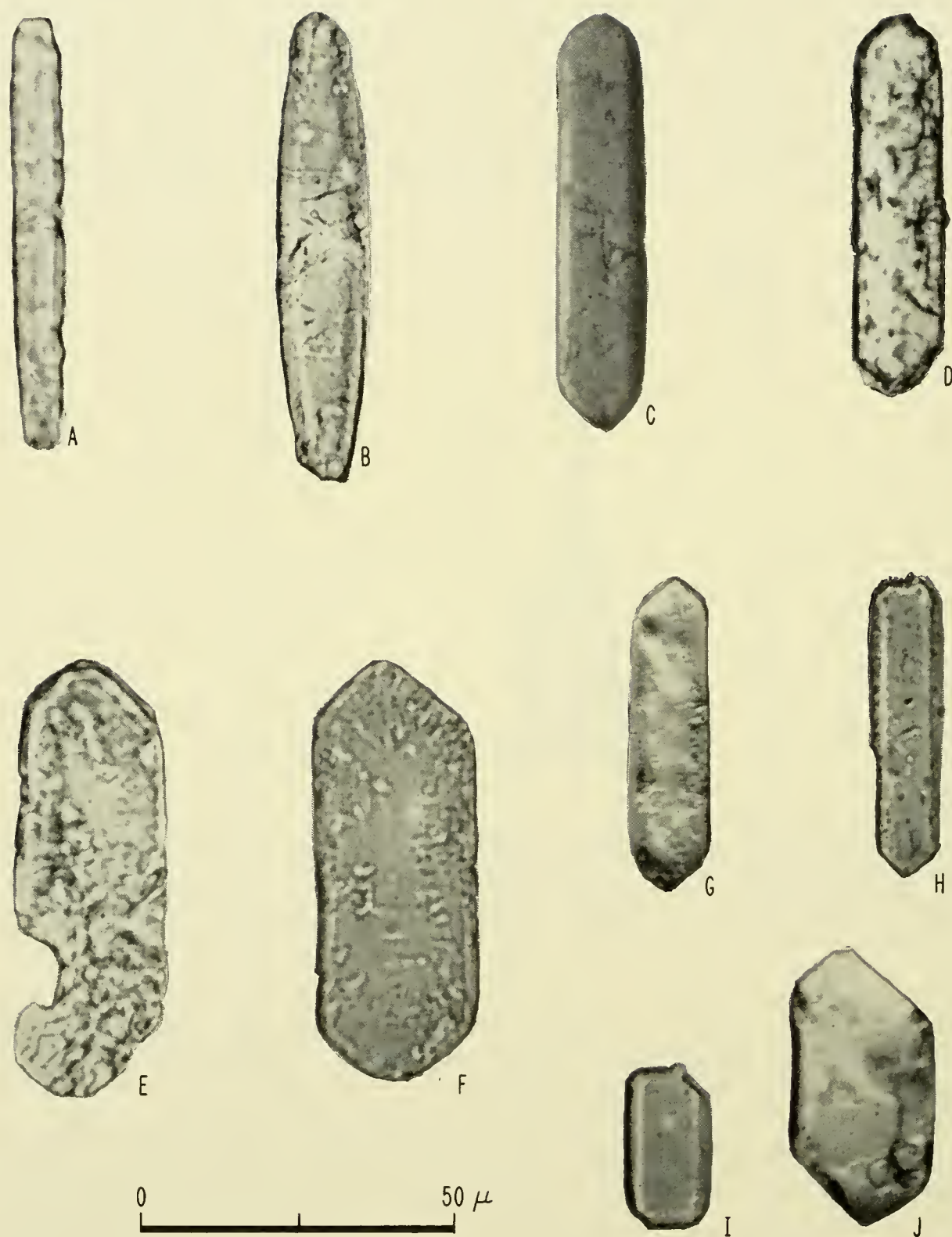


Fig. 13. Authigenic celestobarite from Pacific pelagic sediment showing frequent elongated prismatic habit and barrel-shaped growth form (B). Varying degree of corrosion by aqueous solution at separation is shown by A-H. I and J were protected against corrosion by use of excess sulfate ion at separation.

preservation, separation, and diagnosis of spherules in sediments, polar ice is a promising source for recovery and quantitative study of Pleistocene cosmic accretion (Thiel and Schmidt, 1961).

A material of geophysical significance found on the deep-ocean floor is maghemite (R. Mason, unpublished), which is a diagenetic alteration of magnetite (Hägg, 1935; B. Mason, 1943). The presence of maghemite increases the magnetic susceptibility of the solid. The martite reported by Mellis (1952, 1959) might possibly also be a pseudomorph of maghemite after magnetite.

B. Sulfates

The high concentration of sulfate ion in sea-water, occasionally increased in the interstitial water of the sediment by oxidation of proteinaceous matter, probably limits the solubility of strontium, barium, radium, and lead (Arrhenius, 1959). Radioactive solid solutions of celestite (SrSO_4) and anglesite (PbSO_4) in barite (BaSO_4) thus constitute geochemically important mineral species on the ocean floor (Arrhenius, Bramlette and Picciotto, 1957; Arrhenius, 1959) (Fig. 13). A sample consisting of a large number of celestobarite crystals, obtained from equatorial North Pacific sediments, showed the average amount of substitution to be 5.4 mole per cent celestite and 0.05 mole per cent anglesite.

Comparatively high concentrations of barium, strontium, and lead are found in some marine planktonic organisms, which also contain considerable quantities of other heavy-metal ions (Table III). This suggests that biological extraction from surface sea-water and subsequent sinking is an important mechanism in accreting these elements to the sediment. Among the organisms notable in this respect are some species of Foraminifera, pteropods and heteropods. The acantharid Radiolaria (Schewiakoff, 1926) are particularly efficient in extracting strontium; the celestite (SrSO_4) skeletons of these protozoans contain in addition 0.4 mole per cent of barite in solid solution. The skeletons consist of dart-like spines of radially arranged celestite microcrystals with Y oriented in the radial direction of the spine. At decomposition of the protoplast, the spines become detached and presumably settle at a high rate owing to their shape and high density. In contact with sea-water they are, however, rapidly corroded and dissolve entirely before burial in the sediment occurs.

Thus, marine organisms provide a conveyor mechanism for certain elements from the surface of the ocean to the deep water or the bottom, where the dissolved elements are released by dissolution. Phosphorus, silicon and nitrogen have been found in higher concentrations in intermediate and deep water than in surface water (ref. in Sverdrup *et al.*, 1946). Still higher gradients are found from the near-bottom water and the interstitial water of the sediment for silicon and phosphorus (Koczy, 1950, fig. 2.3; and Table VI of this chapter), for radium (Koczy, 1958), for barium (Chow and Goldberg, 1960), and for nitrate (3 to 15 times excess over bottom-water concentration in interstitial water in South Pacific sediments, Arrhenius and Rotschi, 1953, fig. 29). Part of the ions released into the bottom water or interstitial water are returned to the sediment

TABLE IIIa

Trace-Element Composition of Some Marine Planktonic Organisms. Concentrations in parts per million of ash. The blank consists of spectrally pure quartz treated identically as the samples. Spectrochemical analyses by A. Chodos and E. Godijn. (From Arrhenius, Bradshaw and Kharkar, unpublished.)

Sample no.	Description	Ba	Sr	Mg	Cu	Ag	Zn	Pb	Ti	V	Cr	Mn	Fe	Ni	B
16 256	Foraminifera (listed in Table IIIb)	700	400	1000	25	3	0	10	15	p. tr.	0	8	300	9	0
17 121	Spines of acantharid	5400	major	—	750	0	600	105	300	0	90	0	300	57	0
16 257	Radiolaria Pteropods and heteropods listed in Table IIIe														
16 257-1	Tissue remaining after short treatment with dilute HCl	60	0	—	140	0	660	0	180	0	100	0	—	0	960
16 257-2	Fraction removed by dilute HCl (mainly shells)	31	480	—	15	0	0	0	0	16	0	0	—	0	0
16 257-3	Blank	0	0	—	0	0	0	0	0	0	0	0	—	0	0

p. tr. = possible trace 0 = below sensitivity limit — = no determination

TABLE IIIb

Species Distribution in Composite Sample (16 256) of Planktonic Foraminifera Used for Analysis in Table IIIa. The sample was collected at Tethys Expedition Station 28, 26° 13.9'N, 141° 34.5'W, 9 Aug., 1960, and Station 29, 27° 15.5'N, 137° 58.0'W, 11 Aug., 1960. (Arrhenius, Bradshaw and Kharkar, unpublished.)

<i>Hastigerina pelagica</i> (d'Orbigny)	66.4%
<i>Globigerinoides conglobatus</i> (Brady)	19.5
<i>G. sacculifer</i> (Brady)	6.4
<i>Orbulina universa</i> (d'Orbigny)	3.0
<i>Globerigerinoides ruber</i> (d'Orbigny)	2.6
<i>Candeina nitida</i> (d'Orbigny)	1.5
<i>Globoquadrina conglomerata</i> (Schwager)	0.3
<i>Globorotalia tumida</i> (Brady)	0.2
<i>G. cultrata</i> (d'Orbigny)= <i>menardii</i> (d'Orbigny)	0.1
Total number of specimens	2077
Dry weight	37.5 mg

TABLE IIIc

Relative Abundance of Pteropods and Heteropods in Composite Sample (16 257) Used for Analysis in Table IIIa. The sample was separated from plankton collected at the same stations as Sample 16 256 (Table IIIb)

	Relative abundance
Pteropods	
<i>Styliola subula</i>	3
<i>Hyaloclylix striata</i>	1
<i>Creseis acicula</i>	2
<i>Creseis virgula conica</i>	1
<i>Limacina bulimoides</i>	2
<i>L. lesueuri</i>	3
<i>L. inflata</i>	1
<i>L. trochiformis</i>	1
Heteropods	
<i>Atlanta peroni</i>	2
<i>A. fusca</i>	1
<i>A. turriculata</i>	1
Shells, dissolved by adding dilute HCl drop-wise until effervescence stopped, weighed as CaCl ₂ , anhydr.	685 mg
Ash of soft tissue, oxidized in perchloric acid	10.8 mg

by crystallization of less soluble solids; barium, strontium, and lead separate into harmotome-type zeolites, manganese oxide minerals, possibly including psilomelane, and further crystalline solid solutions of celestite, barite, and anglesite in proportions mentioned above. At slight solution of the celestobarite in distilled water, the crystal faces develop a typical pitted appearance (Fig. 13, A-H). The lack of these etching features in the crystals as found in the sediment (Fig. 13, I-J) indicates that dissolution of celestobarite is not taking place on the ocean floor.

Besides the extensive cation substitution in the celestobarite crystals, replacement of SO_4 by BF_4 and possibly CrO_4 is indicated by the presence of 1000 ppm of boron and 1400 ppm of chromium in this mineral. These and the cation substitutions are of potential interest as indicators of the physico-chemical conditions in the sea-water and in the interstitial solution.

The exceedingly slow crystal growth on the ocean floor probably produces a close approach to thermodynamic equilibrium between the liquid and the solid solution. If in the relation

$$D = \frac{(B_c/A_c)}{(B_1/A_1)},$$

B_c and A_c denote the concentrations of the substituting species and the substituted main species respectively in the crystal, and B_1 and A_1 the corresponding concentrations in the liquid, the partition coefficient, D , indicates the enrichment (if > 1) or depletion of the substituting foreign ion in the crystal structure. If B_c and A_c are known from analysis of the actual crystals, and D from controlled experiments, the ionic ratio, B/A , in the bottom water or interstitial solution from which the crystals formed can be derived. For the cation substitution couple, $\text{Sr}^{2+}/\text{Ba}^{2+}$, the ionic ratio in the halmeic crystals is 0.057, and D has been determined to be 0.030 ± 0.004 (Gordon, Reimer and Burt, 1954). The solution in equilibrium with these crystals should consequently have an ionic ratio, $\text{Sr}^{2+}/\text{Ba}^{2+}$, of 1.9. If 114×10^{-3} mmole/l. (the average strontium concentration in sea-water) is accepted as a minimum concentration value in the interstitial solution of the sediment, then a minimum concentration of 60×10^{-3} mmole/l. of barium is needed to maintain the ratio indicated by the crystal composition. Such a barium concentration would be 136 times higher than that observed in deep water. A part of this apparent discrepancy might be due to lowering of the strontium concentration in the interstitial water by the zeolite and oxide species observed in co-existence with the barite; however, a considerably higher barium concentration in the interstitial water than in the deep water is suggested by these data. Chow and Goldberg (*op. cit.*) have interpreted the deep-water concentrations observed by them as close to saturation with the sedimentary barite. However, considerably higher saturation concentrations should be expected since both the cation and the anion substitution in the barite structure contribute to a markedly increased solubility of the crystalline solid solution above that of pure barite. In pure

water the solubility of celestite is 587 $\mu\text{mole/l.}$ at 25°C and 1 bar¹ as compared with 9.5 $\mu\text{mole/l.}$ for barite. Under the assumption of a linear increase in solubility with substitution, the observed 5.4 mole per cent of celestite in the barite structure would result in a solubility of 40.7 $\mu\text{mole/l.}$, or 4.3 times the solubility of barite. As is seen in Table IV, the other substitutions observed further increase the solubility of the crystal.

TABLE IV
Solubility and Substitution Relations

Solubility, $\mu\text{mole/l.}$ (25°C , 1 atm)	Substitution in pelagic celestobarite (mole per cent)
BaSO ₄ 9.5	94.3
SrSO ₄ 587	5.4
PbSO ₄ 140	0.046
BaCrO ₄ 13	0.12
Ba(BF ₄) ₂ no data	0.11

Gypsum has been observed in several instances in pelagic sediments with a high content of organic matter. Whether these crystals were formed on the ocean floor or during storage of the samples, as a result of sulfide oxidation, is not known.

C. Phosphates

The phosphate concentration in surface sea-water is limited by photosynthetic organisms. These settle toward the bottom or are consumed by higher members of the food chain, and a fraction of the phosphorus is ultimately used by vertebrates for building an apatite skeleton. A continuous transport of phosphorus from the surface layer of the ocean to the bottom is thus maintained. The solubility of the apatite series is not accurately known (Sillén, 1959, p. 566); but it is a well-established fact that skeletal apatite is slowly dissolving on the deep-ocean floor (Koczy, 1952; Arrhenius, 1959), and that no precipitation occurs there of the phosphate formed by hydrolysis of organic matter. It is thus obvious that the solubility of apatite at the temperature and hydrogen ion concentration of present deep-ocean water is higher than the phosphate concentration observed in bottom water and in interstitial water of deep-sea sediments (5.0 $\mu\text{mole/l.}$, Arrhenius and Rotschi, 1953; 5.5 mole/l., Bruejewicz and Zaytseva, 1958). Consequently, all the organic phosphorus and a large fraction of the skeletal apatite reaching the deep-ocean floor are returned to solution in the deep water and ultimately brought back to the upper layer of the ocean. The recycling of phosphate in the ocean due to temperature and pH control of the solubility leads to partial removal of phosphate from the deep-ocean floor and to permanent accumulation of skeletal apatite and of authigenic

¹ Owing to the presence of sulfate ion the solubility is somewhat lower in sea-water (approx. 500 $\mu\text{mole/l.}$ at 25°C and 1 bar) than in pure water (Müller and Puchelt, 1961).

phosphate minerals (mainly francolite, $\text{Ca}_5[\text{F}|\text{PO}_4\text{CO}_3]_3$) in shallow low-latitude areas where saturation is reached. Upwelling of phosphate-rich deep water produces exceptionally high concentrations of phosphate minerals in such areas (Kazakov, 1950). The ensuing increase in organic productivity in the euphotic zone leads to a high rate of accumulation of organic remains on the bottom, and a high rate of crystallization of phosphates is maintained by decomposition of the organic phosphorus compounds (McKelvey *et al.*, 1953). Bruejewicz and Zaytseva (1958) measured concentrations of dissolved phosphorus as high as 27 $\mu\text{mole/l}$. in Pacific sediments of this type.

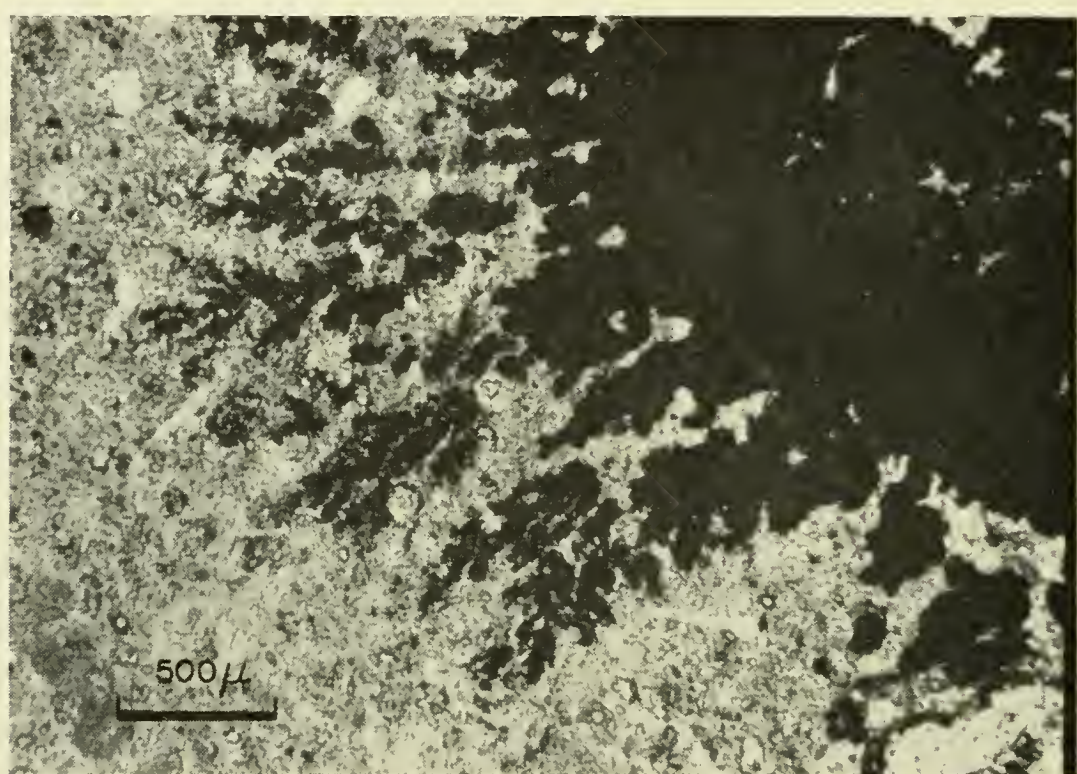


Fig. 14. Dendritic intergrowth of manganese oxide in marine phosphorite from oxidizing environment (Cape Johnson Guyot; $17^{\circ} 10' \text{N}$, $177^{\circ} 10' \text{W}$). Transmitted light.

The solubility relations of francolite are complicated by variable substitution of calcium with zirconium and rare earth ions, which drastically reduce the solubility; zirconium phosphate concentrations up to 2800 ppm Zr have been observed in marine inorganic apatite (Arrhenius and Korkisch, unpublished).

The phosphorite rock accumulating in areas of high organic productivity consists of a microcrystalline matrix of francolite with phosphatized tests of Foraminifera (originally consisting of calcite), skeletal apatite of marine vertebrates, thin flakes of opaline silica derived from diatom frustules, films and grains of glauconite, interspersed dark-colored organic matter and terrigenous minerals. Other widespread deposits of marine phosphorite occur, without association with exceptionally high organic productivity, in shallow areas of the tropical ocean, where calcareous deposits are exposed to relatively warm seawater, such as on seamounts and on drowned coral reefs; some of these are

now elevated above sea-level and commercially exploited. Complete pseudomorphous replacement of calcite and aragonite fossils is attained in some cases (Rex, in Hamilton, 1956, p. 35). In contrast to the phosphorite from areas of high productivity, intergrowth with manganese and ferric oxide minerals is common in this type of phosphorite (Fig. 14), but glauconite and organic



(a)



(b)

Fig. 15. Fish-bone debris: (a) Diaphane mounting medium, phase contrast. Fish-bone fragments labeled 6 and 48 are teeth. (b) Nuclear emulsion, showing tracks of alpha particles emitted from fish debris. [(b) from Picciotto and Arrhenius, unpublished.]

matter are absent. The oxidizing conditions of deposition are further indicated by the low uranium content of this type of marine francolite. Uranium probably prevails in the hexavalent state (ionic radius 0.80 Å) under the normal oxidizing conditions in sea-water, presumably as a carbonate complex (Starik and Kolyadin, 1957), and does not easily substitute for the 20% larger calcium ion in the francolite structure. However, where uranium is locally reduced to the tetravalent state, its increased ionic radius (0.97 Å) is close enough to that of calcium (0.99 Å) to substitute extensively in the crystal structure (Altschuler, Clarke and Young, 1958). Consequently, the concentrations of uranium in the seamount- and reef-type francolite, formed under oxidizing conditions, amount to only one twelfth to one hundredth of the concentrations found in francolite when it is deposited under reducing conditions in areas of high organic productivity (Arrhenius and Korkisch, 1959) (Table V).

TABLE V
Substitution of Uranium in Marine Authigenic (Halmeic) Apatite and in Microcrystalline Fish-Bone Debris

Those apatite deposits which crystallized under reducing conditions, indicated by the presence of organic compounds, glauconite and other ferrous minerals, are high in uranium, presumably substituting as U^{4+} . Conversely, those formed under oxidizing conditions, indicated by lack of organic matter and ferrous minerals and by the coexistence with manganese oxide minerals, have a low uranium content, probably due to the difference in size between Ca^{2+} and U^{6+} , and to the excess charge of the latter ion.

Similar relations appear to govern the sorption of uranium on microcrystalline bone apatite in oxidizing and reducing environments as shown in the lower part of the table.
(Data from Arrhenius and Korkisch, 1959.)

Sample no.	Mineral type	Environment	U, ppm	Description of sample
16 182	Halmeic francolite	Oxidizing	8.5	Pseudomorph after calcite (late Eocene Foraminifera). Guyot 19171, Central Pacific
16 176	„ „ „	Oxidizing	0.7	Pseudomorph after calcite (Foraminifera) Sylvania Seamount, Marshall Is.
16 175	„ „ „	Oxidizing	2.3	Microcrystalline, massive. Cape Johnson Seamount
16 174	„ „ „	Reducing	102	Microcrystalline, massive, with organic matter and glauconite. Coronado Bank
16 803	„ „ „	Reducing	68	Strongly phosphatized surface layer of bark from Pleistocene tree trunk, exposed at sediment surface off Tehuantepec (also described in Goldberg and Parker, 1960)

TABLE V—*continued*

Sample no.	Mineral type	Environment	U, ppm	Description of sample
16 195-8.2	Fish-bone apatite	Oxidizing	1.5	From low organic productivity area, 17–21°N in East Pacific; brown clay sediment with numerous manganese nodules
16 193-10 + + 16 194-6	„ „ „	Oxidizing but less than in 16 195-8.2	8.5	From siliceous-calcareous sediments below Equatorial Current system. Ferrous iron preserved in zeolites, 1–3 mmole NH_4^+ /l. of interstitial solution
16 181-1	„ „ „	Weakly reduc- ing	16.3	Modelo Formation, Calif. (Tertiary). Comparatively rapidly accumulating epicontinental sediment. Organic matter present at the level of 2–4% carbon in the sediment; ferrous iron preserved or generated, no sulfides

Goldberg and Parker (1960) have proposed that the low oxygen content of the bottom water in areas with a high rate of deposition of organic matter is a causal factor in the precipitation of francolite. The widespread occurrence of this mineral, deposited under oxidizing conditions as well as under reducing ones, would seem to point instead to a reaction which is insensitive to the redox state of the system.

The high concentrations of phosphorus, often attaining values of 1–2% P_2O_5 in slowly accumulating clay sediments and zeolitites on the deep-ocean floor, were previously attributed to precipitation of iron phosphate (Goldschmidt, 1954); it now seems quite evident that the phosphate prevails in the form of skeletal debris of fish (Arrhenius, Bramlette and Picciotto, 1957). Apatite is soluble at the deep-ocean floor, so that delicate structures such as scales and minute bone fragments are preserved only in the most recent parts of rapidly accumulating calcareous deep-sea sediments.

In deep-sea sediments, including manganese nodules, which accumulate slowly, only the most resistant structures with a large crystallite size, such as teeth of fish and carbones of whales, remain undissolved. The dissolution of skeletal apatite is counteracted by the incorporation into the crystal structure of large quantities of the rare earth elements thorium and zirconium, adsorbed from solution in sea-water. The ensuing highly insoluble phosphates eventually remain as microscopic crystals after the disappearance of the original skeletal debris in the most slowly accumulating types of deep-sea sediments, such as manganese nodules.

D. Carbonates

The abundant planktonic and benthic organisms which build skeletal structures of calcite or aragonite provide a mechanism for deposition of these minerals over the ocean floor. Quantitatively most important in this respect are Foraminifera, which are Protozoa with calcareous, arenaceous, or chitinous tests (Fig. 16), and coccolithophorids, which are unicellular algae with minute calcite platelets—coccoliths—that have been secreted from the cell

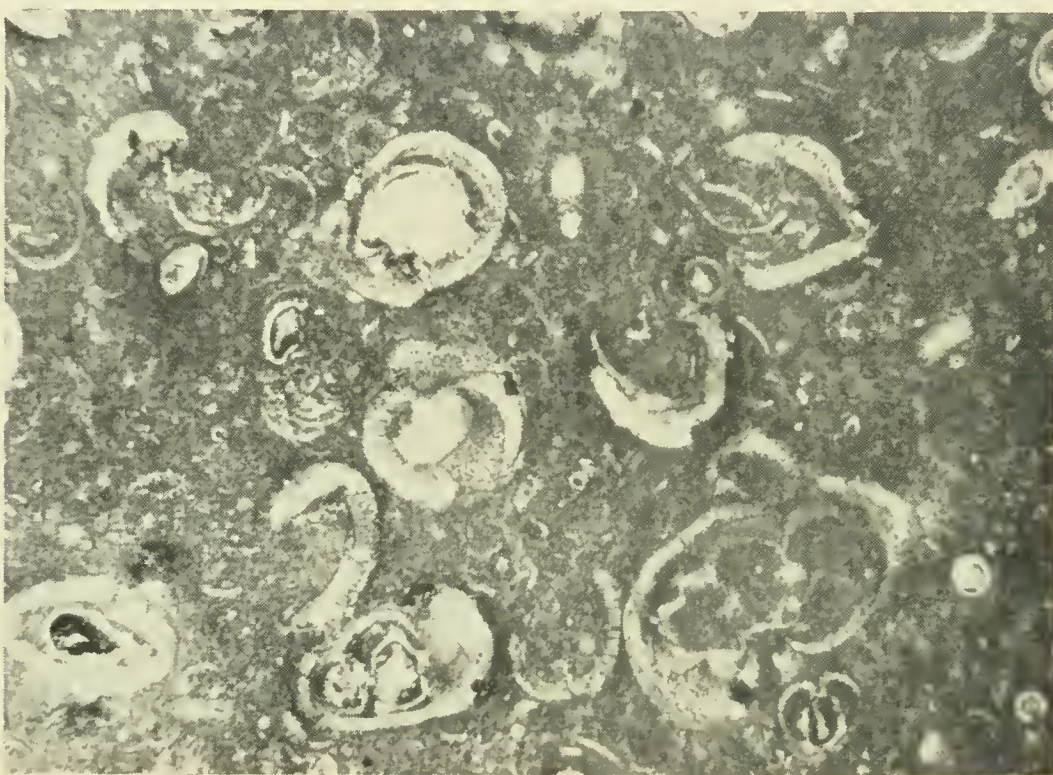
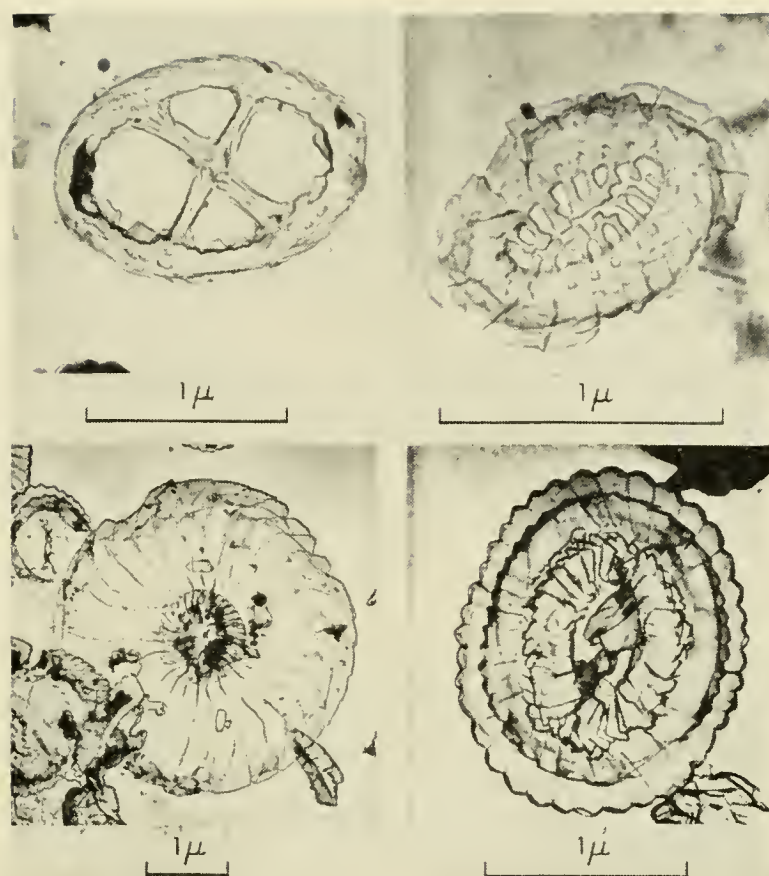
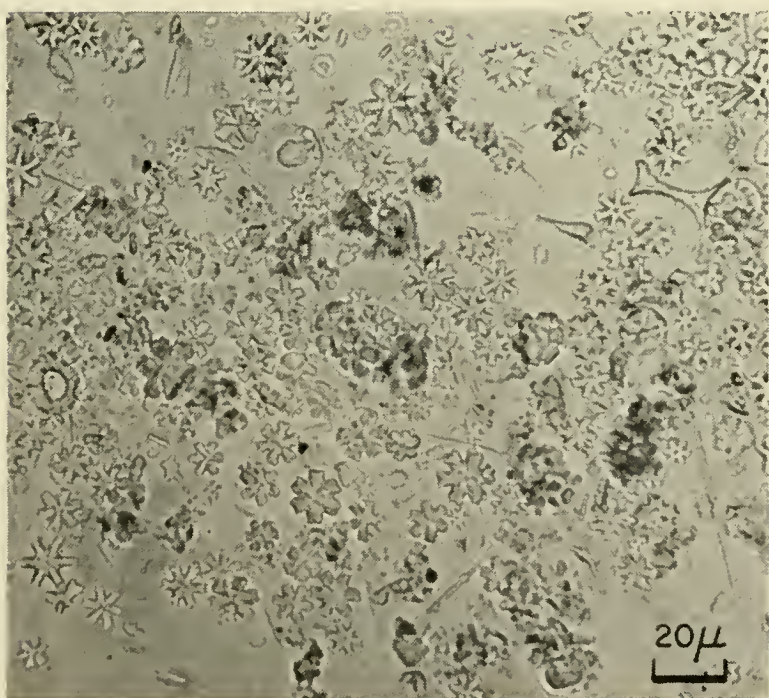


Fig. 16. Calcareous ooze with tests of Foraminifera. Thin section, polarized light.

wall (Fig. 17). Most Foraminifera contributing to the pelagic sediments are planktonic, and all of the planktonic species form calcite tests. Benthonic Foraminifera constitute less than 10% of the fossil assemblages in pelagic deep-sea sediments but are more abundant in shallow-water pelagic sediments such as coral reefs. The variation in species distribution as a function of ambient water temperature has successfully been used, initially by Schott and later by a number of workers (ref. in Phleger, 1960), to trace variations in the surface-water temperature of the ocean in the past. Recently, similar information has been obtained by mass spectrometric determination of the temperature-dependent ratio O^{18}/O^{16} in the carbonate of Foraminifera in deep-sea pelagic sediments (Emiliani *et al.*, see ref. in Emiliani, 1955 and 1956; Ericson and Wollin, 1956) and in the skeletal structures of a number of reef organisms (Lowenstam and Epstein, 1957). The usefulness of pelagic coccolithophorids for this purpose has recently been indicated by Craig (unpublished). A comprehensive survey of marine paleo-temperature work is presented by Emiliani and Flint elsewhere in this volume (Chapter 34).



(a)



(b)

Fig. 17. (a) Coccoliths (electron micrographs of carbon replicas) (from J. Markali, Oslo, unpublished); (b) Coccolith and *Discoaster* ooze (Aquitanian), Equatorial Pacific. (From Bramlette, 1961.)

Owing to relatively rapid and easily distinguished evolutionary changes of the coccolithophorids, it has been possible to use their fossil remains for indication of geological age by highly precise biostratigraphic correlations (Bramlette and Riedel, 1954). The mass of coccoliths in the carbonate fraction of deep-sea sediments sometimes exceeds that of foraminiferal tests; such coccolith oozes were particularly abundant in the Cretaceous and the Tertiary. Coccolith ooze also constitutes the glacial maximum productivity stage below the Pacific Equatorial Divergence (Fig. 36).

In sediments older than the Middle Mesozoic, identifying coccoliths is usually difficult, owing to gradual recrystallization of the calcite; in fact, many fine-grained limestones in older geological formations may be recrystallized coccolith oozes (Bramlette, 1958). Although the calcareous planktonic Foraminifera did not evolve until Mesozoic time, calcium from the continents might thus have been deposited as carbonate over the deep-ocean floor by planktonic organisms early in the history of the Earth.

Aragonite shells are secreted by some groups of planktonic organisms, of which pteropods are the quantitatively most important. Because of the relatively high rate of dissolution of aragonite in sea-water at low temperatures and high pressures, pteropod ooze is accumulating only in comparatively shallow areas.

Extensive substitution in the marine calcium-magnesium carbonate structures is essentially limited to strontium in aragonite. A concentration of other trace elements such as lead, copper, barium, strontium, titanium, and iron is to be found in the protoplasts of some species of Foraminifera (Table III) and in pteropods, whose organic shell structures interlayered with aragonite provide a possible site for heavy-metal ions concentrated from sea-water (Curl and Nicholls, unpublished). Thus, a number of trace elements can be related to calcareous fossils or their dissolution residue (Correns, 1937; Graf, 1960). Several of these organism groups might consequently play an important role in the vertical-transport mechanism mentioned in Section 2-B of this chapter.

Pelagic sediments, as defined in the present work, include shallow-water pelagic carbonate sediments which constitute bioherms of various types and particularly coral reefs. This group of sediments is described elsewhere in this volume (Chapter 22).

Calcite and aragonite are highly soluble, so the original distribution of these minerals over the ocean floor is extensively modified by post-depositional dissolution favored by low temperatures, high hydrostatic pressures, rapid removal of the solution, and high partial pressures of CO₂, generated by oxidation of organic matter at the sediment surface. The dissolution process in a given stratum is slowed as new sediment accumulates above it, producing a diffusion barrier of increasing thickness, separating the carbonate from the solvent. The ultimate rate of accumulation of carbonate at a given depth and circulation is consequently determined by the rate of deposition of carbonate minerals and by the total rate of accumulation of sediment. The regional distribution of calcium carbonate in ocean sediments illustrates the influence of these para-

meters. From the distribution of carbonate concentrations with depth in areas with different productivities, the combined influence of hydrostatic pressure and temperature and likewise the influence of productivity are quite evident (Figs. 18 and 19). Further, at a higher total rate of deposition, providing rapid pro-

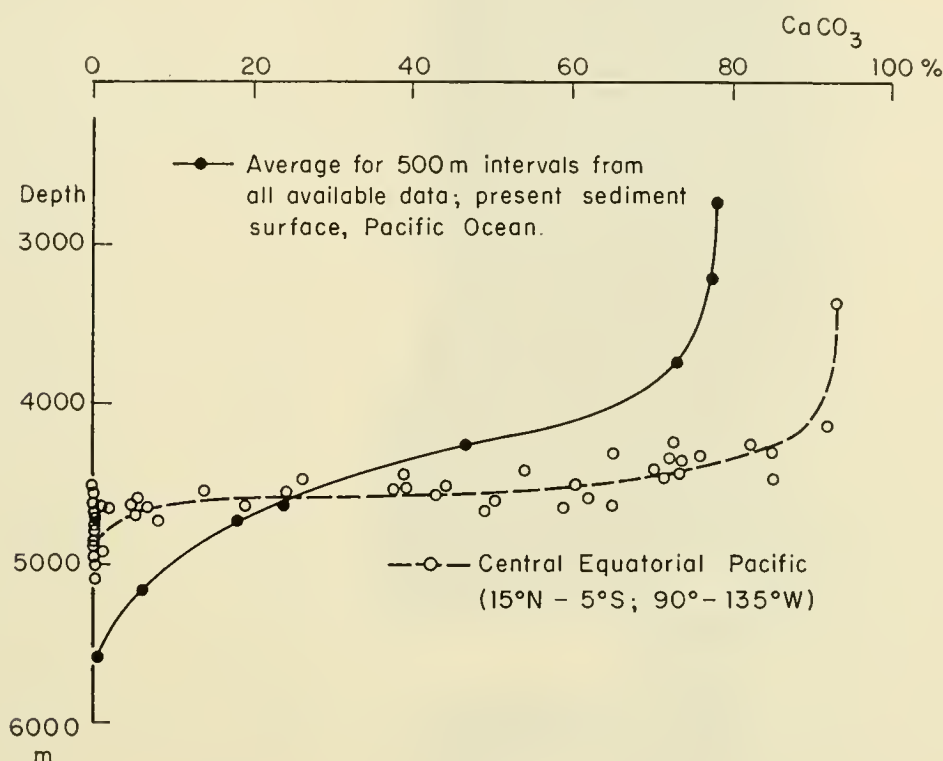


Fig. 18. Concentration of calcium carbonate at the present sediment surface as a function of depth in the Pacific Ocean. The average curve shows a pronounced effect of depth on the rate of solution of carbonate. In the central equatorial Pacific, characterized by a wide regional variability in biological productivity, this latter factor dominates the carbonate distribution. (From Bramlette, 1961.)

tection of the carbonate, the disappearance of the carbonate occurs at greater water depths (Fig. 20). Finally, the influence of the removal of the dissolved calcium ion is demonstrated by the carbonate distribution in the South Atlantic basins; at equal depths the dissolution of calcite is far more extensive in the Brazil Basin, which is flushed by Antarctic deep water, than in the neighboring Congo Basin, which has a slower renewal of the bottom water (Wattenberg, 1933, 1937; Correns, 1939).

At shallow and intermediate depths where the rate of dissolution of calcium carbonate is low, calcite and aragonite are sometimes dolomitized. Outcrops of dolomitized limestone, such as on the Nasca Ridge in the South Pacific (Bramlette, unpublished), are coated with manganese-iron oxide minerals, indicating that the dolomitization was active in the past, and that it has since been replaced by oxide deposition. A similar sequence is observed in many oceanic limestones and phosphorite deposits, which also display a coating of manganese-iron oxide minerals (Fig. 14). Growth of sparse euhedral dolomite crystals in

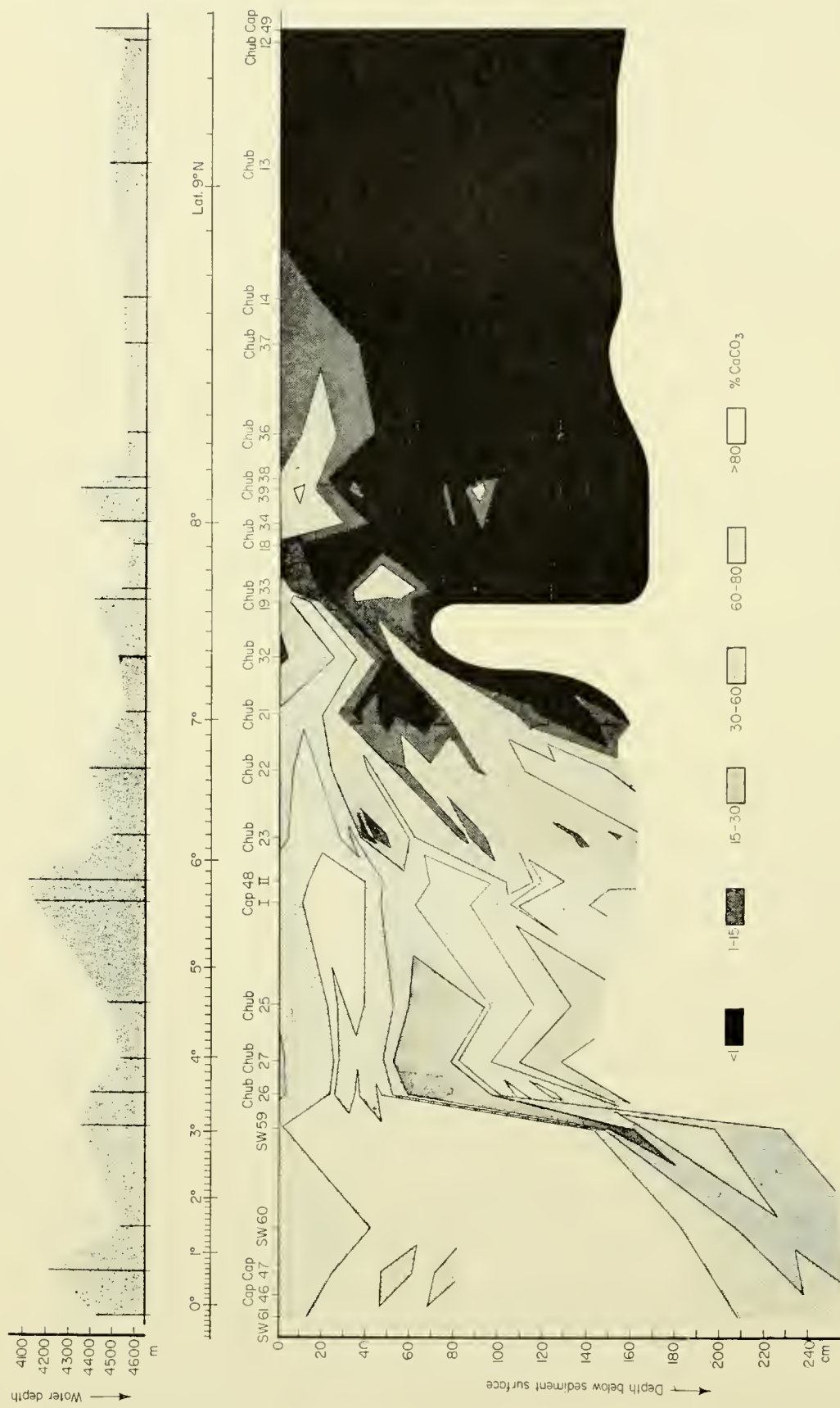


Fig. 19. Distribution of calcium carbonate in a meridional section through the central equatorial Pacific, showing the variation of carbonate content with time (depth of sediment) and with latitude (productivity; falling off from equator). For a general discussion of these features, see Section 3 of this chapter, and Fig. 36, which is based on the section shown above, and its deeper parts. In addition to the productivity effects in time and space, the superimposed effect of water depth (hydrostatic pressure) is manifest as deviations from the regular change with latitude, correlating with the deviations from average depth shown in the upper graph. Diagenetic solution is presumably responsible for the general recession toward lower latitude of the carbonate compensation surface ($\text{CaCO}_3 = 0$) with increasing depth in the sediment. The rate of such solution is low but has a large relative effect on the low original carbonate content of the sediment near the compensation surface.

Recent deep-sea sediments have been observed in several instances, both in the Pacific (Bramlette, unpublished) and in the Atlantic (Correns, 1937; Radczewski, 1937). Extensive dolomitization is observed to occur at the interface of basaltic intrusions, such as the one encountered in the experimental Mohole off Guadalupe Island.

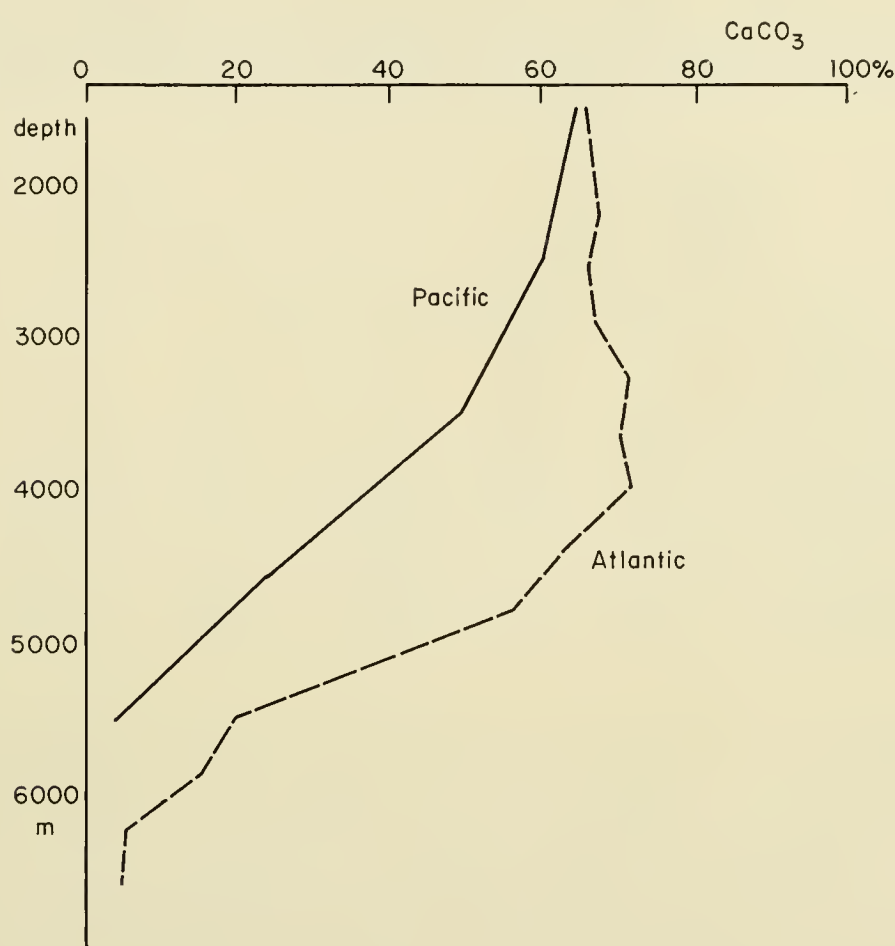


Fig. 20. Average carbonate content as a function of water depth in the Atlantic and Pacific, demonstrating the effect of total rate of deposition on the rate of solution of calcium carbonate at the ocean floor. Under similar depth conditions the ultimate carbonate content of the sediment is, on the average, higher in the Atlantic than in the Pacific. This is due to more rapid burial of the sediment in the Atlantic Ocean, which, per surface area, receives considerably more solid and dissolved material from the continents than does the Pacific. (From Revelle, 1944.)

Much detrital carbonate appears to be carried by wind into the pelagic environment. Calcite and dolomite are often the dominant components of eolian dust, which occasionally also contains small amounts of breunnerite (Radczewski, 1937). In Mediterranean sediments, calcite is the dominant eolian material (Norin, 1958). In deep pelagic sediments most of the fine-grained eolian calcite is dissolved, but in areas with a heavy eolian fallout and a high preservation of accumulating carbonates, eolian calcite and dolomite might be quantitatively important.

E. Silicates

Skeletal structures of opaline silica are secreted by a number of marine organisms, including the planktonic diatoms, radiolarians and silicoflagellates, and some benthic sponges. Much of this opal is dissolved or peptized soon after the death of the organisms; however, the remaining fraction of relatively robust skeletons often forms a significant portion of the sediment, especially below areas of high productivity such as the Subarctic Convergence, the Equatorial Divergence, and the divergences along the west coasts of the

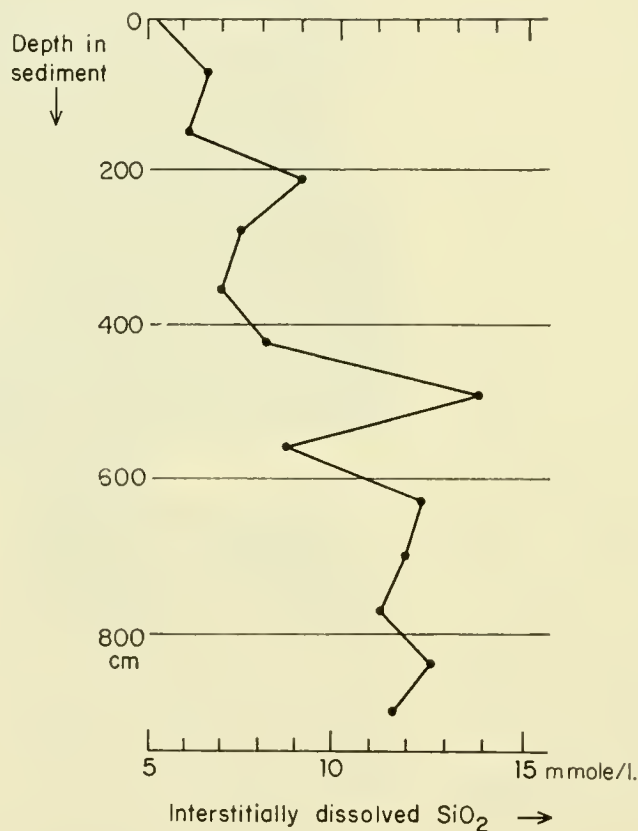


Fig. 21. Monosilicate in interstitial solution at various depths of the core Capricorn 38 BP, South Pacific. The interstitial solution was separated from the sediment by adding a known mass of fresh sediment (with separately determined water content) to a measured volume of filtered sea-water with a low and known silica content. After dispersion, the suspension was centrifuged, and an aliquot of the supernatant liquid was passed through a membrane filter and analyzed colorimetrically. (From Arrhenius and Rotschi, 1953.)

continents (cf. Fig. 1). The instability of silica in the interstitial water of the sediment causes continuous dissolution of the siliceous fossils after deposition; the silicoflagellates disappear first, followed by diatoms, then radiolarians, and finally even the robust sponge spicules. Part of the dissolved silica reacts to form authigenic aluminosilicates observed as overgrowths in partly dissolved siliceous skeletons (see below). In some cases reprecipitation of the silica as opal takes place, resulting in thin flakes of this mineral along the bedding planes in phosphorite, or in laminae of chert, observed to occur at depth in pelagic

sediments in a few instances. Another part of the dissolved silica is returned to the bottom water by diffusion. Thus, a marked vertical gradient is maintained in the concentration of silica in the interstitial solution of the sediment, and at the water interface (Table VI and Fig. 21).

TABLE VI

Concentration of Dissolved Monosilicate in the Water immediately above the Sediment Surface and in the Interstitial Solution of the Sediment in the South Pacific. (Arrhenius and Rotschi, 1953.)

Station	Position		Depth, m	SiO ₂ , μ nole/l.		Sediment type
	Lat S°	Long W°		Bottom water	Interstitial water	
Cap 17 B	19 56	172 40	5730	122	103	Sandy volcanic mud
24 B	19 29	173 44	2780	124	7900	Siliceous volcanic mud
30 B	17 28	160 59	4710	116	12000	Dark brown zeolitite
33 B	12 46	143 33	4380	129	13130	" " "
34 B	11 20	142 26	4500	132	9400	Calcareous brown clay
40 B	14 47	112 08	3020	132	—	Foraminiferal ooze
41 B	13 33	113 21	2940	—	12.4	" "
42 B	07 19	118 40	4230	—	1110	Calcareous brown clay
44 B	03 42	121 03	4170	141	—	Foraminiferal ooze

Wind-transported diatom frustules have been observed in quantity in eolian dust derived from arid areas with exposed diatomaceous deposits (Hustedt, 1921; Radczewski, 1937). Such transport appears to be the most probable explanation of the observation by Kolbe (1955) of freshwater diatoms in equatorial Atlantic sediments. The same author has reported the presence in these sediments of silicified grass cells, presumably suspended in the atmosphere by fires, an explanation which is further indicated by the similar distribution of charcoal fragments (Radczewski, *op. cit.*).

Quartz was recognized as a significant component in deep-sea sediments by Murray and Renard (1884), who drew attention to the importance of wind transport of this mineral. Radczewski (1937, 1939) investigated quantitatively the distribution of eolian dust and found that eolian quartz in pelagic sediments of the equatorial Atlantic frequently exceeded 30% of the total sediment. He further established the regional variations in concentration of eolian quartz and demonstrated a decrease in median size and concentration of the eolian component with increasing distance from the continent. Furthermore, Radczewski found windborne quartz in sediments of glacial and interglacial age as well as in the Recent. Subrounded and pitted quartz has been further reported by Norin (1958) as, together with calcite, the quantitatively most important non-volcanic mineral in the eolian component of Mediterranean sediments.

Revelle (1944) observed notable amounts of silt-size quartz in Pacific pelagic

sediments. The present author found a narrow size frequency distribution of quartz centred at $3-10 \mu$ in north equatorial Pacific clay sediments, and suggested eolian transport as an explanation. Rex and Goldberg (1958), in subsequent extensive studies of Pacific sediments, demonstrated a regional regularity in the quartz distribution (Fig. 22), which they interpreted as an

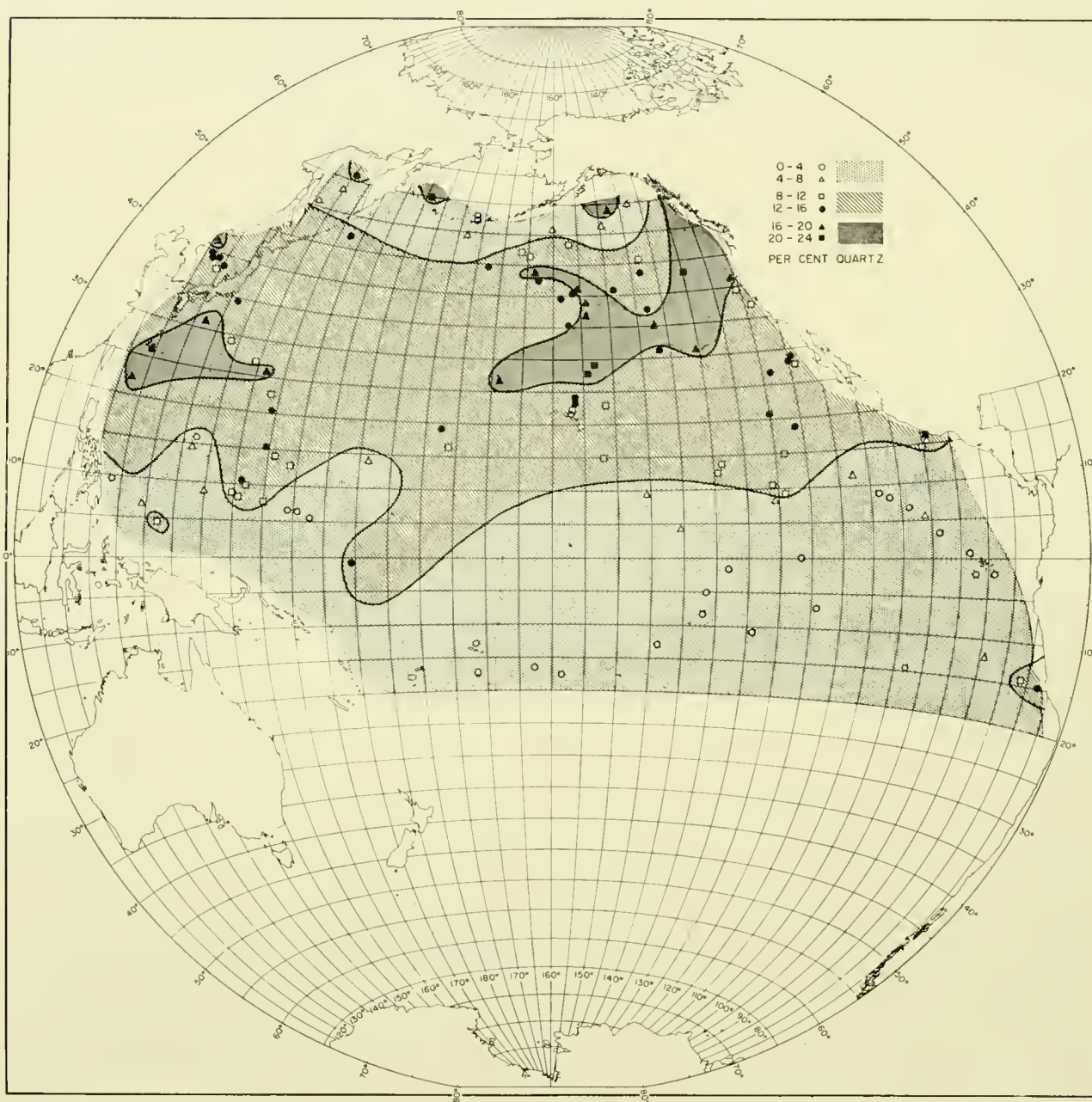


Fig. 22. Areal distribution of quartz in the Pacific. (After Rex and Goldberg, 1958.)

indication of fallout of dust from the high altitude jet streams. The importance of tropospheric transport is indicated by the numerous observations of extensive dust-falls at sea in the equatorial Atlantic (Radezewski, *op. cit.*; Seefried, 1913) and Indian Oceans, and in the South Pacific (Marshall and Kidson, 1929), and further by the correlation between the wind pattern from arid areas and the occurrence of dry atmospheric haze at sea (Fig. 23). Rex and Goldberg (*op. cit.*)

report low concentrations of quartz in the Tertiary pelagic sediments of the North Pacific, as compared to the unconformably overlying Pleistocene, indicating a smaller arid source area or weaker transporting wind currents during Tertiary time. Another indication of low intensity of the Tertiary circulation is the low organic productivity in the Equatorial Divergence during the

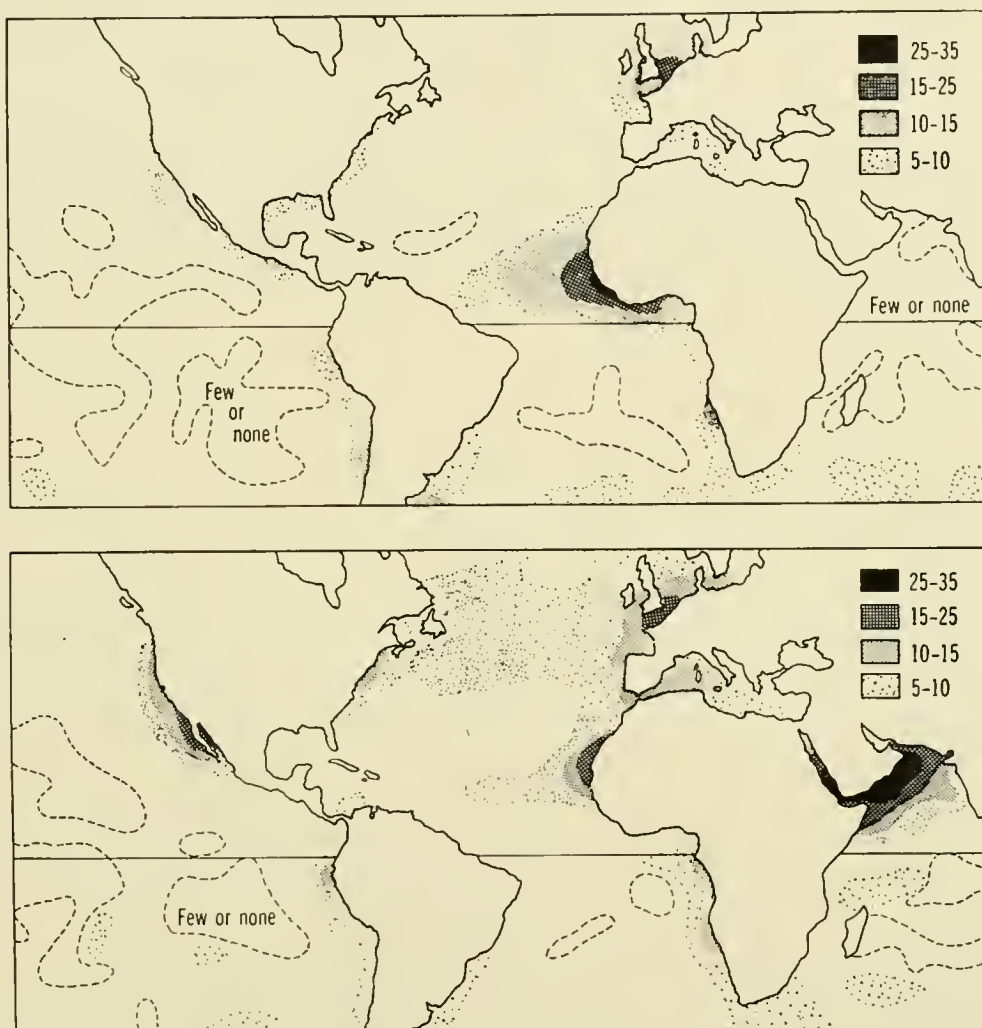


Fig. 23. Tropospheric transport of dust, as indicated by average frequency of haze (dry aerosol) during the northern winter (upper map) and summer (lower map). Frequencies are given in per cent of total number of observations. (From Arrhenius, 1959.)

Pliocene, followed by conditions suggesting a sequence of epochs with markedly increased intensities of zonal winds during the Pleistocene (Fig. 24).

Eolian dust contains little material in the size range below one or a few microns (Fig. 25), though pelagic sediments often display a secondary maximum in this range. Most of this fine-grained pelagic quartz was probably transported together with the aluminosilicate suspensoid in sea-water from the continents to the areas of deposition.

Mixed assemblages of mainly plagioclase feldspar with a grain-size distribution similar to that of quartz are ubiquitous in pelagic sediments. The optical properties indicate that the dominant species range between labradorite and

oligoclase in most Pacific sediments; commonly several species are present together. Large grains of orthoclase, microcline and sanidine, indicating occurrences of acid igneous rocks, are not uncommon within the predominantly basaltic province of the Pacific basin (Revelle, 1944, pp. 10, 18-39). A detailed

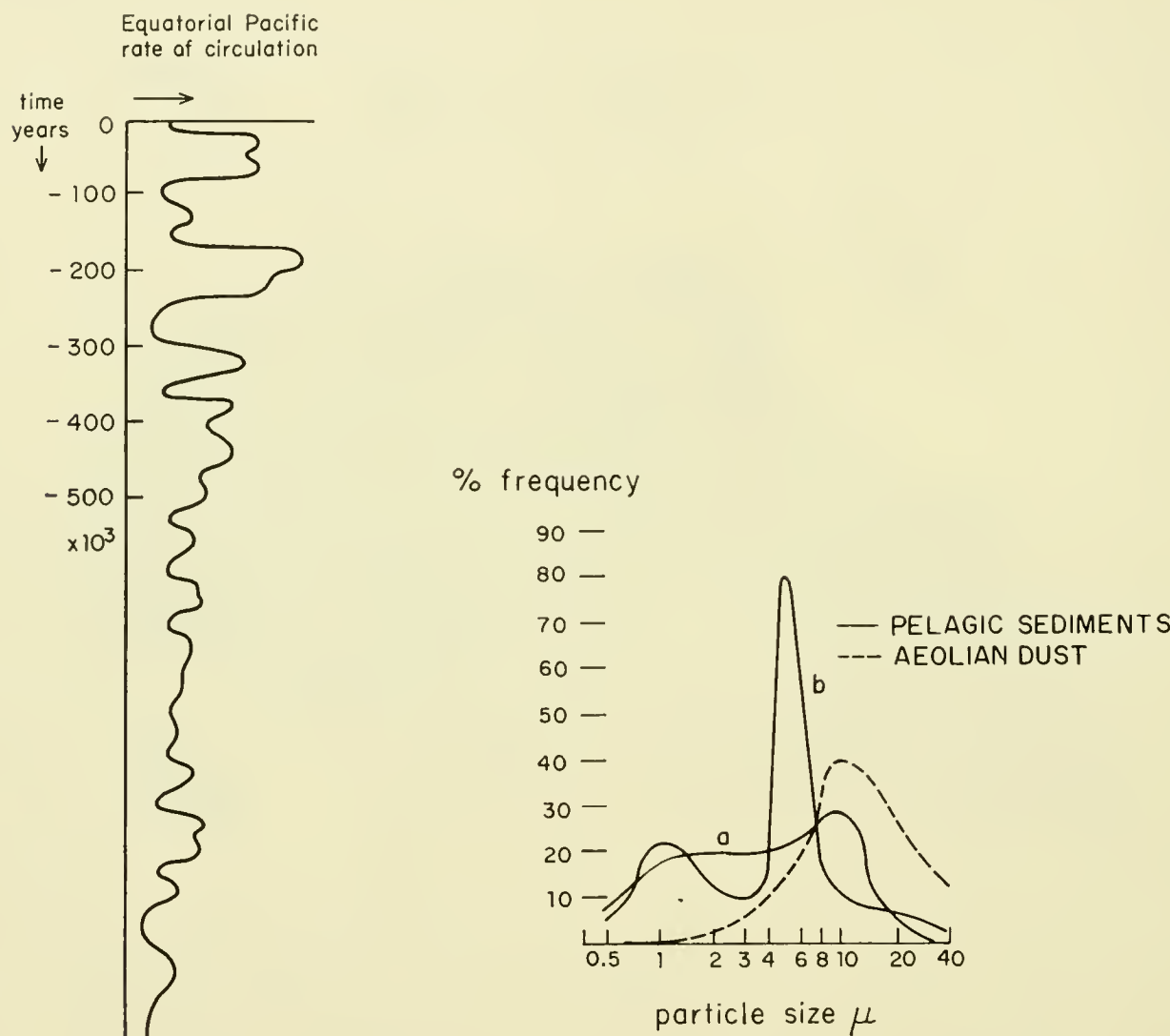


Fig. 24. Relative trade-wind intensity as a function of geological time. The relative intensity is estimated from the ensuing productivity changes at the Equatorial Divergence. (From Arrhenius, 1952.)

Fig. 25. Particle-size distribution in pelagic sediments from the North Pacific and in eolian dust from Illinois. (Data from Rex, 1958; Udden, 1914.)

investigation by Peterson and Goldberg (1962) shows that such feldspar species prevail over a large part of the East Pacific Rise. For the Atlantic, Radczewski (1937) and Leinz (1937) showed that acidic rocks must have been the main source of feldspar in the Cape Verde and the Guinea Basins, inasmuch as the

majority of grains had a composition $An < 30$. As is true of quartz, most of the fine-grained feldspar is probably wind-transported from continental clastics.

Authigenic orthoclase has been observed in a few instances; Mellis (1952, 1959) described a sample from the west Atlantic in which orthoclase had replaced the original plagioclase in altered andesite boulders. This sample indicates highly alkaline conditions during crystallization, as it is known from controlled synthesis experiments that orthoclase grows only above a pH of about 9 at low temperatures; directly below this limit, zeolites form the stable phases.

Rex (1958) attempted to establish the regional variability in the total amount of feldspar in reference to the known amount of quartz in the Pacific. The great variability of X-ray diffraction from given crystallographic planes in the feldspar series, as well as interference from other minerals in the range of inter-

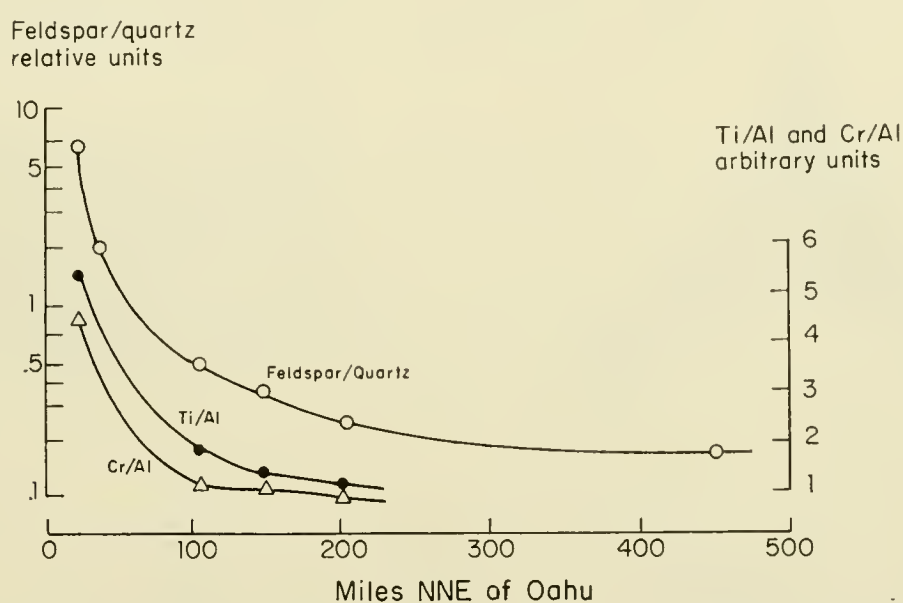


Fig. 26. Relative ratio feldspar/quartz in the North Pacific off Hawaii, showing the rapidly vanishing influence of the basaltic province. This is also reflected by the decrease in the relative concentration of titanium and chromium, mainly occurring in pyroxene crystallites. (From Rex, 1958.)

planar spacings used, limits the interpretation of these data. Nevertheless, some general relationships appear well established, such as an increase in the relative amount of feldspar around the Hawaiian Islands (Fig. 26) indicating the contribution from the basaltic province.

Olivine is unstable on the deep-ocean floor and hence is not observed in quantities in pelagic sediments. However, in association with cosmic nickel-iron spherules, olivine and pyroxene chondrules have been observed which strongly resemble those in chondritic meteorites, and are probably of extra-terrestrial origin (see further page 674 and Fig. 10b).

Pyroxene minerals are ubiquitous and are useful indicators of the origin of pyroclastics. The absence of hypersthene-enstatite among the frequently occurring pyroxene grains in South Pacific sediments indicates an origin within the

province of oceanic basalts, rather than transport from the circum-Pacific andesite regions. Mellis (1959) has found examples of uralitization of pyroxene.

The conditions determining the rate of decomposition and devitrification of volcanic glass in marine sediments are still obscure. While some minute glass shards in Mesozoic sediments are unaltered, some Quaternary deposits of ash and pumice have been entirely altered to montmorillonoid minerals or to phillipsite. The occurrence of unaltered glass in calcareous deposits indicates that a high calcium ion concentration might preserve the glass. Layers and laminae of volcanic glass are potentially useful as stratigraphic markers because of the wide dispersal and the short duration of the supply of volcanic ash. Successful attempts to correlate strata over large distances in marine sediments have been made by Bramlette and Bradley (1942), Mellis (1954) and Nayudu (1962a). A correlation has also been suggested between ash layers observed (Worzel, 1959) off the Middle American coast in the Pacific and in the Gulf of Mexico (Ewing *et al.*, 1959). Further observations of these deposits suggest, however, that they are due to eruptions from different centers and probably at different times.

Kaolinite, which commonly occurs as a weathering product of basaltic glass under acid weathering conditions (Sigvaldason, 1959), has not been found in marine decomposition products of pyroclastics. This agrees with the experimental observations of the influence of hydrogen ion concentration on the stability of low temperature silicates, referred to below.

Palagonitization of basaltic glass is frequently observed on the ocean floor; Correns (1939) and Nayudu (1962) indicate that this alteration takes place mainly at the interaction between hot lava and sea-water or interstitial water, rather than during the continued exposure after cooling.

The zeolite phillipsite was early recognized as quantitatively important in slowly accumulating pelagic sediments (Murray and Renard, 1884). Recently, it has been found that other members of the phillipsite-harmotome series are widespread, although less conspicuous because of their microcrystalline habit, the low intensity of their first order diffraction and their diffractive interference with feldspar. Zeolite concentrations higher than 50% are not infrequent, and zeolite consequently is a common pelagic sediment type. Controlled synthesis of the mineral indicates phillipsite and harmotome to be stable from a lower pH limit between 7 and 8 to an upper between 9 and 10 in a potassium-hydrogen cation system. Above this limit feldspar is stable at low temperatures, and directly below the limit 1M mica forms from solution. These relations might be useful in estimating the hydrogen ion concentration in ancient marine environments.

It is not entirely clear how much of the silicon and aluminum of the zeolite framework, and the interstitial cations, is directly inherited from the igneous silicates and glass decomposing on the ocean floor, and what proportion is derived from ions which have long been in solution and circulation in the ocean. The amount of aluminum passing through the ocean in a dissolved state is of the same order of magnitude as the rate of accumulation of zeolites (Sackett and

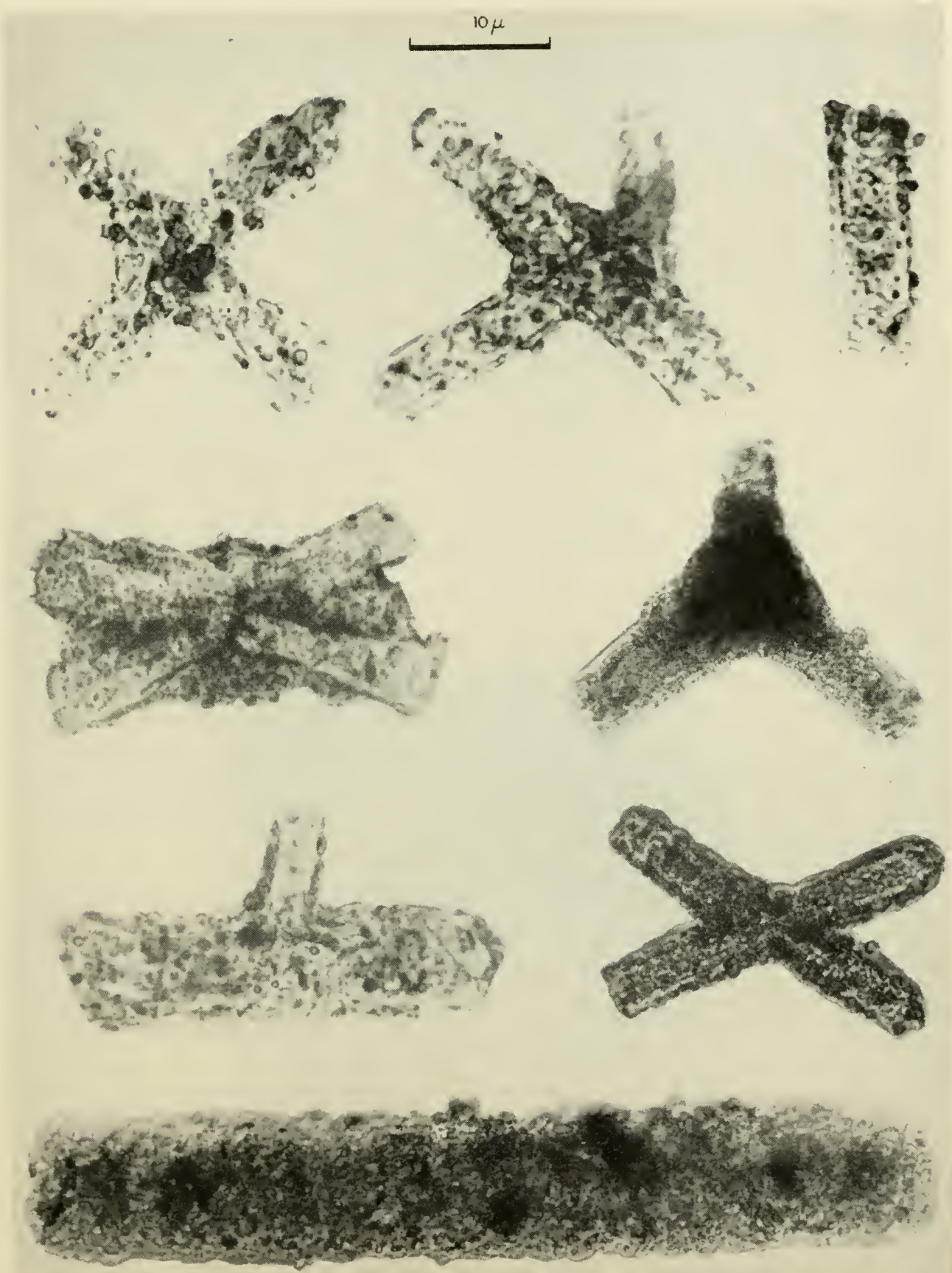


Fig. 27. Twinned zeolites of the phillipsite (K^+ ; Na^+ ; Ca^{2+})–harmotome (Ba^{2+}) series. The crystals typically display extensive intergrowth with other phases, primarily nontronite, which often form as much as one half the volume.

Arrhenius, 1962). The synthesis experiments mentioned above also indicate that precipitation of aluminum species from solution in sea-water would form zeolites rather than phyllosilicates. Finally, microcrystalline zeolite is found within dissolving skeletons of siliceous organisms in sediments without significant quantities of igneous silicates. This suggests that the high concentrations of dissolved silica from biotic sources at the sediment-water interface (cf. Table VI) induce the formation of the zeolites in these cases. On the other hand, phillipsite is frequently observed in intimate physical association with pyroclastics or their remnants on the deep-ocean floor, suggesting that the solution from which the zeolite crystallized is derived directly from the pyroclastic aluminosilicates (Murray and Renard, *op. cit.*).

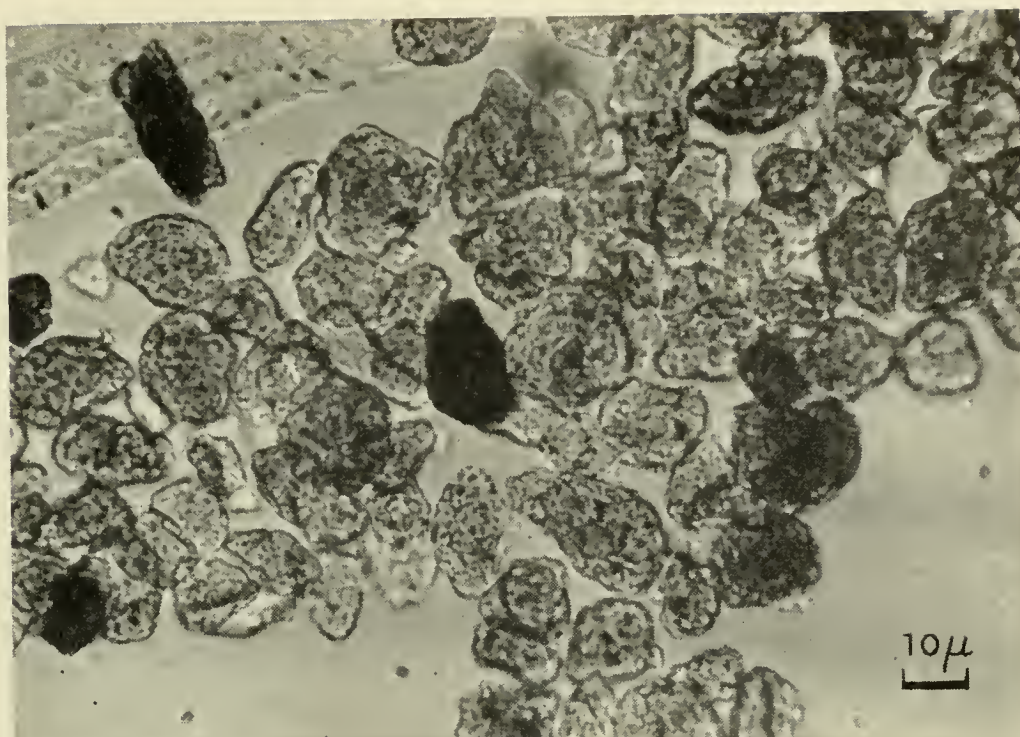
A third mode of formation of zeolites, known to operate on the deep-ocean floor, is the interaction between sea-water or interstitial water and hot basaltic lava during its intrusion. This phenomenon, together with extensive palagonitization of the glass and serpentinization of olivine, is beautifully illustrated in the basalt found at the bottom of the experimental Mohole drilled at Guadalupe Island in 1961.

Phyllosilicates frequently form a major part of the non-biotic fraction in pelagic sediments. Some are clearly terrigenous, with kaolinite the major representative. In solutions containing alkali or alkaline earth ions, kaolinite is a stable phase at only a relatively high concentration of hydrogen ion; it is thus precluded as a mineral forming in the ocean. Oinuma *et al.* (1959; see also Kobayashi *et al.*, 1960) have demonstrated higher concentrations of this mineral on the continental shelf than in the pelagic areas of the Western Pacific. Further, the investigations by Correns (1937) and Yeroshchev-Shak (1961a) indicate considerably higher kaolinite content in Atlantic sediments than in the Pacific. This agrees with the greater influx of terrigenous material in the Atlantic, indicated independently by deposition rates and by the chemical composition of the sediment (Goldberg and Arrhenius, 1958).

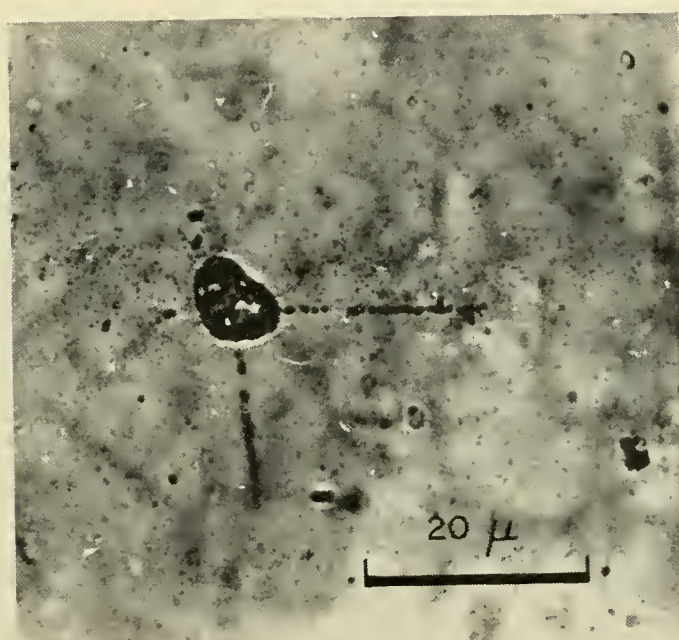
Other phyllosilicate species are obviously halmeic, while a third group, comprising much of the poorly crystallized material with a grain size less than a few microns, is of uncertain origin. Highly ordered polymorphs like biotite and chlorite prevail in relatively large grain sizes (3–30 μ) in areas receiving considerable terrigenous material from metamorphic rocks. However, in the finer fraction of these sediments the crystallinity decreases, and disordered 1*M* mica species¹ dominate. Some of these may have come directly from the continents; their coexistence with coarser, ordered polymorphs seems to indicate that the disordered mica species are partly diagenetic alteration products. Rimšaite (1957) has reported progressive alteration of different mica species.

On the basis of the high boron content and the bonding of the boron in the grain-size fraction containing the 1*Md* micas, Arrhenius (1954 and 1954a) suggested that these micas have crystallized from solution in the ocean with boron

¹ The term illite has been used as a group name for these minerals, together with mixed layer structures (Grim, Dietz and Bradley, 1949). Yoder (1957) has pointed out the need for a modified terminology.



(a)



(b)

Fig. 28. (a) Aggregates of microcrystalline harmotome and nontronite. The aggregates contain Ba^{2+} and Fe^{2+} as principal cations, and often considerable amounts of thorium (in one instance 2200 ppm). The density varies owing to substitution of lighter cations for barium; the highest density measured is 3.2. The aggregates have a high magnetic susceptibility. The microcrystallites rarely exceed a few microns in length. (b) Radio-autograph of harmotome-nontronite aggregate showing emerging alpha particle tracks. [(b) from Picciotto and Arrhenius, unpublished.]



Fig. 29. Chlorite. North Pacific abyssal plain. Polarized light; canada balsam.

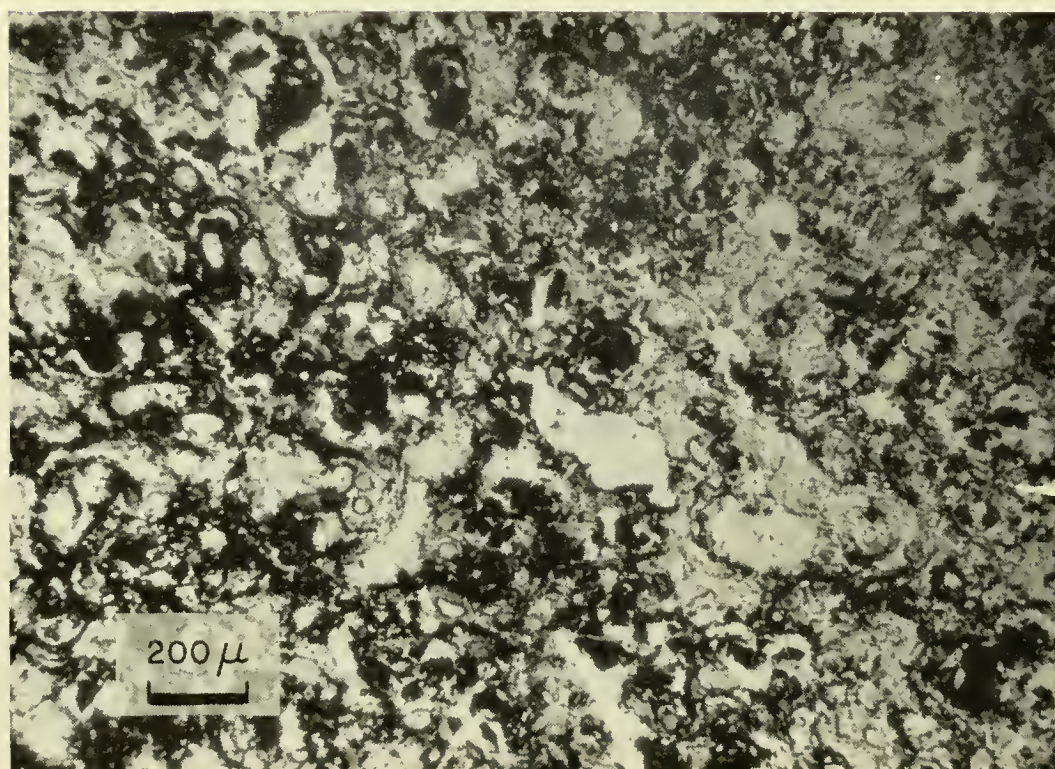


Fig. 30. Nontronite (grey) intergrown with manganese oxide minerals (black) in nodule, (white = voids). Noil Tobe, Timor (Danau Formation).

in coordination with oxygen or fluorine substituting in the tetrahedral silicate sheets. However, Harder (1959) has recently demonstrated that borate ion is readily and irreversibly fixed from solution by natural $1M$ mica. Further, measurements of the rate of passage of dissolved aluminum through the ocean (Sackett and Arrhenius, *op. cit.*) show that only a small fraction of the total aluminosilicate deposition can be accounted for in this way (cf. Sillén, 1961).

Montmorillonoid minerals of nontronite type occur in significant quantities around centers of volcanic activity, like the Cape Verde and the Hawaiian Islands, and in general in areas with a high proportion of pyroclastic sediments (Table VII). These minerals are usually assumed to have formed *in situ* by decomposition of the volcanic glass. The highest relative crystallinity is found

TABLE VII

Concentration and Relative Crystallinity of Montmorillonite Species in Marine Sediments of Varying Geological Age.

A purified sample of the API clay mineral standard 25a, Upton, Wyoming, was arbitrarily selected to represent pure and perfectly crystalline montmorillonite. Concentrations were measured against synthetic boehmite as internal standard.

Sample	Geological age	Montmorillonite	
		Concentration, %	Crystallinity, %
Bentonite, Gotska Sandön, Sweden	Ordovician ^a	33	65
Bentonite, Mossen, Kinnekulle, Sweden	Ordovician ^a	41	49
"Red Clay", Noil Tobe, Timor	Jurassic ^b	36	53
McBride Chalk, Alabama	Tertiary	16	57
Pelagic Clay, S. Pacific, Dwd 61	Quaternary	26	43
Pelagic Clay, S. Pacific, Cap 32B	Quaternary	16	40
Pelagic Clay, S. Pacific, Cap 31B	Quaternary	15	38

^aThorslund (1948, 1958); Waern *et al.* (1948); Hagemann and Spjeldnaes (1955).

^bMolengraaff (1920).

in sediments of Paleozoic and Mesozoic age (Table VII), whereas the Cenozoic-Recent marine montmorillonoid is poorly crystallized and has a limited expansibility. Pelagic montmorillonoids and $1M$ micas may show high disorder because they form as metastable structures, which is often the case at low temperature synthesis; the well ordered zeolites, on the other hand, are stable phases at the composition and in the pH range of sea-water (molar ratio of large cations to magnesium ion = 9, pH approx. 7.3–8.5). This suggestion is supported by laboratory studies of the stability relations of the minerals in question. The higher crystallinity of the ancient montmorillonites may be the result of a diagenetic process active after the removal of the sediment from the original alkaline environment.

F. Organic Matter

At the low rate of deposition characteristic of pelagic sediments, and under the oxidizing conditions usually prevailing at the deep-ocean floor, most of the

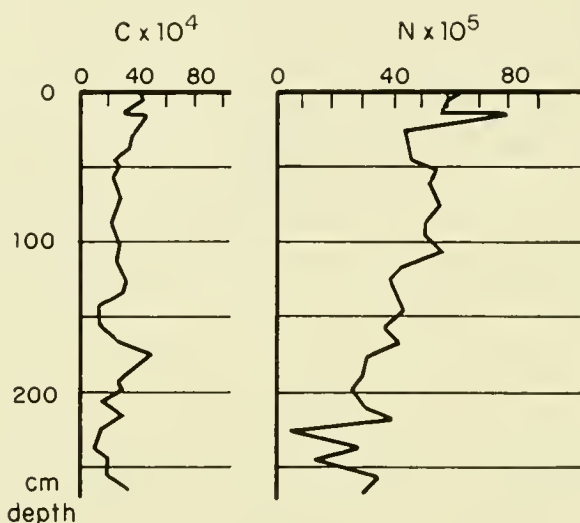


Fig. 31. Carbon and nitrogen concentrations as a function of depth in a pelagic clay sequence (Sw 55, $11^{\circ} 20'N$, $127^{\circ} 37'W$; 4916 m). (From Arrhenius, 1952.)

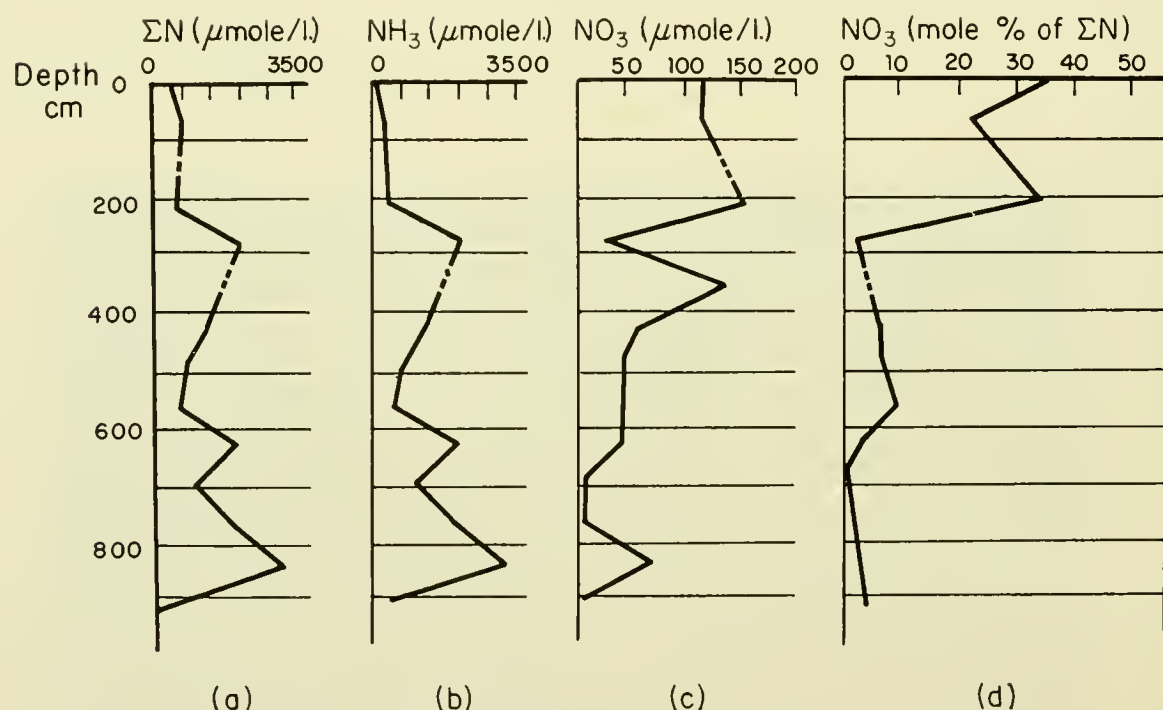


Fig. 32. Distribution of nitrogen between ammonia and nitrate in interstitial solution of core Capricorn 38 BP (South Pacific, $14^{\circ} 16'S$, $119^{\circ} 11'W$; 3400 m). (From Arrhenius and Rotschi, 1953.)

organic matter is oxidized soon after deposition. The oxidation probably is accomplished mainly by bacteria and mud-eating animals concentrated in the surface layer of the sediment (cf. Section 5, and ZoBell, 1946, p. 91). In pelagic sequences far from any terrestrial source of organic matter, the concentration

of organic carbon and nitrogen first decreases rapidly with depth in the sediment and then slowly as the remainder contains an increasingly larger proportion of refractory compounds (Fig. 31) (Mironov and Bordovsky, 1959). Correspondingly, less resistant structures, such as scales of fish and the chitinous beaks of cephalopods, are found only in the surface layer of the sediment. The decomposition of proteins and aminosugar in the sediment produces ammonia and nitrate, which distribute themselves between the interstitial solution and sorption sites on the minerals. Typical values range between 0.1 and 4 mmole of NH_4^+ per kg of solid, and similar amounts per liter of interstitial solution

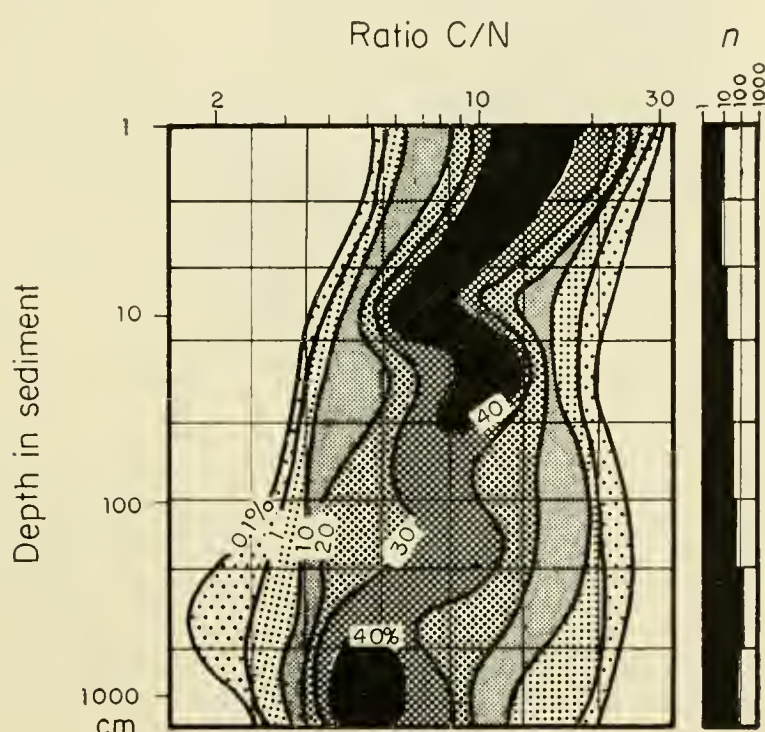


Fig. 33. Frequency distribution of the carbon/nitrogen ratio as a function of depth in Pacific north equatorial clay sediments. The right-hand graph shows the number of samples measured within each of the depth classes limited by horizontal lines. (From Arrhenius, 1952.)

(Fig. 32b) (Bruejewicz and Zaytseva, 1959; Shiskina, 1958). The oxidation state of the interstitially dissolved nitrogen compounds changes rapidly with depth in the sediment, so that at the surface a considerable portion is nitrate whereas at depth ammonium ion predominates in solution (Fig. 32d). In the progressive decomposition of pelagic organic matter, carbon is lost more rapidly than nitrogen and consequently the ratio of carbon to nitrogen in the sediment decreases with depth below the sediment surface, i.e. with geological time (Fig. 33). The combined influence of origin and diagenesis of the organic matter on its composition is illustrated in Fig. 34.

Most of the refractory solid organic matter consists of the original and decomposed organic molecules interstratified with, and protected by, the apatite

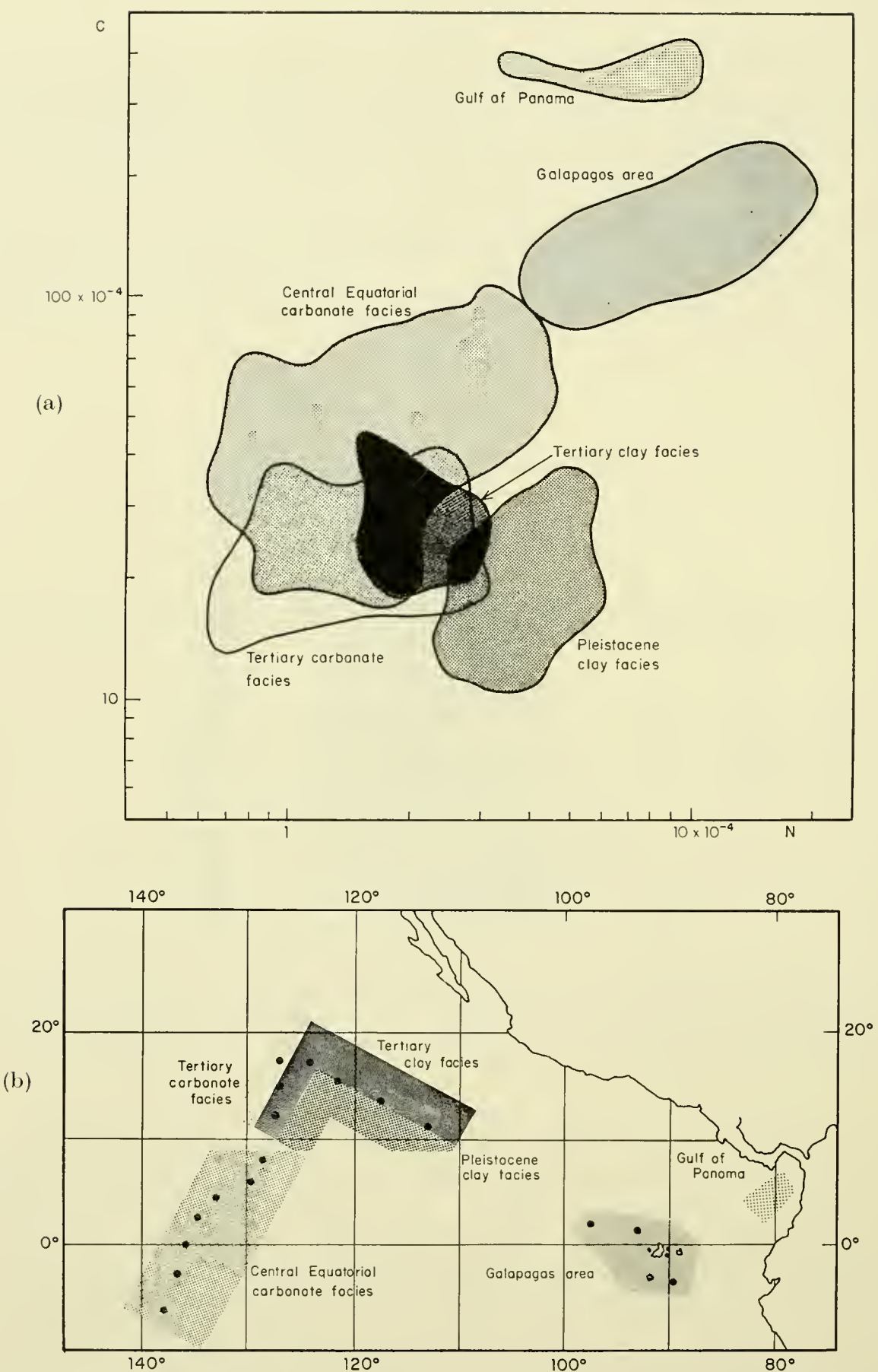


Fig. 34. Influence of origin and diagenesis on the composition of organic matter (a) in sediment cores with location shown in (b). The distribution is based on approximately 2000 analyses. The envelopes in (a) enclose the central 90% of the total number of samples from the respective areas. (After Arrhenius, 1952.)

crystallites in the ubiquitous fish-bone debris (Fig. 15a) (Arrhenius, Bramlette and Picciotto, 1957), and by the calcite crystallites in foraminiferal tests (Correns, 1937). In the former case higher fatty acids form much of the decomposition products precipitated by salt formation with zinc adsorbed from sea-water. Copper, nickel, lead, and silver, also adsorbed from sea-water, are fixed by the proteinaceous residue in the bone debris, whereas the large amounts of rare-earth elements zirconium and thorium from the same source replace calcium in the apatite crystallites. The slow progressive decomposition of the organic matter in the fish debris is further indicated by the gradual disappearance of the deep amber color typical of fragments in Recent strata (Bramlette,

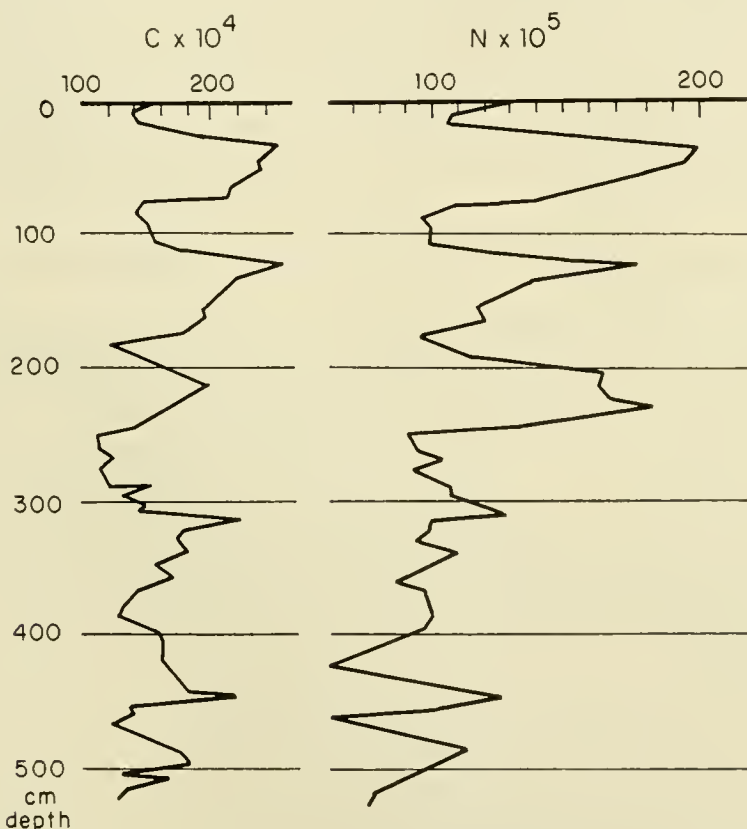


Fig. 35. Variation of carbon and nitrogen concentrations with depth in core Sw 39 from the Galapagos area. The stratigraphic subdivision of this sequence is shown in Fig. 37, and the absolute age of the stratigraphic units is indicated in Fig. 38. (From Arrhenius, 1952.)

unpublished). Complete fading of the color has occurred in pelagic fish debris of Tertiary age.

Variations in geological time of the rate of accumulation of organic matter, large enough to overshadow the diagenetic effects, and the effects of varying dilution with calcium carbonate, have been found only below areas of exceptionally high productivity such as at the eastern end of the equatorial current system in the Pacific. In this area the ensuing sedimentary strata, representing times of low and high organic productivity at the surface of the ocean, differ by a factor of two in their content of carbon and nitrogen (Fig. 35). A similar stratification might be expected below the Peru Current and the Kuroshio.

Because of low density, particles of organic matter from land might spread extensively over adjacent oceanic areas, a minor fraction being windborne (cf. Fig. 21) and the majority transported into the ocean by rivers. Some pelagic sediments, in areas near land with heavy tropical vegetation and protected by marginal trenches (such as on the Pacific side of Middle America), may contain several per cent of terrestrial organic detritus.

The decomposing organic matter on the ocean floor rarely forms well defined organic minerals. Weddellite (calcium oxalate dihydrate) and earlandite (calcium citrate tetrahydrate) have been described by Bannister and Hey (1936) from Antarctic sediment samples, together with authigenic gypsum. Small amounts of strontium and barium substitute for calcium in the organic crystals. Since later attempts to find these minerals in freshly collected Antarctic sediments have failed, and as gypsum is often observed to form in drying bottom samples from calcium carbonate and decomposing proteins, it is possible that the weddellite and earlandite formed during storage of the samples.

3. Productivity Control of Pelagic Sedimentation

One may select approximately level areas of pelagic deposition where the pressure factor and (at least during Pleistocene–Recent times) the temperature factor influencing the post-depositional dissolution of calcite is small compared to the production factor and can be separately estimated (Fig. 19). This facilitates investigating the combined effects of organic production and total rate of deposition on the concentration and rate of accumulation of calcium carbonate. Such studies have been carried out in an approximately level area in the east equatorial Pacific where the Equatorial Divergence maintains a high organic productivity.

The meridional distribution of the rate factors involved, the causative circulation mechanism, and the ensuing sedimentary record are shown graphically in Fig. 36. The top diagram shows a north–south section through the surface layer of the Pacific Ocean at approximately 130°W. The temperature distribution is indicated by the isotherms for 15, 17, 20, 25 and 27°C. The cold intermediate water is represented by a dotted area, and the vertical circulation is indicated by arrows.¹ Divergence of the trade-wind drift currents produces upwelling along the equator of the nutrient-rich intermediate water, resulting in a high rate of production of phytoplankton, sustaining an increased productivity also of higher members of the food chain. At higher tropical latitudes the lack of a mechanism enriching the euphotic layer keeps the productivity low.

The rate of production of skeletal calcium carbonate from coccolithophorids and Foraminifera is illustrated in the middle diagram of Fig. 36, where the full line curve marked “Pleistocene minimum rate of production (interglacial)” corresponds to present-time conditions. The inferred rate of dissolution of calcium carbonate before final burial of the fossils is indicated by the dashed

¹ The heavier shading marks the extension of the Cromwell Current (Knauss, 1960).

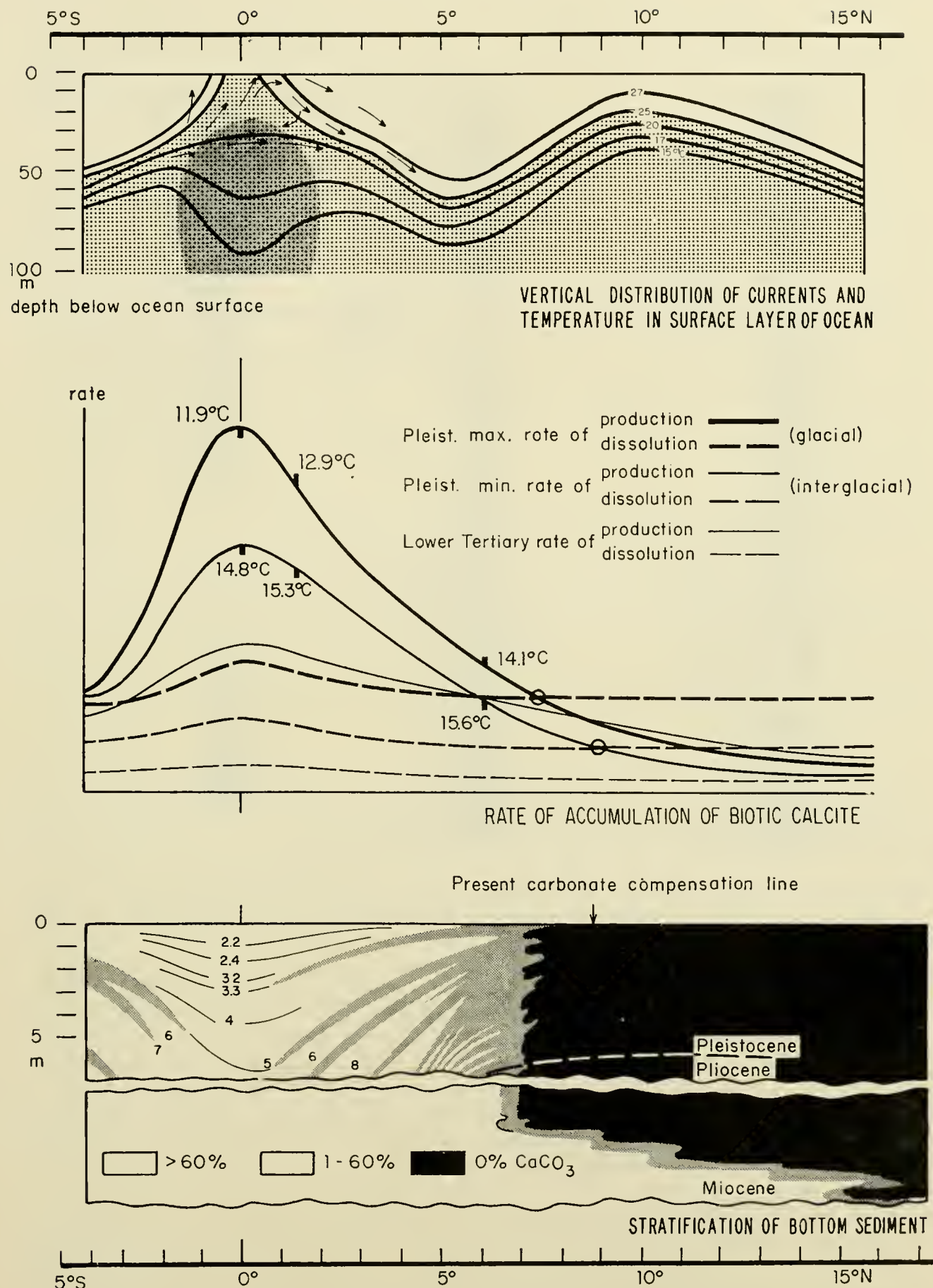


Fig. 36. The equatorial sedimentation mechanism. For explanation, see text.

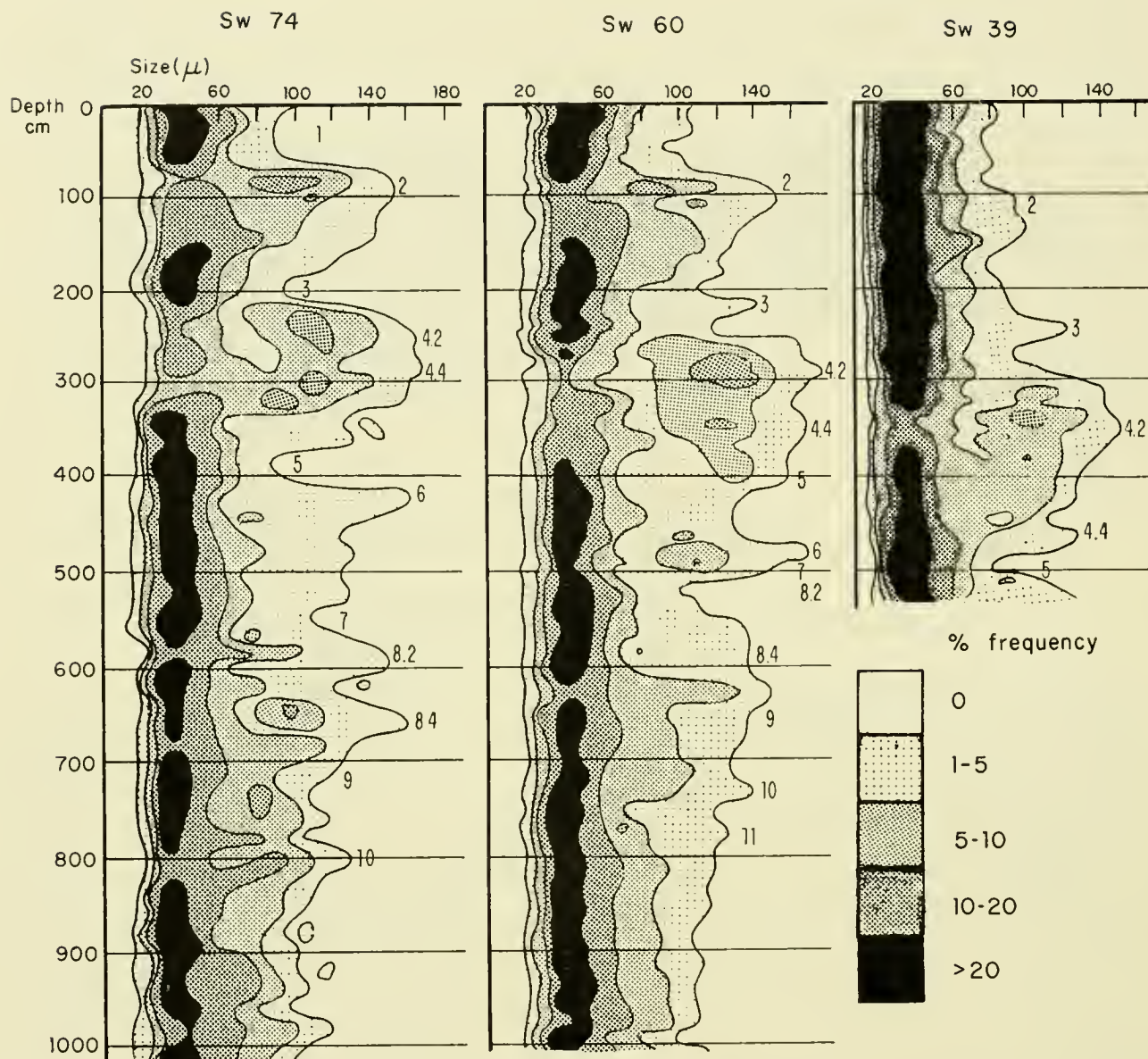


Fig. 37. Size distribution of frustules of the diatom *Coscinodiscus nodulifer* in three widely spaced sedimentary sequences from the equatorial Pacific (Sw 39, long. 93° W; Sw 60, long. 135° W; and Sw 74, long. 150° W). The flat cylindrical frustule of this diatom consists of two halves, the upper one fitting over the lower like a top over a box. At cell division, each daughter cell retains half a frustule as a top and secretes a new bottom (smaller) half. Continuous reproduction by division leads to a distribution of frustule sizes from a few hundred microns to approximately 13μ . In the majority of cases the frustules are shed and sexual reproduction takes place when the frustule has been reduced to 40μ . A naked auxospore is then formed, which grows out to maximum size before a new frustule is secreted.

During times of maximum circulation, as indicated by the rate of accumulation of calcareous, siliceous, and phosphatic fossils (cf. Fig. 38), a secondary maximum at large size occurs in the frustule frequency distribution, indicating a modification of the reproductive cycle. This phenomenon is employed to confirm the correlation of strata over wide distances in equatorial facies. The distance between Sw 39 and Sw 74 amounts to approximately one earth radian. Stratigraphic stages are indicated by numbers in the graphs. (For the age-and-productivity relations of these stages, see Figs. 38 and 35. Also, compare D. Ericson, Chapter 31 of this volume, and Ericson *et al.*, 1955, 1956.)

curve "Pleistocene minimum rate of dissolution (interglacial)", which presupposes an increase under the equatorial productivity maximum due to the effect of carbon dioxide produced by the respiration of bottom-living animals that feed on the rain of organic detritus.

The resultant rate of accumulation of calcium carbonate corresponds to the ordinate difference between the two curves and constitutes the parameter actually measured. At the intersection of the two curves near 9°N the carbonate accumulation accordingly drops to zero. Siliceous clay sediments cover the bottom of the ocean north of the present loci of this intersection, the carbonate compensation line.

Emiliani (1955) has used the calcium carbonate tests of both benthonic and pelagic Foraminifera for paleotemperature measurements in this section. The planktonic results for the present sediment surface are indicated at the present-time production curve in the middle diagram of Fig. 36. The benthonic tests indicate a temperature of about 1°C, in good agreement with the directly measured temperature of the bottom water. The planktonic tests display a gradient, with temperature rising from the equator northward (14.8°C at the equator, 15.3°C at 2°N and 15.6°C at 7°N). This trend agrees with the observed temperature distribution in the surface layer shown in the top graph.¹

The lower diagram in Fig. 36 shows a generalized cross-section through the bottom deposits. The ordinate for the present sediment surface is taken as 0. The lower detached part of the graph, showing the stratification of the Middle Tertiary sediments, lacks detail because of the paucity of observations. The vertical scale is in this latter case relative, and reference to the zero level is not available.

The distribution of carbonate at the present sediment surface is a function of the productivity distribution in the surface layer of the ocean with the superimposed effect of dissolution. From high values below the Equatorial Divergence, the concentration drops toward higher latitudes, and the present northern carbonate compensation line is found near latitude 9°N.

The profile further demonstrates the marked stratification of the calcareous deposits. Below the surface layer, which is characterized by relatively low carbonate concentrations, lies a stratum (2) subdivided into units 2.2, 2.3 and 2.4, high in carbonate and coinciding with the last glaciation in higher latitudes. This stratum is preceded by another low carbonate unit (3) with a small maximum, 3.2, between the minima 3.1 and 3.3.² Below this is a high-carbonate stratum (4) indicating extraordinarily high rates of accumulation of biogenous carbonate and silica. Altogether about nine major carbonate maxima occur in the Pleistocene part of the sequence. The underlying Pliocene sediments are

¹ For no known reason, the magnitudes of temperature derived from the oxygen isotope ratio fall considerably below the temperature range in the top 50-m layer of the ocean, where the meridional gradient occurs, and which is the main habitat of the Foraminifera.

² Not all the details of the stratification are included in this generalized figure, but they can be seen in Figs. 38 and 39.

characterized by less variability with time of the carbonate content. The Pliocene-Pleistocene transition is indicated by a drop in the temperature of the bottom water, shown by the oxygen isotope distribution in benthonic Foraminifera (Emiliani and Edwards, 1953), and by a marked change in the fossil

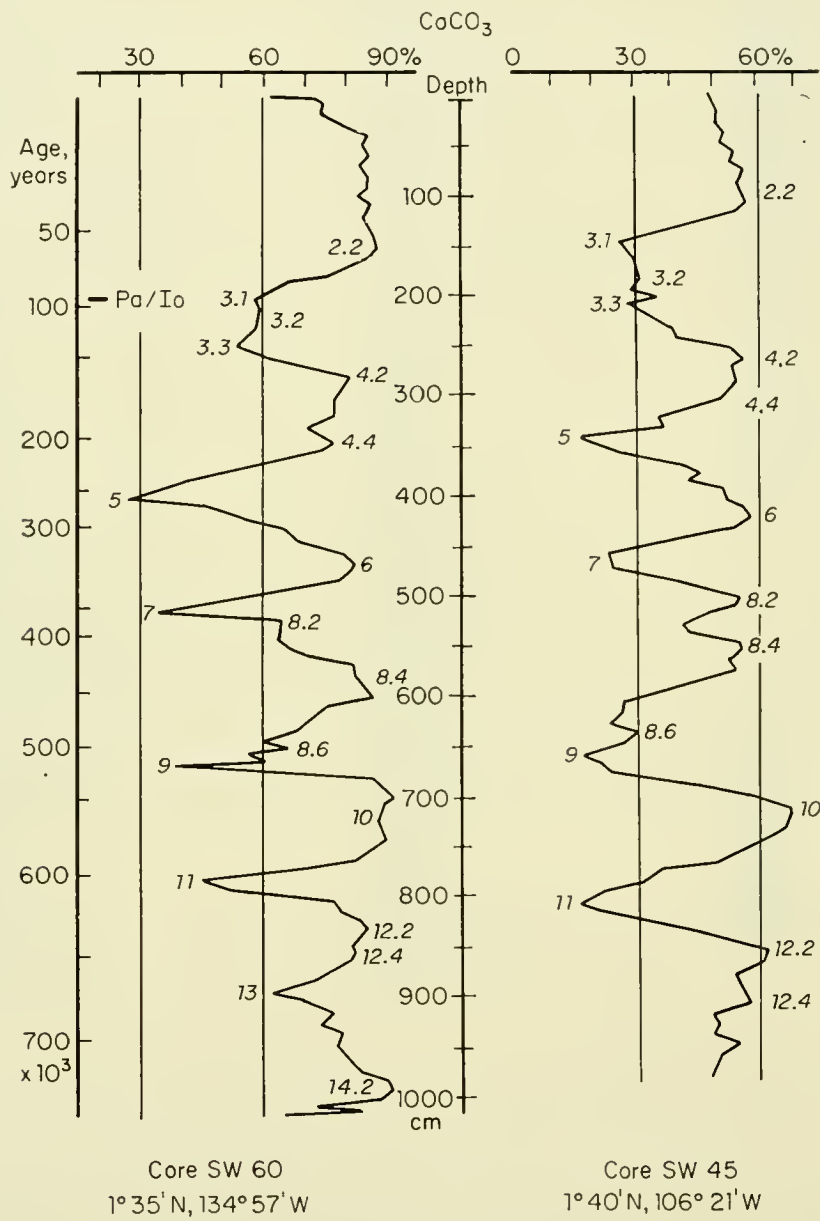


Fig. 38. Age relations of strata in Pacific equatorial carbonate facies as shown by two cores, 3600 km apart. The 95,000-year level in core 60 is determined by the protactinium/ionium ratio at this level, as compared to the sediment surface. The extension of the time scale beyond this age is based on extrapolation assuming a constant rate of deposition of inorganic components but allowing for the wide variability in accumulation of biotic compounds. Strata interpreted as isochronous on the basis of stratigraphic correlation are marked by numbers in the graph (cf. Fig. 37).

assemblages of coccolithophorids (Bramlette, unpublished). In this profile, the transition is marked by a dashed line crossing over the carbonate compensation surface.

From measurements in stratum 4 the full line curve marked "Pleistocene

maximum rate of production (glacial)" in the middle diagram, and the dashed curve marked "Pleistocene maximum rate of dissolution (glacial)" have been constructed. The production appears to have increased greatly, especially in the Equatorial Divergence, and the dissolution seems to have increased somewhat, owing to respiration of benthonic animals, although not enough to counterbalance the greatly increased rate of deposition of calcareous skeletal remains. Thus, the rate of accumulation of calcium carbonate reaches a maximum during this time. The greatest increase occurs at the equator, where values of 5 to 10 g of calcium carbonate per cm^2 in a thousand years are found.

Although the amount of calcium carbonate relative to the inorganic components of the sediment is an analytically convenient measure of past variations

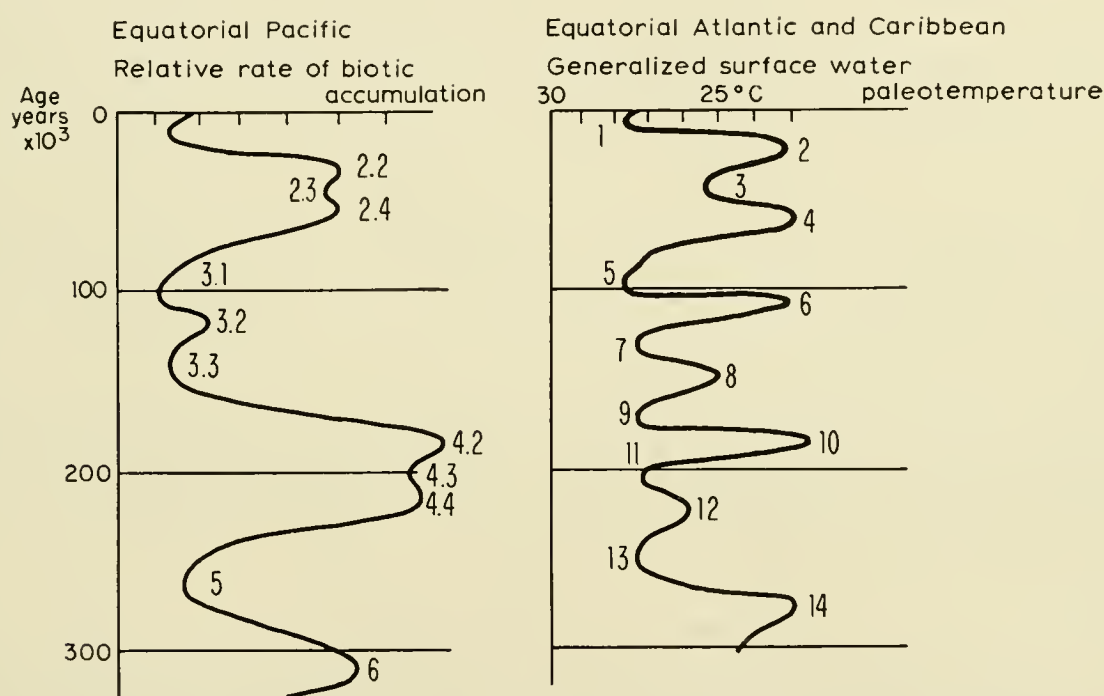


Fig. 39. Age relations and stratigraphic designation of climatically controlled strata in the equatorial Pacific and Atlantic Oceans. (Data from Arrhenius, 1952; Emiliani, 1955; and Emiliani, *in litt.*, 1961.)

in organic productivity, it is not the only one available. The variations described above are accompanied by still more marked changes in the relative amounts of phosphate from fish debris and of opaline silica from diatoms. The diatoms also display characteristic changes in their reproductive cycle (Fig. 37).

As is seen from the planktonic paleotemperature data at the curve "Pleistocene maximum rate of production (glacial)" in the middle graph of Fig. 36 (11.9°C at the equator, 12.9°C at 2°N and 14.1°C at 7°N), the surface temperature gradient away from the equator displayed by the oxygen isotope ratio in the foraminiferal tests is even steeper during the time of circulation maximum (Riss [Illinoian] Glacial Age) than under the present conditions of interglacial type. This further confirms that an increased rate of upwelling in the Equatorial Divergence is the direct cause of the increased productivity. A displacement toward the Equator of the high pressure centers now found between latitudes

20 and 35° could explain this intensified vertical circulation during glacial times. The stratification of biotic components in the Equatorial Pacific under these conditions provides a record of the general climatic evolution of the earth; new drilling techniques now being introduced (Bascom, 1961) could extend the time record beyond the few million years now accessible.

Sediments from Eocene to Pliocene age, outcropping or covered by relatively thin Quaternary strata, have been sampled on topographic highs within the area in question (Arrhenius, 1952, 2.57; Riedel, Chapter 33, this volume). This sedimentation information from the early Cenozoic has been summarized in the lower disconnected part of the bottom graph of Fig. 36, and in the curves marked "Lower Tertiary" in the upper graph of the figure. The northern carbonate compensation line in Lower Tertiary was much farther north than at present, probably north of latitude 45°. However, it was gradually displaced southward, passed latitude 16°N in Miocene time, and approximately reached its present location in Upper Miocene or Pliocene times. Oxygen isotope measurements of benthonic Foraminifera from these strata indicate bottom-water temperatures of approximately 10°C as compared to 1–2° throughout the Pleistocene (Emiliani, *op. cit.*; Emiliani and Edwards, *op. cit.*). Apparently the large meridional extent of carbonate sediments in Lower Tertiary times was due to a decreased rate of dissolution rather than to an increased rate of production.

The meridional drop in concentration of fossils away from the equatorial zone appears also in the Tertiary strata, indicating the operation of the Equatorial Divergence already in early Cenozoic times. Its accurate location in relation to the present equator is not yet known.

4. Physical Stratification

The detailed record on the ocean floor of the climatically induced oscillations in the Equatorial Current system makes it possible to correlate the sedimentary strata of this facies over large distances. Such a correlation is indicated in Fig. 38, which shows two sequences, 3200 km apart, or one-third of the earth's quadrant. The identification of the individual strata is further corroborated by the sequence of properties other than carbonate content, such as the distribution of diatoms shown in Fig. 37.

Attempts have been made to determine the absolute ages of the Pacific equatorial Pleistocene strata by the radiocarbon activity of the carbonate (Arrhenius, Kjellberg and Libby, 1951), and recently by the protactinium/ionium method (Sackett, 1960). Because the short half-life of ^{14}C (5800 years) limits direct age determinations by this method to the Late Glacial and Post-glacial strata (stages 1 and 2.2), the age measurement was used to determine the Late Pleistocene and Recent rate of deposition of inorganic constituents; and the ages of older strata were extrapolated under the assumption of a constant average rate of deposition of inorganic compounds throughout the Pleistocene within the area selected. The error inherent in this assumption is probably not

much larger than the experimental error of the absolute age determination. This statement is based on two facts. First, accumulation measurements have demonstrated that within the area in question and during the Pleistocene time-intervals studied, the rate varies only little, and apparently randomly from one station to another (Arrhenius, 1952, fig. 1.1.6.1). This approximate spatial constancy demonstrates that the depositional area is far enough removed from the source area of the settling particles for the suspension, from which sedimentation takes place, to have assumed a uniform character. The time that the particles have spent in suspension must consequently be long compared to the half-life of the suspension, which is controlled by coagulation or other precipitation mechanisms. If these reactions, as is likely, are of second or higher order, even large variation in the rate of influx of suspensoids in the ocean will have a negligible effect on the terminal precipitation rate (Arrhenius, 1954). Only small variations with time of the rate of accumulation of inorganic components would consequently be expected in an area where the conditions mentioned above are met, and as long as the global ratio of chemical to mechanical weathering is not markedly changed.

Second, the Tertiary clay sediments in the Pacific, as compared with the Quaternary, clearly indicate less dilution of the halmeic and biotic components (such as manganese oxide minerals and skeletal phosphate) with terrigenous material, and a variation of this dilution with time (Fig. 40). The lack of such marked variations in the Quaternary part of the sequences confirms the assumption of a relatively steady inorganic accumulation rate during this time, particularly when averaged over at least one climatic cycle. This conclusion pertains to only one specific region and is not valid in some other areas investigated (cf. section from East Pacific Rise in left part of fig. 1.1.5, Arrhenius, 1952; Broecker *et al.*, 1958). Local deviations from the average conditions, attributed to topographic control, are discussed below (Section 5).

The time scale obtained for the Upper and Middle Pleistocene events is indicated in Fig. 38, together with the recent protactinium/ionium date. This absolute age determination confirms the extrapolated age within the limits of experimental error ($95,000 \pm 13,000$ years for stage 3.1 by protactinium/ionium, as compared to $90,000 \pm 6000$ years by radiocarbon extrapolation).

The Lower Pleistocene and Upper Pliocene strata, which are conformably represented in a few investigated sequences, are beyond the reach of present nuclear age determination methods. In this stratigraphic range two events characterize the Tertiary-Quaternary boundary: a distinct evolutionary change in the coccolithophorids (Bramlette, unpublished) and a marked drop in the surface temperature of the ocean, as indicated by the carbonate paleotemperature (Emiliani, 1955). These events have been recorded in two sequences, one near the equator at an extrapolated age level of 1.4 million years (core Sw 62), the other near the north equatorial carbonate compensation surface (Fig. 36), at 1.7 million years (core Sw 58). Because the first area is smoother, its value is more probable; the second area might contain redistributed sediment from a nearby seamount which causes a rate of accumulation of inorganic

matter higher than average and thus an overestimate for the extrapolated age. These conditions illustrate the desirability of stratigraphic control in sequences where absolute age determinations are attempted.

Methods similar to those applied in the equatorial Pacific have been used by Emiliani (1955) and Broecker *et al.* (1959) to determine the absolute age relations of the Upper Pleistocene climatic stages in the Atlantic Ocean.

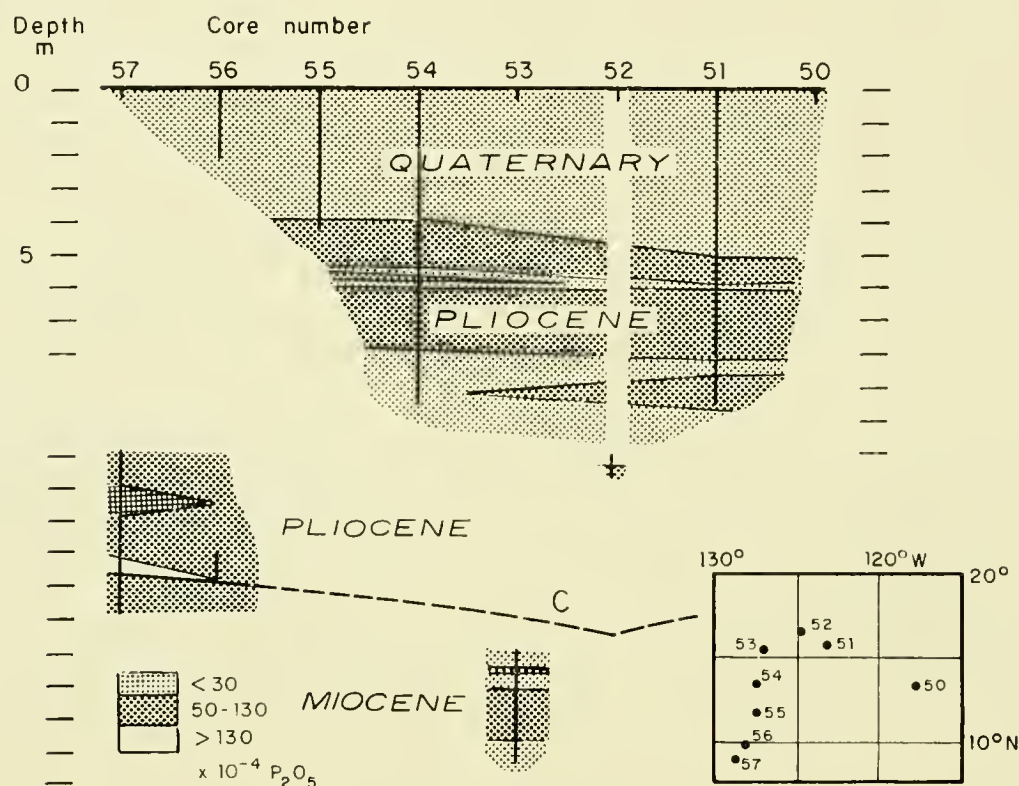


Fig. 40. Stratigraphy of the present north equatorial clay facies in the Pacific on the basis of phosphate content of the sediment. The phosphate is due to skeletal debris of pelagic fish, and the concentration appears to be inversely proportional to the rate of accumulation of terrigenous components. Concentrations are given in g/g.

Vertical lines correspond to the sediment cores indicated by numbers in the graph and in the map insert. The lower detached parts of the figure show older sediments now near the surface below unconformities of various age.

C indicates the heterochronous calcium carbonate compensation surface, separating calcareous from non-calcareous deposits. This boundary moved south past approximately latitude 15°N in the Upper Miocene and appears to have arrived near its present position (cf. Fig. 36) in Pliocene times. (After Arrhenius, 1952.)

Emiliani assumes a low variability in time for both the inorganic and biotic sedimentary components. The stratigraphic subdivision used by Emiliani is based on changes in ocean surface temperature, whereas the stratification in the equatorial Pacific, as mentioned above, is presumably caused by productivity changes, induced by variations in trade-wind intensity. Since certainly both equatorial Pacific circulation and equatorial Atlantic surface temperature were controlled by Pleistocene climatic changes, one would expect agreement in phase but not necessarily in amplitude between the Pacific and Atlantic records.

Fig. 39 shows data for both oceans based on protactinium/ionium dates at approximately the 100,000-year level in both cases, and on extrapolation of the age below this level. A higher resolution is obtained in the Atlantic sequences owing to the higher total rate of deposition, which protects the record more efficiently from the smoothing effects of animal burrowing and post-depositional dissolution. The higher Atlantic resolution indicates a bipartition of the Pacific productivity maximum 3.2 and confirms the bipartition of the Pacific maxima 2 and 4, only vaguely indicated in most Pacific sequences. A cumulative error from extrapolation might account for the difference in apparent age between the Pacific maximum 6 and the Atlantic 14. The suggested interoceanic correlation is summarized in Table VIII. The climatic implications of the stratification are discussed in detail elsewhere (Emiliani, 1955; Arrhenius, 1959a; Emiliani and Flint, Chapter 34 of this volume).

TABLE VIII

Suggested Correlation between Productivity Stratification in Equatorial Pacific Sediments (Arrhenius, 1952) and Paleotemperature Stratification in Atlantic and Caribbean Sediments (Emiliani, 1955)

Stages and substages	
Equatorial Pacific	Equatorial Atlantic and Caribbean
1	1
2.2	2
2.3	3
2.4	4
3.1	5
3.2	6
3.3	7 + 8 + 9
4.2	10
4.3	11
4.4	12
5	13
6	14

The marked effects on circulation and organic production, and ultimately on sediment deposition, caused by the vanishing of the Coriolis force at the equator, open a promising possibility for determining its position in the past. Any displacement of the geographic equator should be accompanied by a corresponding displacement of the thickness maximum of the strata (cf. Fig. 36) and of the maximum in concentration of biotic sedimentary components, resulting from the high productivity in the Equatorial Divergence. If the position of the equator at a given time were established at two points, less than 180° and preferably 90° apart, the position of the poles would also be determined. The estimated possible resolution of this method is of the order of a few degrees of meridional displacement. The sediment cores now existing at the

equator go back to only the Middle Pleistocene, about half a million years. During this time the equator has remained constant within the resolution of the present sampling grid, which is about four degrees of latitude. If 500-m cores could be drilled in the equatorial sediment bulge, Cretaceous or older sediments might be reached, corresponding to postulated positions of the North Pole in the North Pacific (Runcorn, 1956, 1959). Determination of polar wandering by this method would be free from the uncertainty imposed by possible continental drift.

Biostratigraphic means available for subdividing into stages and correlating Upper Cenozoic formation units in their calcareous-siliceous facies are lacking in the adjacent clay and zeolitic facies. The stratigraphic units so far resolved in the North Equatorial Pacific clay facies consist of a Pleistocene-Recent bed of buff clay, comparatively low in halmeic minerals, conformably overlying a series of dark brown clay members (Pliocene), high in manganese-iron oxide minerals and other halmeic phases, and in fish bone apatite (Fig. 40). Older clay sediments (Middle Tertiary) occasionally sampled in outcrops on topographic highs (cf. Section 5) show a petrological composition similar to the Pliocene ones. Where the buff top formation is found without interruption of the sequence by unconformities, the thickness amounts to a few meters, but its lower boundary cannot be defined precisely. Accepting for the north equatorial Pleistocene-Recent clay facies a rate of inorganic accumulation around 2 mm/1000 years, indicated by protactinium/ionium and radiocarbon dates (see above) and ionium/thorium measurements (Goldberg and Koide, 1958), it appears that the buff clay formation comprises the last one or two million years. The stratigraphy suggests a relatively low rate of transportation of terrigenous matter into the area during Tertiary times through Middle Pliocene, periodically varying transition conditions in the Upper Pliocene, and a general increase in terrigenous contribution during Pleistocene and Recent.

5. Topographic and Tectonic Control of Sedimentation

Deformation of the ocean floor into hills, mounts, and fault scarps has undoubtedly occurred many different times. Much of the present small-scale topographic relief in the Pacific was probably created by extensive laccolithic injection of basaltic lava, which updomed the overlying sediments (Arrhenius, 1952, 2.57.0, 3.4.1). This process is assumed to have created the low-relief, hilly topography typical of vast areas in the Pacific Ocean basins (cf. Figs. 41 and 43). Lava erupting at oceanic depths—unlike conditions on land or in shallow water—does not encounter marked discontinuity in the confining pressure at the sediment surface. Lateral flows are consequently not particularly probable at this surface, but are likely to occur at petrological discontinuities at depth in the sediment. Submarine lava flows at great water depth are expected to spread extensively owing to low viscosity resulting from the flow of interstitial water or sea-water into the lava at high water pressure. The discontinuity in sound velocity a few hundred meters below the sediment over wide areas in the east

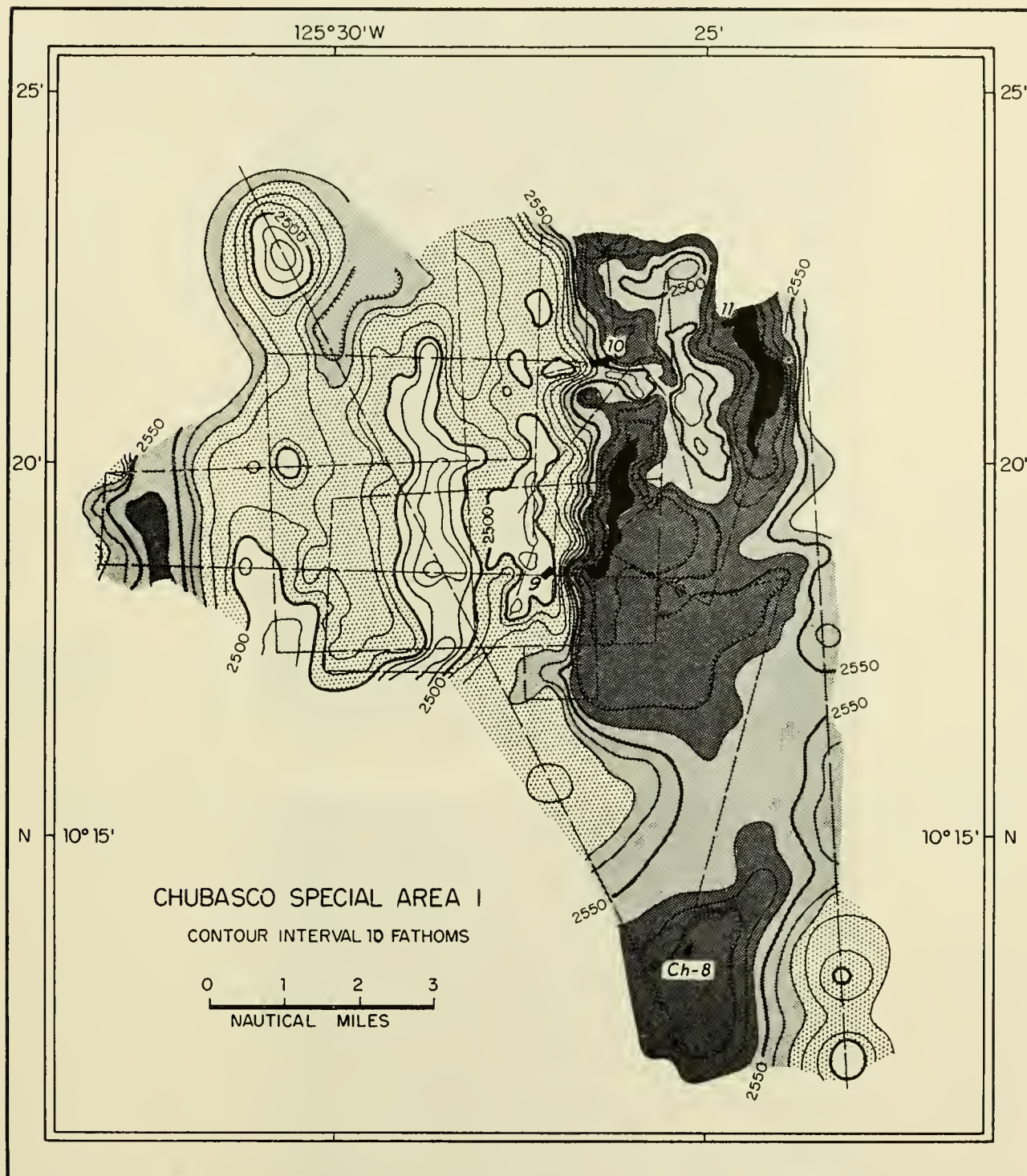


Fig. 41. Topography of area around stations Chub 8, 9, 10 and 11 in North Equatorial clay facies. (Dashed lines indicate the sounding track.) At stations 9 and 10 on the topographic high the Tertiary clay formation is covered only by about 40 cm of Quaternary. The cores 8 and 11, however, which are 160 and 175 cm long respectively, do not penetrate through the Quaternary formation in the valley bottom. The similarity in stratification between cores 8 and 11 suggests that the greater thickness of the Quaternary formation in the valley is not caused by slumping. The abnormal thinness of the Quaternary strata on the slope and crest of the hill consequently appears to be due either to a persistently lower rate of accumulation or to a period of non-deposition represented by the Tertiary-Quaternary unconformity. (From Bramlette and Arrhenius, unpublished; topographic survey by R. L. Fisher.)

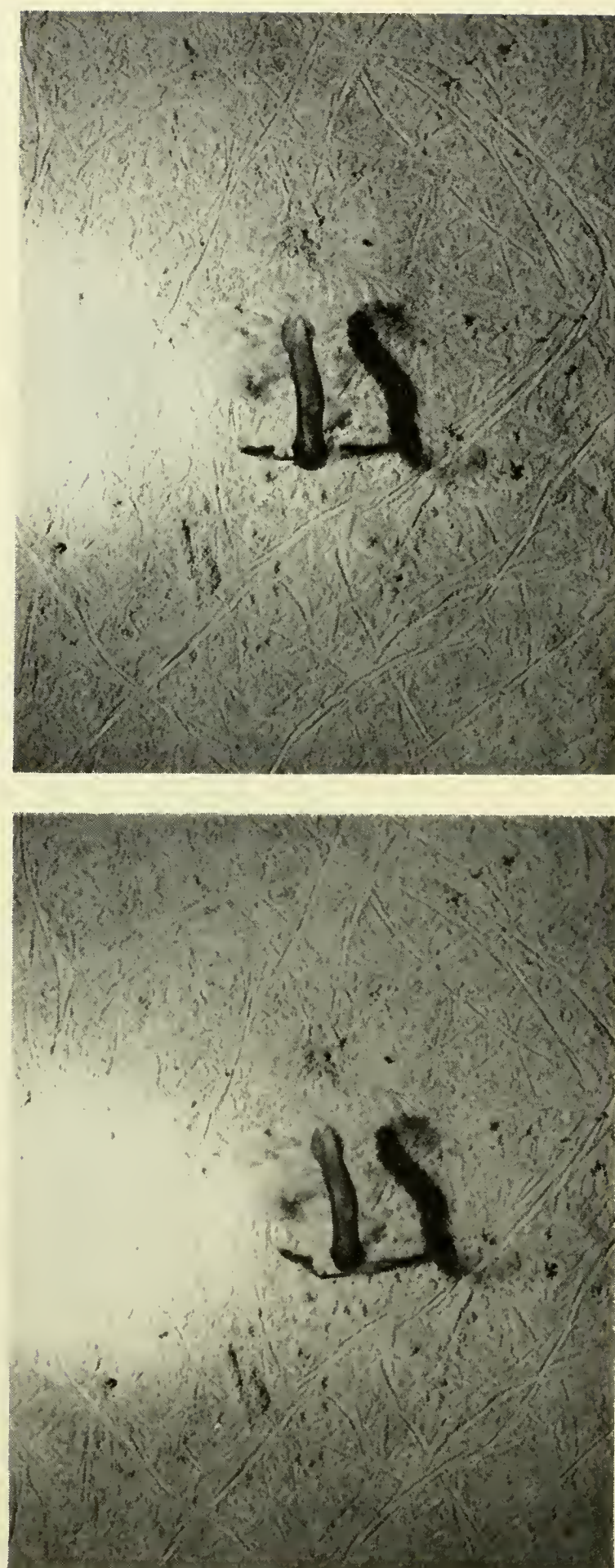


Fig. 42. Sediment suspension cloud stirred up or expelled by a holothurian. (Also visible in the picture: a sea-pen, tracks and burrows of benthic organisms.) $31^{\circ} 22'N$, $117^{\circ} 29'W$; 1930 m (SW of Ensenada, Continental Borderland). (Stereophoto; D. Krause and D. Corrigan.)

Pacific might well be due to such a stratigraphically determined preferred level of intrusion.

Probably because of the uplift, sedimentation appears in many cases to have ceased on the topographic highs for varying lengths of time, except for halmeic minerals accreting by precipitation. In some cases erosion seems to be or has been active on the crests and slopes of the hills, while accumulation continues around them (Fig. 41). The older deposits on the topographic highs, outcropping or covered by relatively thin layers of younger sediments, appear to range in age between Oligocene and Pliocene (Arrhenius, 1952; Riedel, Chap. 33 of this volume). If it is correct to postulate control of the topography by volcanic intrusions, it would then seem that such events have occurred frequently during the Cenozoic era.

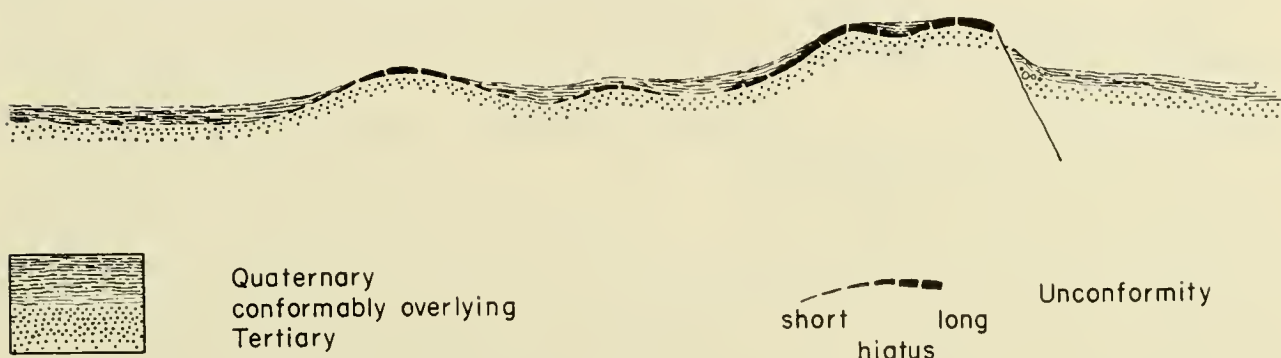


Fig. 43. Hypothetical schematic profile illustrating topographic control of pelagic sedimentation in low, hilly topography. The order of magnitude size of the hills is a few kilometers horizontally and up to a few hundred meters vertically. The thickness scale of the Quaternary formation is exaggerated; the maximum thickness found in pelagic clay facies is a few meters.

Scouring even by weak currents might prevent accumulation of fine-grained clay sediment from taking place on hill-tops and slopes and may account for lateral displacement of resuspended sediment, but is unlikely to be responsible for the resuspension which appears to affect Pleistocene and older sediments with comparatively high shearing strengths. The dispersion of Tertiary Radiolaria through the Pleistocene sediments adjacent to the eroded hills (Riedel, Chapter 33 of this volume) indicates a continuous process of resuspension and transport downhill of the deposit from the topographic highs. This is probably caused by the churning action of benthic animals, some of which have been observed forming a suspension cloud (Fig. 42), which may be displaced by any horizontal movement of the near-bottom water. Repetition of this process seems to result in slow abrasion of the elevated areas and movement of the resuspended sediments downhill, until a level is reached where the streamlines are parallel to the sediment surface. The accumulating sediment, mostly new material and including some redeposited sediment, appears gradually to invade the elevated areas of non-deposition, as schematically indicated in Fig. 43. The upper Cenozoic clay sediments thus form a blanket with frequent holes and thin

spots over hills and seamounts. The smoothing of the topographic irregularities, accompanied by gradual closure of the holes, is apparently more rapid in calcareous sediments on account of their higher accumulation rate.

References

- Altshuler, Z. S., R. S. Clarke and E. J. Young, 1958. Geochemistry of uranium in apatite and phosphorite. *U.S. Geol. Surv. Prof. Paper*, **314-D**.
- Armstrong, F. A. J., 1958. Inorganic suspended matter in sea water. *J. Mar. Res.*, **17**, 23.
- Arrhenius, G., 1952. Sediment cores from the East Pacific. *Reps. Swed. Deep-Sea Exped.*, **5**, Göteborg.
- Arrhenius, G., 1954. Origin and accumulation of aluminosilicates in the ocean. *Tellus*, **6**, 215.
- Arrhenius, G., 1954a. Significance of carbonate stratification in pelagic deposits. *Bull. Geol. Soc. Amer.*, **65**, 228.
- Arrhenius, G., 1959. Sedimentation on the ocean floor. *Researches in Geochemistry*. John Wiley, New York.
- Arrhenius, G., 1959a. Climatic records on the ocean floor. *Rossby Memorial Volume*, edit. B. Bolin, Rockefeller Inst. Press.
- Arrhenius, G., 1961. Geological record on the ocean floor. *Oceanography*. Amer. Assoc. Adv. Sci., Publ. 67. Wash. D.C.
- Arrhenius, G., M. Bramlette and E. Picciotto, 1957. Localization of radioactive and stable heavy nuclides in ocean sediments. *Nature*, **180**, 85–86.
- Arrhenius, G., G. Kjellberg and W. F. Libby, 1951. Age determination of Pacific chalk ooze by radiocarbon and titanium content. *Tellus*, **3**, 222.
- Arrhenius, G. and H. Korkisch, 1959. Uranium and thorium in marine minerals. *Intern. Oceanog. Cong. Preprints*, 497. Edit. M. Sears. Amer. Assoc. Adv. Sci., Wash. D.C.
- Arrhenius, G. and H. Rotschi, 1953. SIO Expedition Capricorn. Unpubl. Rep. Scripps Institution of Oceanography.
- Bannister, F. A. and M. H. Hey, 1936. Report on some crystalline components of the Weddell Sea deposits. *Discovery Reps.*, **12**, 60.
- Barth, T. F. W., 1952. *Theoretical Petrology*. John Wiley, New York, 369 pp.
- Bascom, W., 1961. *A Hole in the Bottom of the Sea*. Doubleday, New York.
- Bramlette, M. N., 1958. Significance of coccolithophorids in calcium carbonate deposition. *Bull. Geol. Soc. Amer.*, **69**, 121–126.
- Bramlette, M. N., 1961. Pelagic sediments. *Oceanography*. Amer. Assoc. Adv. Sci., Publ. 67 Wash. D.C.
- Bramlette, M. N. and W. Bradley, 1942. Geology and biology of North Atlantic deep-sea cores between Newfoundland and Ireland. Lithology and geologic interpretations. *U.S. Geol. Surv. Prof. Paper*, **196**.
- Bramlette, M. N. and W. R. Riedel, 1954. Stratigraphic value of discoaster and some other microfossils related to Recent coccolithophores. *J. Paleont.*, **28**, 385.
- Broecker, W. S., K. K. Turekian and B. C. Heezen, 1958. The relation of deep-sea sedimentation rates to variations in climate. *Amer. J. Sci.*, **256**, 503–517.
- Broecker, W. S., A. Walton, B. C. Heezen and K. Turekian, 1959. Sedimentation rates in the deep ocean. *Intern. Oceanog. Cong. Preprints*, 87. Edit. M. Sears. Amer. Assoc. Adv. Sci., Wash. D.C.
- Bruejewicz, S. V. and E. D. Zaytseva, 1958. The Bering Sea sediments. *Trudy Inst. Okeanol. Akad. Nauk S.S.R.*, **26**, 8–108.
- Buser, W., 1959. The nature of the iron and manganese compounds in manganese nodules. *Intern. Oceanog. Cong. Preprints*, 962. Edit. M. Sears. Amer. Assoc. Adv. Sci., Wash. D.C.

- Buser, W. and A. Grüitter, 1956. Untersuchungen an Mangansedimenten. *Schweiz. Mineralog. Petrograph. Mitt.*, **36**, 49–62.
- Butkevich, E. S. 1928. The formation of marine iron and manganese deposits and the role of microorganisms in the latter. *Verh. Wiss. Meeresinst. Moscow*, **3**, 63.
- Buttlar, H. von and F. G. Houtermans, 1950. Photographische Bestimmung der Aktivitätsverteilung in einer Manganknolle der Tiefsee. *Naturwissenschaften*, **37**, 400–401.
- Castaing, R. and K. Fredriksson, 1958. Analyses of cosmic spherules with an x-ray microanalyzer. *Geochim. et Cosmochim. Acta*, **14**, 114.
- Chow, T. J. and E. D. Goldberg, 1960. On the marine geochemistry of barium. *Geochim. et Cosmochim. Acta*, **20**, 192.
- Correns, C. W., 1937. Die Sedimente des äquatorialen Atlantischen Ozeans. *Wiss. Ergebn. Deut. Atlant. Exped. 'Meteor'*, 1925–1927, **3**, 1.
- Correns, C. W., 1939. Die Sedimentgesteine. Part 2. In Barth, T. F. W., C. W. Correns and P. Eskola, *Die Entstehung der Gesteine*. Springer, Berlin.
- Correns, C. W., 1954. Titan in Tiefseesedimenten. *Deep-Sea Res.*, **1**, 78–85.
- Crozier, 1960. Black magnetic spherules in sediments. *J. Geophys. Res.*, **65**, 2971.
- Dietz, R. S., 1955. Manganese deposits on the northeast Pacific sea floor. *Calif. J. Mines Geol.*, **51**, 209–220.
- Dietz, R. S., K. O. Emery and F. P. Shepard, 1942. Phosphorite deposits on the sea floor off southern California. *Bull. Geol. Soc. Amer.*, **53**, 815–848.
- Dieulafait, L., 1883. Le manganese dans les eaux de mers actuelles et dans certains de leur dépôts. *C. R. Acad. Sci. Paris*, **96**, 718.
- Dorff, F., 1935. *Biologie des Eisen- und Mangankreislaufes*. Springer, Berlin.
- El Wakeel, S. K. and J. P. Riley, 1961. Chemical and mineralogical studies of deep-sea sediments. *Geochim. et Cosmochim. Acta*, **25**, 110.
- Emery, K. O., 1960. *Geology of the Sea Floor off California*. John Wiley, New York.
- Emiliani, C., 1955. Pleistocene temperatures. *J. Geol.*, **63**, 538.
- Emiliani, C., 1956. Oligocene and Miocene temperatures of the equatorial and subtropical Atlantic Ocean. *J. Geol.*, **64**, No. 3, 281.
- Emiliani, C. and G. Edwards, 1953. Tertiary ocean bottom temperatures. *Nature*, **171**, 887.
- Ericson, D. B., M. Ewing, B. Heezen and G. Wollin, 1955. Sediment deposition in deep Atlantic. *Geol. Soc. Amer. Spec. Paper* 62, 205–220.
- Ericson, D. B. and G. Wollin, 1956. Correlation of six cores from the equatorial Atlantic and Caribbean. *Deep-Sea Res.*, **3**, 104–125.
- Ericson, D. B. and G. Wollin, 1956a. Micropaleontological and isotopic determinations of Pleistocene climates. *Micropaleontology*, **2**, 257.
- Ewing, M., B. C. Heezen and D. Ericson, 1959. Significance of the Worzel deep-sea ash. *Proc. Nat. Acad. Sci.*, **45**, 355.
- Fredriksson, K., 1958. A note on investigations of cosmic spherules and other small meteoritic particles. *Astronomical Notes*. Univ. of Göteborg, Sweden, p. 21.
- Fredriksson, K., 1959. On the origin, age, and distribution of cosmic spherules. *Intern. Oceanog. Cong. Preprints*, 456. Edit. M. Sears. Amer. Assoc. Adv. Sci., Wash. D.C.
- Fredriksson, K., 1961. Origin of black spherules from Pacific islands, deep-sea sediments and Antarctic ice. *Symposium Abst. 10th Pacific Sci. Cong.*, Honolulu.
- Goldberg, E. D., 1954. Marine geochemistry I. Chemical scavengers of the sea. *J. Geol.*, **62**, 249–265.
- Goldberg, E. D. and G. Arrhenius, 1958. Chemistry of Pacific pelagic sediments. *Geochim. et Cosmochim. Acta*, **13**, 153–212.
- Goldberg, E. D. and M. Koide, 1958. Ionium-thorium chronology in deep-sea sediments of the Pacific. *Science*, **128**, 1003.
- Goldberg, E. D. and R. H. Parker, 1960. Phosphatized wood from the Pacific sea floor. *Bull. Geol. Soc. Amer.*, **71**, 631.

- Goldberg, E. D., C. Patterson and T. Chow, 1958. Ionium-thorium and lead isotope ratios as indicators of oceanic water masses. *2nd U.N. Intern. Conf. Peaceful Uses of Atomic Energy*, 15/P/1980.
- Goldberg, E. D. and E. Picciotto, 1955. Thorium determinations in manganese nodules. *Science*, **121**, 613–614.
- Goldschmidt, V. M., 1954. *Geochemistry*. Clarendon Press, Oxford.
- Gorbunova, Z. N., 1960. Fine grained minerals in the sediments of the Indian Ocean. *Doklady Akad. Nauk S.S.R.*, **134**, 935.
- Gorbunova, Z. N., 1960a. Composition of clay minerals in different horizons of the bottom deposits of the Indian Ocean. *Doklady Akad. Nauk S.S.R.*, **134**, 1201.
- Gordon, L., C. C. Reimer and B. P. Burtt, 1954. Coprecipitation from homogeneous solution. *Anal. Chem.*, **26**, 842.
- Grabau, A. W., 1904. On the classification of sedimentary rocks. *Amer. Geol.*, **33**, 228.
- Graf, C. L., 1960. Geochemistry of carbonate sediments and sedimentary carbonate rocks. Part III; minor element distribution. *Ill. State Geol. Surv.*, Urbana, Ill. Circular 301.
- Graham, J. W., 1959. Metabolically induced precipitation of trace elements from sea water. *Science*, **129**, 1428.
- Grim, R. E., R. S. Dietz and W. F. Bradley, 1949. Clay mineral composition of some sediments from the Pacific Ocean off the California coast and the Gulf of California. *Bull. Geol. Soc. Amer.*, **60**, 1785–1808.
- Gripenberg, S., 1934. A study of the sediments of the North Baltic and adjoining seas. *Fennia*, **60**, No. 3, Helsingfors.
- Grütter, A. and W. Buser, 1957. Untersuchungen an Mangansedimenten. *Chimia*, **11**, 132–133.
- Hagemann, F. and Spjeldnaes, N., 1955. The Middle Ordovician of the Oslo region, Norway. 6. Notes on bentonite (K-bentonites) from the Oslo-Asker District. *Norsk Geol. Tidsskr.*, **35**, 29–52, Oslo.
- Hägg, G., 1935. The crystal structure of magnetic ferric oxide. *Z. physik. Chem.*, **29**, 95.
- Hamilton, E. L., 1956. Sunken islands of the mid-Pacific mountains. *Geol. Soc. Amer. Mem.*, **64**.
- Harder, H., 1959. Beitrag zur Geochemie des Bors. *Nachr. Akad. Wiss. Göttingen*, **6**, 123.
- Heezen, B. C., M. Tharp and M. Ewing, 1959. The floors of the oceans. *Geol. Soc. Amer. Spec. Paper* 65.
- Hunter, W. and D. W. Parkin, 1960. Cosmic dust in Recent deep-sea sediments. *Proc. Roy. Soc. London*, **A255**, 382–397.
- Hurley, R. J., 1960. Unpublished manuscript, SIO ref. 60–67.
- Hustedt, F., 1921. Untersuchungen über die Natur der Harmattantrübe. *Deut. Übersee. Meteorol. Ber.*, **23**.
- Inman, D. and T. Chamberlain, 1960. Littoral sand budget along the southern California coast. *21st Intern. Geol. Cong. Copenhagen*, 245.
- Jerlov, N. G., 1953. Particle distribution in the ocean. *Reps. Swed. Deep-Sea Exped.*, **3** (Fasc. 2), 73–97.
- Kalinenko, V. O., 1949. The origin of Fe–Mn concretions. *Mikrobiologiya*, **18**, 528.
- Kato, K., 1955. Accumulation of organic matter in marine bottom and its oceanographic environment in the sea to the southeast of Hokkaido. *Bull. Fac. Fish., Hokkaido Univ.*, **6**, 125–151.
- Kazakov, A. V., 1950. Geotectonics and the formation of phosphorite deposits. *Bull. Acad. Sci. U.S.S.R., Ser. Geol.*, **5**, 42–68.
- Knauss, J. A., 1960. Measurements of the Cromwell Current. *Deep-Sea Res.*, **6**, 265–286.
- Kobayashi, K., K. Oinuma and T. Sudo, 1960. Clay mineralogical study on Recent marine sediments. *Oceanog. Mag.*, **11**, 215 (Tokyo).
- Koczy, F., 1950. Die bodennahen Wasserschichten der Tiefsee. *Naturwissenschaften*, **37**, 360.

- Koezy, F. F., 1952. On the properties of the water layers close to the ocean floor. *Assoc. Oceanog. Phys. Procès-Verbaux.*, No. 5, 146.
- Koezy, F., 1958. Natural radium as a tracer in the ocean. *Proc. 2nd U.N. Intern. Conf. Peaceful Uses of Atomic Energy, Geneva*, **18**, 351–357.
- Kolbe, R. W., 1955. Diatoms from equatorial Atlantic cores. *Reps. Swed. Deep-Sea Exped.*, **7**, 3.
- Kriss, A. Y., 1959. *Marine Microbiology*. Moskva (in Russian).
- Kuenen, Ph. H., 1950. *Marine Geology*. John Wiley and Sons, New York.
- Laevestu, T. and O. Mellis, 1955. Extraterrestrial material in deep-sea deposits. *Trans. Amer. Geophys. Un.*, **36**, 385.
- LaGow, H. E. and W. M. Alexander, 1960. Satellite measurements of cosmic dust. *IGY Bull. U.S. Nat. Acad. Sci.*, **12**.
- Leinz, V., 1937. Die Mineralfazies der Sedimente des Guinea-Beckens. *Wiss. Ergebn. Dcut. Atlant. Exped. 'Meteor', 1925–1927*, **3**, 245.
- Ljunggren, P., 1953. Some data concerning the formation of manganeseiferous and ferriferous bog ores. *Geol. Fören. Stockholm Förhandl.*, **75**, 277.
- Lowenstam, H. A. and S. Epstein, 1954. Paleotemperatures of the Post-Aptian Cretaceous. *J. Geol.*, **62**, 207.
- Lowenstam, H. A. and S. Epstein, 1957. On the origin of sedimentary aragonite needles of the Great Bahama Bank. *J. Geol.*, **65**, 364.
- Marshall, P. and E. Kidson, 1929. Dust storms of October, 1928. *N.Z. J. Sci. Tech.*, **10**, 291.
- McKelvey, V. E., R. W. Swanson and R. P. Sheldon, 1953. The Permian phosphorite deposits of western United States. *C. R., XXIX, Cong. Géol. Intern., Alger 1952*, **11**, 45.
- Mason, B., 1943. Mineralogical aspects of the system FeO–Fe₂O₃, MnO–Mn₂O₃. *Geol. Fören. Stockholm Förhandl.*, **65**, 95.
- Mellis, O., 1952. Replacement of plagioclase by orthoclase in deep-sea deposits. *Nature*, **169**, 624.
- Mellis, O., 1954. Volcanic ash horizons in deep-sea sediments from the Eastern Mediterranean. *Deep-Sea Res.*, **2**, 89.
- Mellis, O., 1959. Gesteinsfragmente im roten Ton des Atlantischen Ozeans. *Meddel. Oceanog. Inst. Göteborg*, Ser. B., **8**, No. 6, 1–17.
- Menard, H. W., 1959. La topographie et la géologie des profondeurs océaniques. *Coll. Intern. Centre Nat. Rech. Sci.*, **83**, 95.
- Menard, H. W. and C. J. Shipek, 1958. Surface concentrations of manganese nodules. *Nature*, **182**, 1156–1158.
- Mero, J. L., 1960. Mineral resources on the ocean floor. *Sci. Amer.*, **203**, No. 12.
- Mero, J. L., 1960a. Mineral resources on the ocean floor. *Mining Cong. J.*, **46**, 48–53.
- Mironov, S. I. and O. K. Bordovsky, 1959. Organic matter in bottom sediments of the Bering Sea. *Intern. Oceanog. Cong. Preprints*, 970–974. Edit. M. Sears. Amer. Assoc. Adv. Sci., Wash. D.C.
- Molengraaff, G., 1920. Manganknollen in Mesozoische Diepzeeafzettingen van Nederlandsche-Timor. *Versl. Wisen. Nat. Afd., Koninkl. Akad. Wetenschap. Amsterdam*, D. 1.29, 677.
- Moore, D. G., 1960. Submarine slumps. *J. Sediment. Petrol.*, **31**, 343.
- Müller, G. and H. Puchelt, 1961. Die Bildung von Coelestin aus Meerwasser. *Naturwissenschaften*, **48**, 301.
- Murray, J. and A. F. Renard, 1884. On the nomenclature, origin and distribution of deep-sea deposits. *Proc. Roy. Soc. Edinburgh*, **12**, 495.
- Murray, J. and A. F. Renard, 1891. Deep-sea deposits. *Rep. 'Challenger' Exped.*, London.
- Nayudu, Y. R., 1962. A new hypothesis for origin of guyots and seamount terraces. *Amer. Geophys. Un. Monog.*, 6.
- Nayudu, Y. R., 1962a. Volcanic ash deposits in the Gulf of Alaska and problems of correlation of deep-sea ash deposits. *J. Sediment. Petrol.*, in press.

- Niino, H., 1959. On the distribution of organic carbon in the deep-sea sediments of the Japan Sea. *Intern. Oceanog. Cong. Reprints*, 974-6. Edit. M. Sears. Amer. Assoc. Adv. Sci., Wash. D.C.
- Norin, E., 1958. The sediments of the central Tyrrhenian Sea. *Reps. Swed. Deep-Sea Exped.*, **8**, 1.
- Oinuma, K., K. Kobayashi and T. Sudo, 1959. Clay mineral composition of some Recent marine sediments. *J. Sediment. Petrol.*, **29**, 56-63.
- Olausson, E., 1961. Remarks on Tertiary Sequences of two cores from the Pacific. *Bull. Geol. Inst. Univ. Uppsala*, **40**, 299.
- Ostroumov, E. A. and L. S. Fomina, 1960. On the forms of sulfur compounds in the bottom deposits of the Marianas trench. *Doklady Akad. Nauk S.S.R.*, **126**, no. 1-6.
- Peterson, M. N. and E. D. Goldberg, 1962. Feldspar distribution in South Pacific pelagic sediments. *J. Geophys. Res.*, **67**, 3477.
- Pettersson, H., 1945. Iron and manganese on the ocean floor; a contribution to submarine geology. *Göteborgs Kungl. Vet. o. Vitterh. Samh. Handl.*; 6. följd, ser. B, **2**, no. 8, 1-43.
- Pettersson, H., 1945a. Oceanbotttnens problem. *Ymer.*, 161-178.
- Pettersson, H., 1955. Manganese nodules and oceanic radium. *Deep-Sea Res.*, **3**, Suppl. 335-345.
- Pettersson, H., 1959. Manganese and nickel on the ocean floor. *Geochim. et Cosmochim. Acta*, **17**, 209-213.
- Pettersson, H., 1959a. Frequency of meteorite falls throughout the ages. *Nature*, **183**, 1114.
- Pettersson, H. and K. Fredriksson, 1958. Magnetic spherules in deep-sea deposits. *Pacific Sci.*, **12**, 71-81.
- Pettijohn, F. J., 1949. *Sedimentary Rocks*. Harper, New York.
- Phleger, F. B., 1960. *Ecology and Distribution of Recent Foraminifera*. Johns Hopkins Press, Baltimore.
- Radczewski, O. E., 1937. Die Mineralfazies der Sedimente des Kapverden-Beckens. *Wiss. Ergebni. Deut. Atlant. Exped. 'Meteor'*, 1925-1927, **3**, 262.
- Radczewski, O. E., 1939. Eolian deposits in marine sediments. *Recent Marine Sediment Symposium* (P. D. Trask, ed.). Amer. Assoc. Petrol. Geol., Tulsa, 496-502.
- Revelle, R. R., 1944. Marine bottom samples collected in the Pacific Ocean by the Carnegie on its seventh cruise. *Carnegie Inst. Wash. Pubs.*, 556, Washington, D.C.
- Revelle, R. R., M. N. Bramlette, G. Arrhenius and E. D. Goldberg, 1955. Pelagic sediments of the Pacific. *Geol. Soc. Amer. Spec. Paper* 62, 221-236.
- Rex, R., 1958. Quartz in sediments of the Central and North Pacific Basins. Unpub. thesis, University of California.
- Rex, R. W., and E. D. Goldberg, 1958. Quartz contents of pelagic sediments of the Pacific Ocean. *Tellus*, **10**, 153-159.
- Riley, J. P. and P. Sinhaseni, 1958. Chemical composition of three manganese nodules from the Pacific Ocean. *J. Mar. Res.*, **17**, 466.
- Rimšaitė, J., 1957. Über die Eigenschaften der Glimmer in den Sanden und Sandsteinen. *Beitr. Min. Petrol.*, **6**, 1.
- Runcorn, S. K., 1956. Paleomagnetism, polar wandering and continental drift. *Geol. Mijnb.*, **18**, 253-256.
- Runcorn, S. K., 1959. Rock magnetism. *Science*, **129**, 1002-1012.
- Sackett, W. M., 1960. Protactinium-231 content of ocean water and sediments. *Science*, **132**, 1761.
- Sackett, W. M. and G. Arrhenius, 1962. Distribution of aluminum species in natural waters. *Geochim. et Cosmochim. Acta*, **26**, 955.
- Schewiakoff, W., 1926. Fauna e flora del golfo di Napoli. Acantharia, *Pub. Staz. Zool. Napoli*, Mono. **37**.
- Schott, W., 1935. In G. Schott, *Geographie des Indischen und Stillen Ozeans*. Boysen, Hamburg, 110-111.
- Seefried, V., 1913. Untersuchungen über die Natur der Harmattantrübe. *Mitt. Deut. Schutzgeb.*, Bd. H.I. **26**.

- Shepard, F. P., 1948. *Submarine Geology*. Harper, New York.
- Shipek, C. J., 1960. Photographic study of some deep-sea floor environments in the eastern Pacific. *Bull. Geol. Soc. Amer.*, **71**, 1067-1074.
- Shiskina, O. V., 1959. On the salt composition of the marine interstitial waters. *Intern. Oceanog. Cong. Preprint Abst.* Edit. M. Sears. Amer. Assoc. Adv. Sci., Wash. D.C., 977.
- Sigvaldason, G. E., 1959. Mineralogische Untersuchungen über Gesteinszersetzung durch postvulkanische Aktivität in Island. *Beitr. Min. Petrol.*, **6**, 405.
- Sillén, L. G., 1961. Chemistry of sea water. *Oceanography*. Amer. Assoc. Adv. Sci., Publ. 67. Wash. D.C.
- Skornyakova, N. S., 1960. Manganese concretions in sediments of the north-eastern Pacific Ocean. *Doklady Akad. Nauk S.S.R.*, **130**, 653-656.
- Smoluchovski, M. von, 1917. Versuch einer Mathematischen Theorie der Koagulationskinetik Kolloider Lösungen. *Z. physik. Chem.*, **92**, 129.
- Starik, I. Ye. and L. B. Kolyadin, 1957. The conditions of occurrences of uranium in sea water. *Geokhimiya*, no. 3, 213.
- Starik, I. Ye. and A. P. Zharkov, 1961. Rate of sediment accumulation in the Indian Ocean by C^{14} . *Doklady Akad. Nauk S.S.R.*, **136**, 203.
- Strunz, H., 1957. *Mineralogische Tabellen*. Akad. Verlagsges., Leipzig.
- Sverdrup, H. U., M. W. Johnson and R. H. Fleming, 1946. *The Oceans: Their physics, chemistry and general biology*. Prentice-Hall, New York.
- Teodorovich, G., 1958. *Autigennye mineraly osadochnykh porod*. U.S.S.R. Acad. Sci. Press (translation into English; Consultant's Bureau, N.Y., 1961).
- Thiel, E. and R. A. Schmidt, 1961. Spherules from the Antarctic Ice Cap. *J. Geophys. Res.*, **66**, 307.
- Thorslund, P., 1948. Silurisk bentonit från Gotland. *Geol. Fören. Stockholm Förhandl.*, **70**, 245-246.
- Thorslund, P., 1958. Djupborrningen på Gotska Sandön. *Geol. Fören. Stockholm Förhandl.*, **80**, 190.
- Udden, J. A., 1914. Mechanical composition of clastic sediments. *Bull. Geol. Soc. Amer.*, **25**, 655.
- Waern, B., P. Thorslund and Q. Henningsmoen, 1948. Deep boring through Ordovician and Silurian strata at Kinnekulle, Västergötland. *Bull. Geol. Inst. Uppsala*, **32**, 433-474.
- Wattenberg, H., 1933. Kalziumkarbonat- und Kohlensäuregehalt des Meerwassers. *Wiss. Ergebn. Deut. Atlant. Exped. 'Meteor'*, 1925-1927, 8.
- Wattenberg, H., 1937. Die Bedeutung anorganischer Faktoren bei der Ablagerung von Kalziumkarbonat im Meere. *Geol. Meere u. Binnengewäss.*, **1**, 237.
- Wedepohl, K. H., 1960. Spurenanalytische Untersuchungen an Tiefseetonen aus dem Atlantik. *Geochim. et Cosmochim. Acta*, **18**, 200.
- Worzel, J. L., 1959. Extensive deep sea sub-bottom reflections identified as white ash. *Proc. Nat. Acad. Sci.*, **45**, 349.
- Yeroshchev-Shak, V. A., 1961. Kaolinite in the sediments of the Atlantic Ocean. *Doklady Akad. Nauk S.S.R.*, **137**, 695-697.
- Yeroshchev-Shak, V. A., 1961a. Illite in the sediments of the Atlantic Ocean. *Doklady Akad. Nauk S.S.R.*, **137**, 941-953.
- Yoder, H. S., Jr., 1957. Experimental studies on micas: a synthesis. *Proc. 6th Nat. Conf. on Clay and Clay Minerals*, no. 1284, 42-60.
- Zen, E-An, 1959. Mineralogy and petrology of some marine bottom sediment samples off the coast of Peru and Chile. *J. Sediment. Petrol.*, **29**, 513-539.
- Zenkevitch, N. L., 1959. Methods and some results of photographing the floor of the Pacific Ocean. *Intern. Oceanog. Cong. Preprints*, 493. Edit. M. Sears. Amer. Assoc. Adv. Sci., Wash. D.C.
- ZoBell, C., 1946. *Marine Microbiology*. Chronica Botanica Co., Waltham, Mass.